UNIVERSITY OF NAPLES FEDERICO II

FACULTY OF AGRICULTURE

RESEARCH DOCTORATE IN
IMPROVEMENT AND MANAGEMENT OF AGRICULTURAL AND FOREST RESOURCES

Analysis and Modeling of Agricultural systems and Forestry

XXIII CYCLE

LAND USE CHANGES IN ASWA BASIN-NORTHERN UGANDA: OPPORTUNITIES AND CONSTRAINS TO WATER RESOURCES MANAGEMENT

Martine NYEKO

Thesis submitted to Faculty of Agriculture in partial fulfilment for the requirement of the award of a degree of Doctor of philosophy of the University of Naples Federico II.

Tutor:	Professor Eng. Guido D'Urso
Co-Tutor:	Dr. Walter Immerzeel
Coordinator:	Professor Antonio Cioffi

PORTICI, NOVEMBRE 2010

Acknowledgement

The years that I have been working on my PhD were very inspiring and challenging. It would have not been possible without the funding from the University of Naples Federico II and individuals I take great honor to acknowledge. First of all I would like to express my gratitude to Professor J.H Nyeko Pen-Mogi, Professor C. W Baliddawa and Professor Guido D'Urso for initiating this PhD endeavor. Professor Guido D'Urso enthusiastically accepted to supervise this PhD and together, we worked more closely throughout the years. I dedicate my special thanks to him for intellectual and comprehensive supervision and for believing in me. I am also very grateful to my Co-tutor Dr. Walter Immerzeel of FutureWater, the Netherlands for his brilliant and technical advice, without which I would not been able to wrap up this thesis.

Many individuals and colleagues through their great company and encouragement made this endeavor to become a reality. In particular, I deeply appreciate Mrs. Paola Di Fiore who helps me in analyzing my soil data and for many support she offered and to Dr. Mario Palladino who generously shared his vast knowledge and expertise with me and showing me directions.

I would also like to express my gratitude to all the institutions and individuals who provided me with the data that supported my work: Engineer Bart of FAO-NILE, Mr. Musoke of the department of Meteorology Kampala and the staff of the directorate of water resources development (DWD) Entebbe. On personal note, I would like to thank Professor George Kraft of University of Wisconsin who introduce me to model SWAT and Johannes Hunink of FutureWater, the Netherland for the technical support on SWAT model calibration.

Finally, I express my sincere gratitude to God the almighty father for unconditionally giving me health I enjoyed throughout the three years and to my family and friends for their support and encouragement. I take special honor to dedicate this piece of work to my wife Beatrice, my son Eugene and daughter Faith, who patiently waited for me while I was away. Your continued love and prayer kept me motivated and focused.

Abstract

Modification of the Earth's surface i.e. land use change, is the main human activity for survival and is the key player in the management of natural resources, including water. Little attention has, however, been given to understand the role territorial vegetation changes may play in strategic management of water resources. In the basin of Aswa northern Uganda, the changes in land use due to complex demographic and social economic factors is among the numerous challenges faced in management of the limited water resources in the area. The aim of the current study was to explore the opportunities land use changes in the basin may offer to water resources management, looking mainly at the expansion in future agriculture and afforestation as the critical land use change issues. The study was structured into four broad objectives: The first objective was to generate the reference land use dataset (1986 & 2001). The available techniques (the supervised and the unsupervised image classification) were explored using Landsat multi-spectral images. Through careful evaluation, the supervised image classification with the best classification accuracy of 81.48% was used to generate 1986 and 2001 land use maps. The second objectives of the study was to generate experimental land use scenarios required for testing the effect of spatial land use policies on hydrologic processes in the basin. The Multi-criteria-GIS methodology was developed and six experimental land use scenarios were generated using simple but consistence set of bio-physical and socio-economic parameters. The third objective was to customise the hydrologic process model SWAT that was used to simulate the hydrologic impact of the land use change scenarios. The calibration of the hydrologic model SWAT used monthly historical streamflow records from 1970 to 1974 recorded at the basin outlet. The model was manually calibrated using the Nash-Sutcliffe coefficient as objective function. The efficiency of the model during calibration was 0.46. Validation of the model using an independence monthly streamflow records from 1975 to 1978 was done and the model efficiency was 0.66, much better than in calibration period. An independent validation of the model to identify the validity of extending the optimal parameters set in simulation of 2001 hydrologic processes and the hydrologic impact of land use change scenarios was carried out by comparing the simulated actual evapotranspiration fraction with estimated actual evapotranspiration fraction obtained using surface energy balance method and the thermal MODIS images. Validation indicated acceptable model performance in simulating 2001 hydrologic processes, with a spatial correlation coefficient of 0.45. The forth and last objective of the study was to

simulate the hydrologic processes in the reference years and the hydrologic processes impacted by the land use change scenarios and to evaluate how this impact affects water resources management strategies. The results of the hydrologic processes simulation in the reference years showed that 2001 had more water yield than 1986 by 9.2 mm, equivalent to $112.10^6 m^3$. The analysis of the hydrologic impact of land use change in the reference years indicated an increase of 2.52 mm i.e. 30 million cubic meters of water yield in the year 2001. Simulation of the hydrologic impact of the experimental land use indicated that Land use types, which in this study were restricted to plantation forest and generic agriculture, land use extent and location of the land use with respect to climatic zoning, greatly influence the hydrologic process of the basin and the net water yield. It was noted that the water yield of the basin can be significantly decreased by over 15%, if more than 37% of the plantation forests are introduced in the wet zone. In the dry sub-basins however, afforestation of up to 42% had insignificant effect on water yield, which could be taken advantage of in offsetting the afforestation pressure in the wet sub-basin while at the same time enhancing the basin water yield. The effect of agricultural land use change on water yield was however less sensitive to climatic zones. 53% increase in agricultural land cover showed an increase in water yield by about 27%. In conclusion, afforestation increases the actual ET at the expense of runoff, while expansion of agricultural land decreases actual ET and enhances runoff, the degree of the effects depending on the location of the land cover with respect to precipitation.

Abbreviations and acronyms

AE	Average Error
AHP	Analytic Hierarchy Process
AOI	Area of Interest
ARS	Agricultural Research Service
ASCE	American Society of Civil Engineers
CDM	Clean Development Mechanism
CN	Curve Number
ETM+	Enhanced Thematic Mapper Plus
ET_f	Evapotranspiration fraction
FAO	Food and Agriculture Organisation
GDP	Gross Domestic Product
GIS	Geographic Information System
GWQ	Groundwater contribution to streamflow
HRU	Hydrological Response Units
ISODATA	Interactive Self-Organising Data Analysis Technique
IWRM	Integrated Water Resources Management
LAI	Leaf Area Index
LATQ	Lateral flow contribution to streamflow
LCCS	Land Cover Classification Systems
LSST	Land Surface Temperature
MCDM	Multi-Criteria Decision Making
MODIS	Moderate Resolution Imaging Spectroradiometer
NDVI	Normalised Difference Vegetation Index
NFA	National Forest Authority
NSE	Nash-Sutcliffe Efficiency
OECD	Organisation for Economic Cooperation and Development
PREC	Precipitation
RE	Relative Error
SCS	Soil Conservation Service
SEA	Soil and Terrain Database for north-eastern Africa
SEBAL	Surface Energy Balance Algorithm for Land

SSEB	Simplified Surface Energy Balance
STRM	Shuttle Radar Topographic Mission
SURQ	Surface Runoff contribution to streamflow
SW	Soil Water
SWAT	Soil and Water Assessment Tool
TM	Thematic Mapper
TR-55	Technical Release 55
UNESCO	United Nations Educational, Scientific and Cultural Organisation
USDA	United State Department of Agriculture
USGS	United State Geological Survey
USLE	Universal Soil Loss Equation
UTM	Universal Transverse Mercator
WGS84	World Geodetic System 1984

List of symbols

Symbols		Units
C_p	Specific heat of air	kJ/Kg K
d_r	Inverse relative earth-sun distance	-
ET_a	Actual evapotranspiration	mm
ET_o	Reference evapotranspiration	mm
ET_p	Potential plant transpiration	mm
e_a	Air vapor pressure	-
e_s	Saturated vapor pressure	-
G_{sc}	Solar constant	$MJm^{-2}min^{-1}$
K_e	Effective hydraulic conductivity	mm/s
q_{lat}	Lateral flow	mm d^{-1}
r_a	Aerodynamic resistance	s m^{-1}
R_a	Extraterrestrial radiation	$MJm^{-2}day^{-1}$
r_c	Canopy resistance	s m^{-1}
R_c	Recharge	mm
R_n	Net radiation	$MJm^{-2}day^{-1}$
V_{sa}	Shallow aquifer storage	mm
Θ_d	Drainable porosity	mm
ρ_λ	Surface reflectance at wavelength λ	-
ω_s	Sunset hour angle (radiant)	-
ω_λ	Weighting coefficient for solar extraterrestrial irradiance	-
$Alpha\_Bf$	Baseflow recession constant	-
$Cn2$	Curve number for moisture condition II	-
$ESCO$	Soil evaporation compensating factor	-
G	Soil heat flux	$MJm^{-2}day^{-1}$
$GWQMN$	Threshold depth in shallow aquifer for return flow	mm
Gw_Revap	Groundwater revap coefficient	-
J	Julian day (day of the year)	days
Sol_Awc	Available soil water capacity	mm
Sol_Z	Soil depth	m
$canmx$	Maximum canopy storage index	-

$revap$	Root water uptake from shallow aquifer	mm
γ	Psychrometric constant	kPa K^{-1}
δ	Solar decimal (radiant)	-
λET	Latent heat flux density	$MJm^{-2}day^{-1}$
φ	Latitude (radiant)	-

Content

Figures

Tables

Chapter 1

1. Contextual analysis

1.1 Background

Water is a valued resource, to be beneficially managed. Management of water resources frequently must deal with complex systems composed of many interconnected parts. One of the challenges faced in contemporary water resources management is how to use water sustainably to respond to the increasing demand and how to mitigate the environmental consequences related to human quest for survival that affects the quality and quantity of water for the desired use. The contemporary approach to water resources management requires a clear quantitative understanding of the water balance in order to provide secure and sustainable allocations. Water balance is controlled by catchment characteristics and climate. Climate factors are natural and cannot be directly influenced, but catchment modification is main human activity for survival. Understanding the catchment processes and how modifications affect hydrologic systems is very important in the management of water resources; however, this is always limited due to inherent uncertainties in the processes and complexities of the systems, which themselves are dynamics (Pagan and Crase, 2004). To respond to the challenges of systems complexity and uncertainty, a new philosophy of adaptive management is now being advanced. Adaptive management is considered as an approach that involves learning from management actions, and using that learning to improve the next stage of management (Holling, 1978).

Water resources managers need to develop effective and adaptive polices on how to manage water resources for sustainability and also improve their management through understanding the past, predicting the futures and appreciates factors that drives hydrologic systems at a given management unit. Territorial vegetation has been acknowledged as the key player in the water balance (Gerten et al., 2004). The composition and distribution of plant communities on a given landscape are of fundamental important for evapotranspiration and runoff generation (Dunn and Mackay, 1995).

In principle, the need to integrate land use planning in water resources management relates to site specific issues such as demand and supply and may be a matter of urgent where

human livelihood is directly dependence on land. Numerous studies have suggested that changes in land use e.g. afforestation may reduce water yield (Li et al., 2007; Bosch & Hewlett, 1982), unfortunately, the knowledge of such findings cannot be generalized and use as management tool in land use planning and water resources management, due to known issues of uniqueness of the hydrologic processes (Kiersch & Tognetti, 2002). This limitation creates an incentive towards site specific assessment of hydrologic impact of land use change for an effective management of land and water resources.

1.2 Land use change and hydrologic processes

Hydrologic response varies within a watershed as a function of topography, soil, land cover and climate. Land cover controls process of evaporation, transpiration, infiltration, groundwater flow and streamflow. These processes are central to energy, carbon, water and solute balances (Zhang, et al., 2002). Changes in any of the above process affect the others and there is need to consider the dynamic interactions and feedback between the processes. Li et al., (2007) and Bosch & Hewlett, (1982) reported that changes in vegetation cover of a watershed may or may not have any impact on watershed hydrology. This means that there exists a threshold, below which the impact of land use change on hydrology is insignificant. The threshold, which is attributed by Li et al., (2002) to the competition between increasing evaporation and decreasing transpiration, is a function of land use type and location in watershed.

The land cover types affect evapotranspiration, interception losses and the soil water processes. Site specific factors such as climate (precipitation rates and amount), geology, topography and management practices (Kiersch & Tognetti, 2002) also greatly affect the hydrologic response due to land cover changes in a watershed. For example location of deep rooted vegetation in wetland may decrease water yield. In areas receiving high precipitation rates, hydrologic response is highly sensitive to land use change and to the changes in canopy structure and roughness (Bosch and Hewlett, 1982). According to Hibbert (1983), a watershed receiving an amount of yearly precipitation greater than 450 mm can experience a significant change in water yield when deep rooted vegetation are replaced by shallow rooted vegetation. Beside vegetation cover, management practices that affect soil surface characteristics also influence the hydrologic processes (Brooks, et al., 2003).

1.3 Management of water resources

Water resources development and management are specific issues relating to demand and supply, geographical, historical, cultural, political and economic context of any country, territory or basin. Many authors have differently defined water resources management. Arnold, et al., (1998) defined water resources management as the process centered on the need for water, policy to meet the needs, and management to implement the policy. Molden, (2007) considered water resources management as broad discipline covering social, ecological and political aspect, which address multiple use, feedbacks and dynamic interactions between water and production system, livelihood and environment. The Organization for Economic Cooperation and Development (OECD, 1980) has defined water resources management as a production function, which transforms the quantity, quality, time and location characteristics of surface and groundwater resources into the quantity, quality, time and location characteristics of the desired output. In Agricultural perspectives, water resources management covers development of new water supply, use of water conservation, rational use of rain water and institutional development (Tanji & Enos, 1994).

The wide range of definitions given to water resources management indicates the level of complexity and uncertainty involved. Internationally accepted approaches to water resources management however address the connections between resources and services under the theme “Integrated Water resources Management” (IWRM). The basis of IWRM is that different uses of water are interdependent. That is water allocations and management decisions consider the effects of each use on the others.

1.4 Management of water resources in Uganda; issues and outlook

1.4.1 Uganda’s fresh water resources

Uganda's freshwater resources consist of direct rainfall, water in lakes and rivers, and groundwater (shallow and deep aquifer). Rainfall feeds agriculture, rivers, lakes and recharge groundwater and the patterns influence the local land use potential and population distribution. The average annual rainfall varies from less than 900 mm in the north-eastern semi-arid areas of Kotido to 2000 mm on the Lake Victoria island (Uganda Nation Water Development Report, 2005). In the semi-arid areas, most of the rainfall is evaporated due to

high evaporative demand and little is left as storage in the soil, runoff and recharge to shallow aquifer.

Open water (surface water) in Uganda covers about 15% of the total surface area and its annual yield is estimated at 66 Km3 including runoff (Uganda Nation Water Development Report, 2005). This supply, however, faces significant spatial and temporal variability rendering many parts of the country water stressed in most periods of the year. Harvesting of the runoff for use during water scarcity is yet to be explored in most area.

Groundwater (water from springs, boreholes and dug wells) is dominant and in some places, constitutes the only source of daily water to many Ugandans. Unreliability of surface water resources, coupled with poor quality, puts dependency level on groundwater resources very high. The crystalline basement rock that provides over 90% of the productive aquifers in Uganda (occurring either as shallow aquifers in the weathered overburden or as deep aquifers in the fractured bedrock) often have very low yield (Howard et al., 1992). The groundwater resources especially in Aswa basin is highly vulnerable to changes in vegetation, especially forest cover that can significantly affects the recharge of the aquifers.

1.4.2 Management outlook

In Uganda, IWRM planning processes is focusing on how to attain the UN Millennium Development Goals on reducing poverty and hunger, diseases and environmental degradation, including halving the proportion of people without access to basic drinking water and sanitation services.

There are multiple challenges being faced in the country as a result of population growth wanting expansion in services and development of economy to attain the UN Millennium Development Goals. In the frontage of these challenges are: the needs to increase food production, through improved rain-fed agricultural production or Irrigated agriculture; the needs to provide access to clean water; and the needs to meet energy demand while at the same time complementing environmental sustainability.

Growth in food production can be achieved through primarily expansion of agricultural land and increase in water use (irrigated agriculture). However there may be no more land available for expansion of farmland in most part of Uganda by 2022 (Jorgensen, 2006). The outlook into future agricultural development in the country therefore relies mainly on

increasing the productivity of the available land through water use innovation in rain fed agriculture, which includes water harvesting, drip irrigation and conservation farming technologies.

The increasing demand for fuel (wood and charcoal), and timber as a result of population growth has consequently resulted into deforestation in many parts of the country. To balance the effects of deforestation, the National Forest Authority (NFA), Uganda's institution in charge of forest resources, has undertaken reforestation project, with funding from World Bank (Wandera & Izama, 2009). The expansion of wood resources, which are mainly pines and eucalyptus, is considered crucial for the country to meet its growing demand for wood and reduce the pressure on the remaining native forests. This campaign has been well taken up by the communities and it has gained significant momentum meant to propel it to a near future. The results are continuous increases in areas under forest mainly in gazetted land and in marginal land.

As noted previously, changes in land use due to expansion of farmland and introduction of new plantation forest pose some constrains and opportunities to water resources management. The introduction of pines, eucalyptus and other new plantations as a substitute to indigenous plantation (deciduous and conifers), the location of the new plantations and the extent of the plantations are likely to have a significant impact on the hydrologic response and net water yield. The extended agricultural lands may potentially increase the sediment loads to reaches, besides being potential non-point pollutant sources.

1.5 The study area

The case study area is the lower part of Aswa basin (Figure 1) located in Northern Uganda. The area covers approximately 12,225 km^2, almost half the area of the entire basin (27,601 Km^2), with over 1 million people inhabitants who derive their livelihood directly on land. Altitude ranges between 870 to 1908 meters above sea level and slope is gentle with most part (>97%) having slope less than 20%. Both land use and geology are complex. Land cover comprises mainly of wood lands and Savannah grassland. The natural forest, which is mainly deciduous trees covers very little area of the catchment (>0.5%).

Rainfall distribution significantly varies from less than 900 mm annually in the North-eastern part to over 1800 mm at the higher altitude. Water availability is a critical issue as

most of the streams and tributaries dries out during the dry season, which normally extend from December to March. Groundwater is used as major source of water in the basin providing portable water to meet domestics and livestock water demand. Increased demand for water is expected to be intense especially in the agricultural sector, to boost food production, and in the rapidly growing urban centres.

Agriculture is purely subsistent and it is practiced on small parcels of land. Nonetheless, the agricultural sector provides the basic raw materials to the agro-based industries and account for over 90% of the economic activity of the inhabitants together with animal husbandry. A combination of social, economic, and technological factors are known to be major drivers of land use in the basin. Most notably are incentives towards afforestation and commercialisation of Agriculture. Technology adoption in agriculture has been expanding, thus creating major shift in land use. Local and international markets are opening and access to information are all exciting faster rate of land use change in the near future, which shall require proper planning and management.

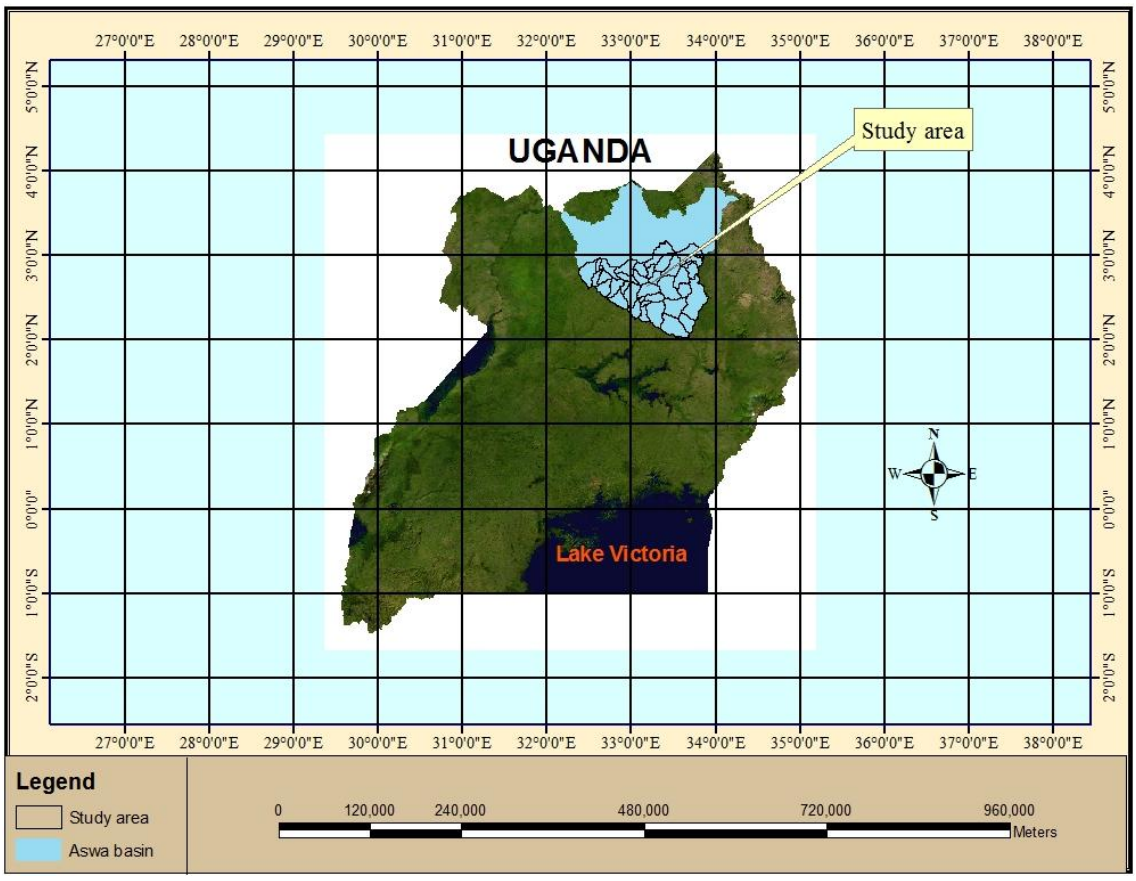

Figure 1.1: The study area

1.6 Statement of the research problem

Water resources management problems in Aswa basin are twofold. The first and foremost is lack of quantitative knowledge of the hydrologic processes in the basin. No major study has been conducted so far to quantify how much water is available, how the available water is distributed over space and time and how much water is needed now and in the near future. The second problem is the unstructured land use changes taking place at considerable scale and rate compared to recent past. The two problems coupled with climatic constrain and the hydrogeological complexities of the basin present a significant threat to the current and the future water use.

1.7 Objective of the study

The objective of the study is to explore the involvement of land use change in management of water resources. The study investigates the relationship between the hydrologic processes; mainly water yield, and groundwater storage and the land use change attributes; defined in this study as land use types, land use location and land use extent. The land use types considered in this study were plantation forest (Pine and Eucalyptus) and agricultural land use generic. The hydrologic impact of the land use changes were simulated using the hydrologic process model SWAT. Input data required to run the model were processed in chapter III and IV. In particular, the GIS Multicriteria methodology was developed and used to generate the land use scenarios based on the bio-physical and the socio-economic parameters.

1.7.1 Specific objectives

To meet the objective of this study and manage the issues of data unavailability, the study was structured into four broad areas each with specific objectives:

1- Land use change evaluation
   a. To develop land cover maps using remote sensing image classification techniques
   b. To analyse the changes in the land cover
2- Land use change scenarios
   a. To develop GIS based multi-criteria approach to simulate anticipated forest land cover and agricultural land cover changes in the basin

3- Hydrologic impact assessment of land use change
    a. To setup hydrologic process model SWAT
    b. To calibrate and validate the hydrologic model for scenario simulation
    c. To quantify the hydrologic processes in the basin using the model &
    d. To simulate the hydrologic impact of land use change scenarios
4- Impact evaluation
    a. To examine how the hydrologic impact of land use change affects water resources availability, capacity and technological choices in sustaining future water demand in agriculture and other sectors.

1.8 Limitation

The main limitations to this study were the availability and accessibility of quality data required to implement the hydrologic process model SWAT. The streamflow records, the climatic data on daily time steps (precipitation, temperature minimum and maximum, wind speed, solar radiation and relative humidity), and the soil data were available but with missing values, limited descriptions and details required. The soil data was missing the soil hydraulic properties and the important soil attributes like organic carbon content, wet soil albedo, erodibility factors and textural classes. The available streamflow records for the gauges ASWA86201 & ASWA86202 were available for the years 1960 to 1980 and had significant gaps in the records especially after 1977. The weather data obtained from FAO-NILE had extensive historical records covering the periods between 1940 and 2000 but was without the daily solar radiation record and lots of gaps in wind speed, humidity and temperature records.

Land use maps for the periods of interest, preferably 1970's and 2009 were not available. The land use maps had to be prepared using the available satellite images. The available satellite images were obtained from Landsat archives and were downloaded for free. There were no Landsat scene earlier than 1983, and the available earliest image with good visibility was Landsat scene of January 1986. Land cover maps representing the 1970's situation was needed for tuning up the hydrologic model using the 1970's streamflow records. Since it was impossible to get this land cover, it was assumed that the 1986 land cover was good representation of the 1970's land cover situation. The most recent land use map was also required to represent the current land use. However, the available satellite image, particular

with high resolution that could be used to classify the most recent land use map, was Landsat scene of January 2001.

The soil data was the most difficult dataset to process in this study. Effort to estimate the fundamental soil hydraulic properties were made using a known correlation between textural classes, bulk density and organic matter content. Soil survey was carried out in the study area in the year 2007 and soil samples were collected for the analysis of textural classes, bulk density and the organic matter contents. The analyses were carried out at the soil hydraulic laboratory in the University of Naples Federico II. The results obtained from the soil sample analyses together with other information provided in FOA soil database, the harmonised world soil database and the publication of soil of Northern Province, the representative textural classes, the bulk density and organic matter content for the different soil units were derived.

There was a significant time lag between the model calibration periods (1970-1974) and the model implementation period (2001). To be sure that the time lag had no effect in the model application in simulating the hydrologic processes in 2001 and the land use change scenarios, an independent validation of the model in 2001 was necessary. However, the streamflow records required to carry out the validation in these periods was lucking. An attempt was therefore made to validate the model in 2001 by comparing the actual evapotranspiration simulated by the model with the actual evapotranspiration estimated using the energy balance method and the MODIS thermal images.

1.9 Organisation of the thesis

The thesis is presented in ten chapters as briefly described below:

1. Chapter I: Contextual analyses: Provides background information and the research concept, the research problem and the research objectives and is concluded with an outline of the thesis.
2. Chapter II: Hydrologic systems and models: The chapter reviews fundamental literature on the hydrologic systems, hydrologic systems analysis and modeling and the hydrologic process model SWAT.
3. Chapter III: Land use change in Aswa basin, quantification using remote sensing image classification: In this chapter, the spectrally based image classification techniques are

evaluated. The superior classification technique is used in the classification of 1986 and 2001 land use map and the changes in the land cover between 1986 and 2001 are quantified.

4. Chapter IV: Land use scenario modeling, an integrated approach of GIS Multi-criteria analysis: The formulation of land use change model based on integrated approach of GIS and multi-criteria analysis, using bio-physical and socio-economic parameters is presented and the experimental land use scenarios are simulated using the model formulated.
5. Chapter V: SWAT model set-up, calibration and validation: The hydrologic process model SWAT set-up, parameterization and verification are discussed. Detail description of data processing and analysis of sensitivity of streamflow prediction to model parameters are presented.
6. Chapter VI: Implementation of the hydrologic model SWAT in 2001: This chapter evaluates the validity of using the model to simulate the hydrologic processes in 2001 and the subsequent application in analyzing the land use change impact on hydrologic processes. The evaluation of the model was done using the actual ET fraction derived using the Simple Surface Energy (SSEB) balance approach based on MODIS Land Surface Temperature, since the streamflow records were missing in these periods.
7. Chapter VII: Simulation of the hydrologic processes and the hydrologic impact of reference land use change scenario: The objectives of this chapter were to quantify the hydrologic processes in 1986 and 2001 and to simulate the hydrologic impact of the land use change between 1986 & 2001. The chapter presents the analysis of the hydrologic impact of the land use change using variables climate and using non-variable climate.
8. Chapter VIII: Simulation of the hydrologic impacts of experimental land cover: Six experimental land use scenarios, showing different land cover extend and location are presented for simulation of hydrologic impact of land use change in this chapter. The analyses are presented at two spatial scale, the sub-basin scale and basin scale. The effects of spatial locations with respect to climatic zoning are discussed.
9. Chapter IX: Impact evaluation: This chapter examines how the effect of land use change on water balance affects water resources management strategies in the area. The chapter addresses two particular questions that form the basis of this thesis: The first question was "*to what extent can water yield be manipulated by altering the vegetation cover at sub-basins and basin scale*?" and the second question was "*can vegetation manipulation complement water resources management objectives in the study area*?"

10. Chapter X: Discussion and conclusion: This chapter provides the discussion and conclusion of the entire chapters in the thesis and presents the main conclusion of the study.

Chapter 2

2. Hydrologic systems and the hydrologic process model SWAT

The objective of this chapter was to review the fundamental literature on the hydrologic systems, hydrologic systems analysis and modeling and the hydrologic process model SWAT as a requirement for identifying the appropriate model structures for simulating the hydrologic impact of land use change.

2.1 Hydrologic systems

Dooge (1973) gave a more general definition of hydrologic systems. His definition, consider hydrologic systems as set of physical, chemical and/or biological processes acting upon an input variable(s), to convert it (them) into an output variable(s). A variable here is understood to be a characteristic of a system which may be measured, and which assumes different values when measured at different times. Meanwhile, quantities that define the characteristics of hydrologic systems that may remain constant in time or may vary are termed parameters.

Most hydrologic systems are extremely complex, and cannot be understood in detail. Therefore, abstraction is necessary if one is to understand or control some aspects of their behaviour. The abstraction of hydrologic systems is done through hydrologic systems analysis or modeling. Hydrologic modeling has gained a theoretical base from advances of systems theory. Systems theory recognizes the fact that although real systems may be physically totally different, they may still obey the same systems laws, therefore allowing equivalent mathematical descriptions or computer simulation (Bossel, 1986). The objective of hydrologic system analysis or modeling is to study the system operation and predict its output using hydrologic systems models.

The watershed can be considered as a hydrologic system with the system boundary as the watershed divide. The accounting of input and output of water into a system is based on the principle of conservation of mass, which state that any change in the water content of a given control volume during a specified period must equal the difference between the amount of

water added to the control volume and the amount of water withdrawn from it. This concept widely known as water balance can simply be represented mathematically as:

$$I - O = \Delta S \qquad 2.0$$

where I is input, O is output and ΔS is change in storage

In thermodynamics and fluid mechanics, a control volume defines a fixed region in space where one studies the masses and energies crossing the boundaries of the region.

Using the concept of system analysis, effort is directed to construct a model relating inputs and outputs rather than to the extremely difficult task of exact representation of the system details, which may not be important from a practical point of view or may not be known. Nonetheless, good knowledge of the physical system helps in developing a good model and verifying its accuracy.

In principles, the systems of equation representing the hydrologic system are expressed as function of time that is,

$$Q(t) = \Omega\, I(t) \qquad 2.1$$

where Ω is a transfer function between the input and the output. The transfer function describes the hydrologic processes that transform the input into output. The schematic diagram of the hydrologic systems (Figure 2.1) shows some of the hydrologic process that transforms the input variables "precipitation" into output variables "streamflow".

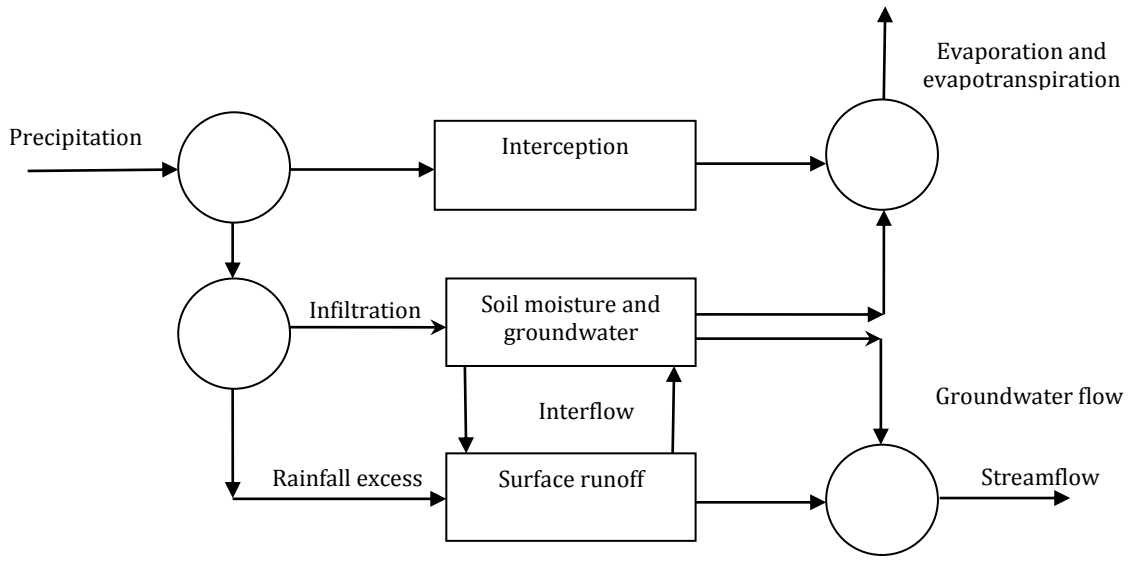

Figure 2.1: schematic representation of hydrologic systems of watershed (Chow et al., 1988)

At the root zone, these processes can be identified as; interception loss, transpiration, evaporation, infiltration, interflow (sub-surface flow) and deep drainage (drainage below root zone). The schematic representation of the hydrologic systems at root zone can be expressed mathematically as,

$$\Delta S = P - I_c - T - E - SR - D \qquad 2.2$$

where ΔS is the change in root zone soil water storage over the time period of interest, P is precipitation, I_c is interception loss, E is direct evaporation from the soil surface, T is transpiration by plants, SR is surface runoff or overland flow, and D is deep drainage out of the root zone. All quantities are expressed in terms of volume of water per unit land area or equivalent depth of water over the period considered.

Equation 2.2 is the basis of water balance calculation. In the equation, precipitation is the largest term and can be directly measured using rain gauges. Interception loss is a complex process affected by factors such as rainfall regime and canopy characteristics. Soil evaporation is often lumped together with plant transpiration as total evapotranspiration. Evapotranspiration represents the second largest term in water balance equation. Evapotranspiration can be estimated from the meteorological (Penman, 1948; Thornthwaite, 1948; Priestly and Taylor, 1972; Hargreaves, 1975 and Blaney-Criddle, 1960) and soil moisture data or measured directly. Runoff significantly varies with the scale of measurement. At field scale, the amount of surface runoff may be considered negligible. However, at catchment scale, runoff may be significant compared to major components of water balance. The storage term depends on the time periods over which the water balance is computed. In long term, the change in storage is likely to be small in relation to total water balance and can be neglected, while in the short term storage can be significant.

2.2 Hydrologic process model SWAT

2.2.1 Description

The Soil Water Assessment tool (SWAT) model (Arnorld, et al., 1998) is a distributed conceptual physically based hydrologic model developed to predict the effect of land management practices on water, sediment and agricultural chemical yield in large complex watershed with varying soil, land use and management condition over long periods of time.

The model was developed for the USDA Agricultural research service (ARS). The model has an explicit spatial parameter space and to simplify the pre and post processing of spatially distributed data, the model is coupled to GIS. The objective in SWAT model development was to predict the impact of management on water, sediment and agricultural chemical yield. The model component thus includes: weather, hydrology, soil temperature, plant growth, nutrients, pesticides and land management (Arnold, et al., 1998).

The application of the hydrologic process model SWAT in this study was due to the capability of the model in simulating land phase of the hydrologic processes using an extensive inbuilt land use and management database, the relatively few input data required by the model and the ability of the model to use the inbuilt weather generator to fill in gaps in weather records and generate missing weather record during simulation.

2.2.2 Hydrologic processes in SWAT model

The hydrologic processes in SWAT model are based on conceptual understanding of the hydrologic systems and the different pathways that water takes within the hydrologic systems. The hydrologic processes simulated by SWAT are based on the water balance equation (Equation 2.3):

$$SW_t = SW_o + \sum_{i=1}^{t}\left(R_{day} - Q_{surf} - E_a - w_{seep} - Q_{gw}\right) \qquad 2.3$$

where SW_t is the final soil water content (mm H_2O), SW_o is the initial soil water content on day i (mm H2O), t is the time (days), R_{day} is the amount of precipitation on day i (mm H_2O), Q_{surf} is the amount of surface runoff on day i (mm H_2O), E_a is the amount of evapotranspiration on day i (mm H_2O), w_{seep} is the amount of water entering the vadose zone from the soil profile on day i (mm H_2O), and Q_{gw} is the amount of lateral flow on day i (mm H_2O).

The hydrologic processes presented in equation 2.3 are predicted separately for each HRU and aggregated (routed) to obtain the total sub-basins and basin values. In other words, the HRU is the operational unit of the model. In studying complex basin, the model divides the basin into a number of sub-basin units each drained by a reach. Each sub-basin is further divided into HRU (where hydrologic process is treated as homogeneous) using unique combination of land use, soil type and slope. The SWAT HRU water balance is presented by

four storage volumes: snows, soil profile (0-2m), shallow aquifer typically 2-20m) and deep aquifer (>20m) (Figure 2.2).

Surface runoff process

Runoff results from excess precipitation occurring on the watershed. Rainfall excess is part of the rainfall that is not lost to infiltration, depression storage and interception. Surface runoff contributes majorly to streamflow in most basins. In classical hydrology, streamflow is defined in term of three components: 1) surface runoff, 2) interflow, 3) groundwater flow.

In order to model surface runoff, one needs to determine the rainfall loss rate (infiltration rate). The excess rainfall is then transformed by the catchment into direct runoff. Conceptually, surface runoff occurs in SWAT model whenever the rate of water application to the ground surface exceeds the rate of infiltration. The model provides two methods for the estimating surface runoff. The SCS curve number procedures (SCS, 1972) and the Green and Ampt infiltration method (Green and Ampt, 1911).

The SCS Curve Number method relates a calculated Runoff Curve Number (CN) to runoff, accounting for initial abstraction losses ($I_a = 0.2S$) and infiltration rates of soils. The initial abstraction I_a includes surface storage, interception and infiltration prior to runoff and the retention parameter S. S varies spatially due to changes in soils, land use, management and slope and temporally due to changes in soil water content.

The fundamental rainfall-runoff equations are as follows (SCS, 1972):

$$Q = \frac{(P-0.2S)^2}{(P+0.8S)} \qquad 2.4$$

In which, Q = runoff, P = precipitation (maximum potential runoff), S = potential maximum watershed retention. S is related to the soil and cover conditions of the watershed through the CN. CN has a range of 0 to 100, and the relationship between S and CN id given by:

$$CN = \frac{1000}{S+10} \qquad 2.5$$

Conceptually, SWAT model runoff only when $P > I_a$. That is:

$$Q = \frac{(P-0.2\,s)^2}{P-0.8\,s}, \qquad P > 0.2\,s \tag{2.6a}$$

$$Q = 0.0 \qquad P \leq 0.2\,s \tag{2.6b}$$

The SCS curve number is a function of the soil's permeability, land use and antecedent soil water condition. The SCS defines three antecedent moisture conditions: moisture condition I referring to dry or wilting point, moisture condition II referring to average moisture and moisture condition III referring to wet or field capacity moisture. The curve number for moisture condition I and III is calculated using curve number for moisture condition II (Neitsch et al., 2005).

The second methodology provided in SWAT for the estimation of runoff is the Green-Ampt Mein and Larson excess rainfall method. The original Green and Ampt equation was developed to predict infiltration assuming excess water at the surface at all time (Green and Ampt, 1911). Mein and Larson (1973) developed a methodology for determining ponding time with infiltration using the Green and Ampt equation. The Green-Ampt Mein and Larson infiltration rate is defined as,

$$f_{inf,t} = K_e\left(1 + \frac{\varphi_{wf\times\Delta\theta_v}}{F_{inf,t}}\right) \tag{2.7}$$

where $f_{inf,t}$ infiltration rate at time t K_e is the effective hydraulic conductivity $F_{inf,t}$ is the commutative infiltration at time t φ_{wf} is the wetting front matric potential and $\Delta\theta_v$ is the change in volumetric moisture content across the wetting front.

The effective hydraulic conductivity is conceptually calculate as a function of curve number and saturated hydraulic conductivity. The volumetric moisture content across the wetting front is also calculated at the beginning of each day as a function of soil water content, amount of water in the soil profile at field capacity and the porosity of the soil (Neitsch et al., 2005). The wetting front matric potential is the function of porosity, percentage sand constituents and percentage clay constituents (Rawls and Brakensiek, 1985).

Two approaches for estimating the peak runoff rate is provided in SWAT: the modified rational formula and the SCS TR-55 method (USDA SCS, 1986). A stochastic element is included in the rational formula to allow realistic simulation of peak runoff rates, given only daily rainfall and monthly rainfall intensity.

Evapotranspiration process

Evapotranspiration estimation in SWAT takes two broad steps. The first step is the estimation of the reference evapotranspiration ETO and the second step is the estimation of the actual evapotranspiration ETa.

Three methods have been incorporated in SWAT for the estimation of ETO, the Penman-Monteith (Monteith, 1965), Priestley-Taylor (Priestley and Taylor, 1972) and the Hargreaves methods, (Hargreaves, et al., 1985). Penman-Monteith is considered most robust and has been adapted and recommended by FAO (Allen, 1998).

The original Penman-Monteith equation (Penman, 1948), combined the energy balance with the mass transfer method and derived an equation to compute the evaporation from an open water surface from standard climatological records of sunshine, temperature, humidity and wind speed (Equation 2.8).

$$\lambda ET = \frac{\Delta(R_n - G) + \rho_a c_p \frac{(e_s - e_a)}{r_a}}{\Delta + \gamma\left[1 + \frac{r_s}{r_a}\right]} \qquad 2.8$$

where R_n is the net radiation, G is the soil heat flux, $(e_s - e_a)$ represents the vapour pressure deficit of the air, ρ_a is the mean air density at constant pressure, c_p is the specific heat of the air, Δ represents the slope of the saturation vapour pressure temperature relationship, γ is the psychrometric constant, and r_s and r_a are the (bulk) surface and aerodynamic resistances.

The aerodynamic resistance to sensible heat and vapour transfer (r_a) is calculated in SWAT model as logarithmic function of wind speed measurement height, humidity and temperature measurement height, the zero plane displacement of wind profile, the roughness length for momentum and vapour transfer and it decreases with increase in wind speed at a given height.

The canopy resistance (r_c) is calculated in SWAT using the equation according to Jensen, et at., (1990), which considered that for a well-watered reference crop;

$$r_c = \frac{r_l}{(0.5 \times LAI)} \qquad 2.9$$

where r_l is the minimum effective stomatal resistance of a single leaf

The introduction of resistance factors to cropped surfaces extends the application of Penman-Monteith equation to direct calculation of any crop evapotranspiration as the surface and aerodynamic resistances are crop specific (Allen et al., 1998).

Once ETO has been determined, SWAT calculates ETa. Rainfall intercepted by the plant canopy is first allowed to evaporate and the maximum amount of plant transpiration and soil evaporation is calculated (Neitsch et al., 2005). If the Penman-Monteith method is used as the reference evapotranspiration method, potential daily transpiration is calculated using the extended application of Penman-Monteith equation that directly calculate any crop evapotranspiration using the surface and aerodynamic resistance of the specific crop (Neitsch et al., 2005).

For the other methods (Priestley-Taylor and the Hargreaves), potential plant transpiration (ET_p) is estimated as,

$$ET_p = \frac{ET_o \times LAI}{3.0} \qquad 0 \leq LAI \leq 3.0 \qquad 2.10a$$

$$ET_p = ET_o \qquad 0 > 3.0 \qquad 2.10a$$

ETa is calculated from ET_p using the plant water uptake equation given by,

$$w_{up,z} = \frac{ET_p}{1-\exp(-\beta_w)} \times \left[1 - \exp(-\beta_w \times \frac{z}{z_{root}}\right] \qquad 2.11$$

where $w_{up,z}$ is the potential plant water uptake from the soil surface to a specified depth of the soil on a given day, β_w is the water use distribution parameters, z is the depth from the depth from the soil surface (mm) and z_{root} is the depth of root development in the soil (mm). Actual plant water uptakes is equals is exponentially reduced when soil water content drops below field capacity.

The maximum amount of soil evaporation in a given day is a function of reference evapotranspiration and the soil cover index. During the period of high water use by plants, the maximum soil evaporation is reduced using the relationship

$$E_s' = \min\left(E_s, \frac{E_s.ET_o}{E_s+E_p}\right) \qquad 2.12$$

where E_s' is the maximum soil evaporation adjusted for plant water use and E_s is the maximum soil evaporation.

SWAT partition the soil evaporation between different layers and estimate soil evaporative demand for each layer differently. The depth distribution of the soil evaporation is a function of the maximum soil evaporation and the soil depth. Each soil layer must meet its evaporative demand; however, if the soil layer is unable to meet its evaporative demand, a compensating factor ESCO can be adjusted to modify the depth distribution used to meet the soil evaporative demand. The actual soil evaporation is limited by soil water content and is reduced when the water content of the soil layer is below field capacity according to the equations:

$$E_{sl}' = E_{sl} \times \exp\left(\frac{2.5 \times (SW_l - FC_l)}{FC_l - WP_l}\right) \quad 2.13$$

where E_{sl}' is the evaporative demand for the layer adjusted for the water content, E_{sl} is the evaporative demand for the layer, SW_l is the layer soil water content, FC_l is the layer soil water content at field capacity and WP_l is the layer soil water content at wilting point.

The soil water process

The soil water process include: infiltration, evaporation, plant uptake, lateral flow and percolation to lower layers. Infiltration process is modelled during runoff estimation using either the SCS curve number approach (SCS, 1972) or the Green and Ampt equation (Green and Ampt, 1911).

Soil percolation component of SWAT uses a storage routing technique combined with crack flow model to predict flow through each soil layers in the root zone. Once the water percolates below the root zone, it is lost from the watershed and become groundwater or appears as return flow. The soil profile is divided into multiple layers (up to 10 layers). Downward flow occurs when the field capacity of a soil layer is exceeded and below is not saturated. Downward flow is governed by saturated hydraulic conductivity of the soil layer. Upward flow may also occur, when the lower layer exceed field capacity. Movement of water between adjoining layers is governed by soil water to filed capacity ratios of the two layers. The equations governing the soil water process are given in Neitsch, et al., (2005).

Lateral flow in the subsurface profile (0-2m) is calculated simultaneously with percolation. A kinematic storage model (Sloan et al., 1983) based on slope, slope length, and saturated conductivity is used (Equation 2.8).

$$q_{lat} = 0.024 \frac{(2S\ SC\ \sin(\propto))}{\Theta_d L} \quad 2.14$$

where q_{lat} is the lateral flow ($mm\ d^{-1}$), S is the drainable volume of soil water (mh^{-1}), α is slope (mm), Θ_d is the drainable porosity (mm) and L is length. If the saturated zone rises above the soil layers, water is allowed to flow to the layer above. To account for multiple layers, the model is applied to each soil layers independently, starting at the upper layers.

Groundwater water process

Groundwater contribution to streamflow is simulated by creating shallow aquifer storage (Arnold, et al., 1993). Percolation from the bottom of the soil profile recharges the shallow aquifer (groundwater recharge). A recess constant derived from daily streamflow records lags flow from the aquifer to stream. Total groundwater recharge is simulated by SWAT as: water that passes past the bottom of the soil profile, channel transmission losses, and seepage from the ponds or reservoir. The water balance for shallow aquifer is given by (Arnold, et al., 1998)

$$V_{sai} = V_{sai-1} + R_c - revap - rf - perc_{gw} - WU_{SA} \quad 2.15$$

where V_{sai} is the shallow aquifer storage on day i (mm), V_{sai-1} is water storage in shallow aquifer on day $i-1$ (mm), R_c is the recharge (percolate from the bottom of soil profile) (mm), revap is the root uptake from the shallow aquifer (mm), rf is the return flow (mm), $perc_{gw}$ is percolation into deep aquifer (mm) and WU_{SA} is the water withdrawal from shallow aquifer. Return flow from shallow aquifer to stream is estimated with the equation (Arnold, et al., 1993):

$$rf_i = rf_i e^{-\alpha \Delta t} + Rc(1.0 - e^{-\alpha \Delta t}) \quad 2.16$$

where α is a constant of proportionality or reaction factor. Figure 5.1 show pathways available for water flow in SWAT.

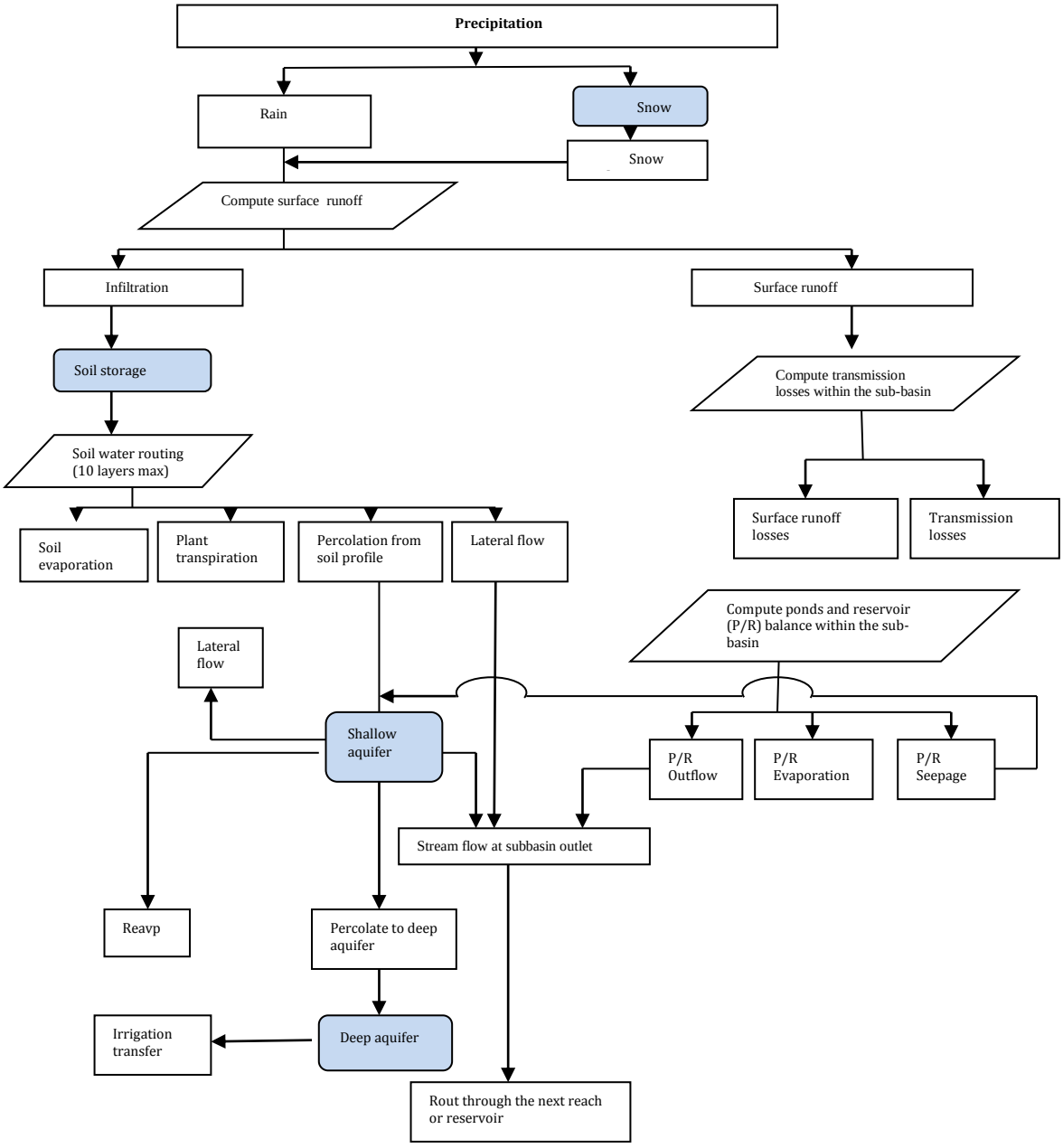

Figure 2.2: schematic pathways available for water movement in swat model at HRU (Arnold, et al., 1998)

2.2.3 The appropriate model structures

SWAT model is design to suit different modeling objectives and input data quantity and quality available. Understanding the general structure, parameter space and input variables of the SWAT model is first major step to successful application of the model. For the case of land use change simulation, the model structures must be able to adequately describe all the relevant hydrological processes. The sections below discuss the model structures selected in the simulation of land phase and routing phase of the hydrologic processes in this thesis.

1. Climate

In SWAT model, climatic variables are either input from records or generated using customized weather generator (section 5.2.1). Daily precipitation and daily temperature minimum and maximum records from the weather stations were used as inputs. Solar radiation, wind speed and relative humidity were generated using the customized weather generator (WXGEN) during simulation. The distribution of precipitation used to generate representative streamflow was calculated using the skewed distribution proposed by Nicks (1974). The exponential distribution, which provides an alternative to the skewed distribution is mainly applied where limited data on precipitation are available, however, in this study, an extensive records on precipitation from the three stations were available. The daily maximum half hour rain values used in calculation of peak discharge was estimated using the triangular distribution. The assumption made is that the randomness of the triangular distribution in generating daily values was more appropriate for the large study watershed.

2. Hydrology

The SCS curve number method developed provide a consistent basis for estimating the amount of runoff under varying land use and soil type (Rallison and Miller, 1981). The retention parameter can vary with soil profile water content (Neitsch, et al., 2005) and the initial abstraction includes the canopy storage terms. These attributes makes the SCS curve number methods to have more physical meaning in estimation of runoff in the study of hydrologic impact of land use change.

For the estimation of evapotranspiration, the Penman-Monteith method was adopted. The Penman-Monteith equation combines components that account for energy needed to sustain evaporation, the strength of the mechanism required to remove the water vapour and

aerodynamic and surface resistance terms (Neitsch et al., 2005). The aerodynamic and surface resistance are specific to a given land cover. The evapotranspiration estimated using the Penman-Monteith equation is therefore more representative.

The management file in SWAT model contain and extensive plant growth database that control the growth cycle of plant. Management options allows user to schedule plant growth using either dates or heat units. The study area consists of generic land cover and the agricultural practices are also generic with no fertilizer, pesticide and or irrigation application. Besides, planting dates for crops are not specific and crop rotations are haphazardly done. The heat unit scheduling was therefore found more suitable in this scenarios. All plant growth cycle in this study was controlled using the heat unit.

The loading of water in each HRU was routed through the stream network of the watershed using the variable storage coefficient method developed by Williams (1969). The variable storage routing technique proposed is advantageous over the Muskingum technique in that the parameters required by the variable storage routing techniques are readily available from the channel morphological data.

2.3 Conclusion

Hydrologic systems are complex, however, with the advent of modern computers and the development of systems theory, complex hydrologic systems analysis has become practically possible. The representation of key hydrologic processes in a watershed using hydrologic models varies with degree of complexity required, the data available and expertise on the part of the user. In this study, SWAT model was used because of the detail spatial representation of parameters, the ability to adequately represent the land phase of the hydrologic systems and the great flexibility of the model to data input.

Chapter 3

3. Land use change in Aswa basin. Quantification using remote sensing image classification

3.1 Introduction

Recent rapid growth in the population and the needs to increase food production and meet the basic energy demand has triggered a peculiar land use change phenomena in Aswa basin. The pattern and extent of the new land uses can be of environmental concern. In particular, the composition and distribution of the new land uses are of fundamental important to the management of water resources in the basin. Proper planning and management of the land use changes in the basin required to mitigate the possible environmental consequences, can only take place when the land use change itself is quantified and the objective of the environmental benefits defined.

In this chapter, the principle objective was to quantify the land use changes between 1986 and 2001. Before this could be done, the available image classification techniques, the supervised and the unsupervised image classification were first evaluated and the superior technique used mapping the land use for the year 1986 and 2001 using Landsat images. The supervised and the unsupervised classification techniques were particularly chosen for evaluation because of its simplicity and effectiveness in this particular situation where data was a limiting factor in the implementation of more sophisticated technique such as knowledge-based systems, hierarchical processing, artificial neural network analysis, and or Object Oriented Image Analysis.

3.2 Materials and methods

3.2.1 Ground truth data acquisition

The ground truth data collection campaign was done between July and September 2009 and was mainly aimed at qualitative information gathering concerning the land cover and few geographic positions of land covers such as forest, agriculture, range land, wetland, grass

land and water that were expected not to have changed between 2001 and 2009. The ground truth data were few and were used in the validation phase.

Considering the difficulties in ground truth data acquisition, which is typical in many other studies in Africa, where dataset for training and evaluation of supervised classification procedures are difficult to collect or are scarcely available, a procedure based on spatial and temporal pattern analysis were developed to collect training dataset for supervised classification. The spatial pattern recognition using relationships of pixels and its surrounding e.g. proximity, feature size, shapes, textures and repetition were used in identifying different land cover pattern and in collecting training pixels. The temporal pattern recognition was applied to aid in distinguishing between agricultural land cover, which would appear similar to grass land during dry season. Images taken in dry and wet seasons were analyzed to determine pattern in vegetation changes. Nonagricultural land cover was expected to have high vegetation density in wet months. Similarly, in the dry season only coniferous trees and vegetation in wetland and or areas with high water table would exhibit high reflectance values in the near-infrared region due to their chlorophyll content, diversely from deciduous trees and grasses.

3.2.2 Landsat data acquisition

Landsat 7 and 5 images covering Row 58 and Path 171 and 172, were downloaded from the achieved data site http://edcsns17.cr.usgs.gov/EarthExplorer. The technical characteristic of TM and ETM sensors can be found at http://landsat.usgs.gov/tools_project_documents.php. Both images (1986 and 2001) were 100% cloud free. 2000 image was acquired in wet seasons and was used in temporal pattern recognition.

3.2.3 Image processing

Landsat images distributed after December 23 2003 are already orthorectified. Products include Landsat Enhanced Thematic Mapper (ETM) +, Pansharpened ETM+, and Thematic Mapper (TM) data from Landsat 4, 5 and 7 missions. Only bands 1 to 7 of Landsat 7 images were processed for use. The panchromatic band with low spectral resolution was considered not be very useful in discriminating different vegetation types. The level of the image rectification by USGS (UTM-WGS84 grid) was considered satisfactory for the present study. Atmospheric correction of the images was carried out by using the ATCOR 9.3 algorithm,

embedded in ERDAS IMAGINE software, which also incorporate haze reduction and topographic effects.

3.2.4 Classification schemes

The purpose of land cover classification scheme is to provide a framework for organizing and categorizing the information that can be extracted from the data (Jensen et al., 1983). There are several land cover classification systems e.g. FAO land cover classification scheme (LCCS), UNESCO and the United State Geological survey land use classification scheme. In this study, U.S. Geological Survey Land Use/Land Cover Classification systems/scheme according to Anderson et al. (1976) was adopted. By using this scheme, 8 land cover classes were carefully selected and defined as follows: Agricultural land, Range land herbaceous (semi-arid range), Range land grass, Range land brush, Forest mixed, wetland mixed, Ponds/reservoir and Urban/settlement (Table 3.1).

Table 3.1: Land cover classification scheme

Land cover class	Description
Agricultural land	Cropland, with mixed settlement, horticultural areas, and fallow agricultural
Range land	Herbaceous, shrubs/brush and mixed range land
Forest land	Deciduous, evergreen and mixed forest land
Wetland	Forested and non-forested
Water	Stream and canal, lakes, and reservoirs
Settlement	Residential, with mixed settlement, urban or built-up land

3.2.5 Image classification

1. Supervised image classification techniques

The accuracy of supervised classification depends on the representativeness of the signatures obtained from the training data (Lillesand & Kiefer, 1987). In this study, the training data were collected using pattern recognition in the images. The process of collecting the training data was well spatially managed to give maximum representation of the land cover of interest. The adoption of this method proved more robust in collection of training data than the ground truth campaigns, which are normally limited by accessibility factor.

Signature samples for training were extracted using area of interest (AOI) and or seed growing properties. For more homogenous area, AOI was used to extract the signature

samples. This method provides quicker way of extracting signatures sample. The AOI tool was used to create polygons around homogenous land cover, which define the training areas. Seed growing at inquire cursor was used for less homogenous areas. In this procedure, polygons/regions based on spectral similarities were created. Geographic Constraints and spectral Euclidean distance were used to constrain the growth of the polygon within the mean of the seed pixel.

Fifteen or more signature clusters were identified for each land cover type, except for water and forest, due to their limited extent. If the same information class appears different in two or more locations e.g. in semi-arid environment and humid tropical environment, training signature were collected separately for each site and the final information classes merged later after classification.

The extracted signatures were evaluated using histogram techniques (Figure 3.1a & b). The histogram plot for each training set 'signature' was scrutinized by looking at the frequency or distribution of pixels that have each data value. Acceptable signatures were expected to exhibit a "unimodal" distribution in each band (Figure 3.1 (a) and (b)). The rejected signature (training pixels) were then later merged or deleted and replaced with training pixels that accurately represent the classes to be identified. Maximum likelihood classifier because of its robustness (Richards, 1993), was used.

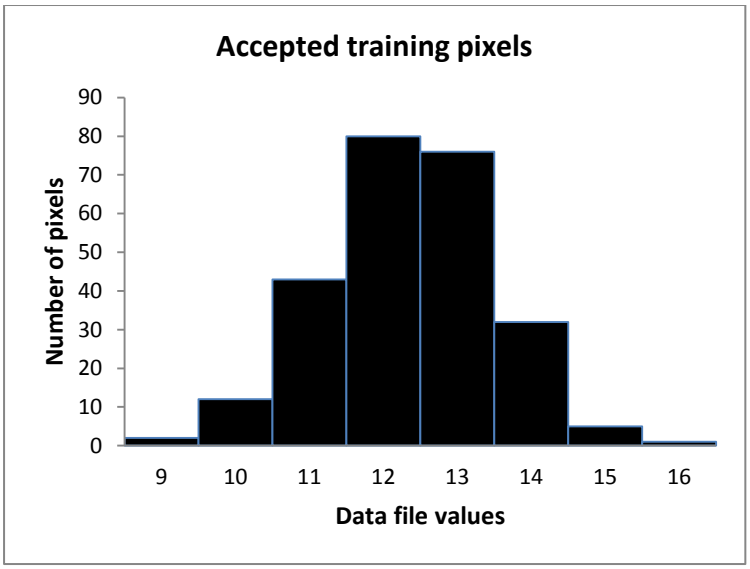

Figure 3.1(a): Histogram of accepted training pixels picked as the training region for forest land cover

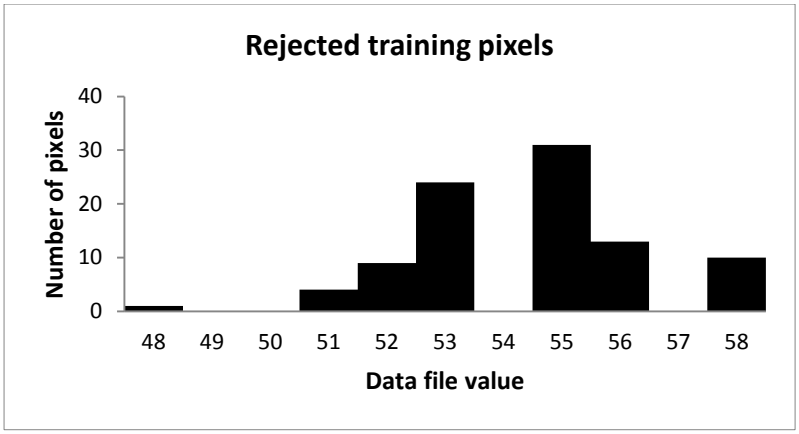

Figure 3.1 (b): Histogram of rejected training pixels picked as the training region for forest land cover

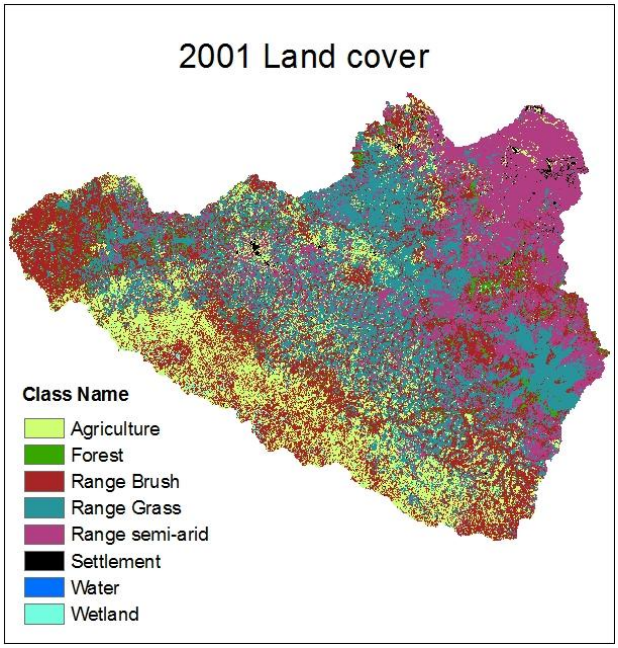

Figure 3.2: Land cover derived from supervised classification

2. Unsupervised image classification

Several unsupervised classification algorithms are available for use in remote sensing image classification software. The two most frequently used algorithms are the K-mean and the ISODATA clustering algorithm. Both of these algorithms are iterative procedures. In general, both of them assign first an arbitrary initial cluster vector and classify each of the pixels to the closest cluster. The algorithms next calculate the mean vector for the new cluster based on all the pixels in one cluster. These processes are repeated until the change between the iteration is small. The change can be defined in several different ways; either by measuring the distances the mean cluster vector has changed between successive iteration, or by the percentage of pixels that have changed between iterations.

The ISODATA algorithm has some further refinements by splitting and merging of clusters (Jensen, 1996). Clusters are merged if either the number of members (pixels) in a cluster is less than a certain threshold or if the centers of two clusters are closer than a certain threshold. Clusters are split into two different clusters if the cluster standard deviation exceeds a predefined value and the number of members (pixels) is twice the threshold for the minimum number of members.

The requirement for unsupervised image classification is minimal. However, the task of interpreting the classes that are created by means of clustering techniques is quite a demanding one. According to the parameters specified for each clustering process, the resulting cluster can later be merged, disregarded, otherwise manipulated, or used as the basis for defining a spectral signature. The unsupervised classification package in ERDAS is based on the Iterative Self-Organizing Data Analysis Technique (ISODATA), firstly developed by Tou and Gonzalez (1974). The clustering technique uses spectral distance as in the sequential method, but iteratively classifies the pixels, redefines the criteria for each class, and classifies again, so that the spectral distance patterns in the data gradually emerge.

In this study, the ISODATA clustering was performed and the numbers of clusters were varied from 15 to 20. Using more than 20 clusters resulted into redundant unrecognized spectral classes. Using both spatial and temporal pattern recognition as described earlier, land use classes were attached to the different clusters. The classes were then later recorded and filtered using majority filter with 3x3 moving windows.

The land cover map produced as the result of unsupervised classification is shown in figure 3.3. The method was unable to classify water. This resulted into seven land cover classes instead of eight as was obtained with the supervised image classification. The spectral characteristics of water appeared similar to dry grass land according to this method.

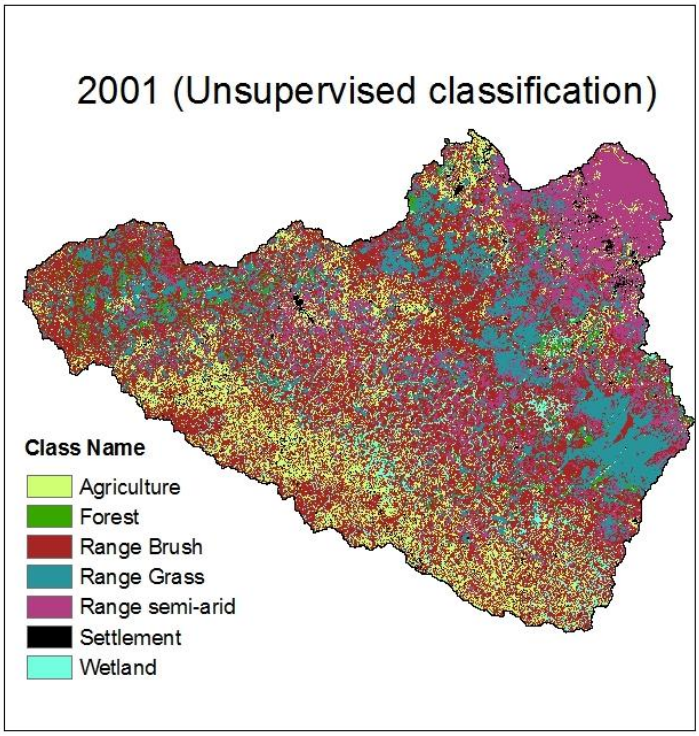

Figure 3.3: Land cover derived from unsupervised classification

3.3 Results and discussion

3.3.1 Evaluation of the classification techniques

To validate the classification procedures described above, accuracy assessment were conducted using ground truth data obtained independently of the training data except for water. The accuracy reports were generated and the summary of the classification accuracy is presented in table 3.2 for supervised image classification and table 3.4 for unsupervised image classification.

The overall classification accuracy for supervised classification was obtained as 81.48%, with the Kappa coefficient expressing the proportionate reduction in error generated by a classification process as 0.782 (Congalton 1991).

The accuracy report reveals that, supervised classification was able to accurately classify water, forest and wetland (Table 3.2). This could partly be due to the homogeneity of the spectral properties of these land cover types. With the image acquired in dry season, wetland vegetations are distinctly bright with unique spectral signatures. This is similar to coniferous forest. The classification accuracy assessment for water was biased because the same dataset

used in training was used in validation. This was because of limited access to many water points whose dataset could be divided between training and validation.

Table 3.2: Accuracy report generated from supervised classification and ground truth data

Class Name	Reference Totals	Classified Totals	Number Correct	Producers Accuracy	Users Accuracy
Agriculture	7	8	6	85.71%	75.00%
Settlement	2	2	2	100.00%	100.00%
Forest	4	3	3	75.00%	100.00%
Grass land	3	2	1	33.33%	50.00%
Grass land semi arid	1	1	1	100.00%	100.00%
Range brush	4	4	4	100.00%	100.00%
Wetland	2	3	2	100.00%	66.67%
Water	1	1	1	100.00%	100.00%
Overall Classification Accuracy = 81.48% KAPPA (K^) STATISTICS Overall Kappa Statistics = 0.7816					

Considering that, the ground truth data were few and very likely to compromise the accuracy report, 500 additional random points were generated and reference values to these point assigned using expert knowledge of the land cover categories. Using this new set of data, error matrix presented in Table 2.4, was generated. The error matrix indicates that the accuracy and the reliability of supervised classification can be considered good. It however showed that the main confusion occurred in discriminating settlement from agricultural land and settlement from semi-arid grass land. This is mainly due to mixed settlements within the farmsteads which are normally smaller in size compared to farmland and due to bare soil exposed in semi-arid grass during dry season.

The accuracy report using random points, showed a general improvement in the classification accuracy, however with discrepancies in individual classification accuracy most notably settlement and semi-arid range (Table 3.3).

The error matrix report also showed misclassification between grass land semi-arid and settlement. The satisfactory classification of forest, wetland and grass land can be explained by their unique signatures presented during the dry season. Similarly, water bodies present unique signatures within the study area and its classification reliability and accuracy was excellent.

Table 3.3: Error matrix of the supervised classification of 2001 Landsat image using random points

Classified Data	Agriculture	Settlement	Forest	Grass land	Semi-arid range	Range brush	Wetland	Water	Row Total	Accuracy
Agriculture	71	6	0	4	0	1	0	0	82	0.87
Settlement	0	4	0	0	4	0	0	0	8	0.50
Forest	0	0	9	0	0	0	0	0	9	1.00
Grass land	7	0	0	92	1	0	0	0	100	0.92
Semi-arid range	1	8	0	7	44	0	0	0	60	0.73
Range brush	0	0	0	9	1	71	4	0	85	0.84
Wetland	0	0	2	0	0	1	8	0	11	0.73
Water	0	0	0	0	0	0	0	1	1	1.00
Column Total	80	18	11	112	50	73	12	1		
Reliability	0.89	0.22	0.82	0.82	0.88	0.97	0.67	1.00		

Table 3.4: An Error matrix generated from unsupervised classification and ground truth data

Class Name	Reference Totals	Classified Totals	Number Correct	Producers Accuracy	Users Accuracy
Agriculture	5	2	2	40.00%	100.00%
Settlement	5	5	3	60.00%	60.00%
Forest	4	3	3	75.00%	100.00%
Grass land	2	3	2	100.00%	66.67%
Grass land semi arid	3	3	3	100.00%	100.00%
Range brush	3	5	3	100.00%	60.00%
Wetland	3	3	2	66.67%	66.67%
Overall Classification Accuracy = 70.37% KAPPA (K^) STATISTICS Overall Kappa Statistics = 0.6609					

For unsupervised image classification, validation was also done using the same validation dataset as for the supervised classification. The accuracy report is presented in table 3.4. The overall classification accuracy for unsupervised classification was obtained as 70.37% and the Kappa coefficient is 0.6609.

Detail accuracy report showed low classification accuracy for settlement (60%), agricultural land (40.0%) and forest cover (75%). In particular, there was high confusion between settlement and bare soil (semi-arid range). This resulted into delineation of "fault settlement", which is extensive in the extreme north east of the study area, which in the actual sense is dry semi-arid range, left bare due to intensive grazing.

3.3.2 Quantification of the land use change

1986 land cover map (figure 3.4) was later derived using supervised classification techniques. The land cover map was derived with overall classification accuracy of 80.96%. The two thematic land cover maps (1986 and 2001) were then analyzed for extent and percentage change in land use using ArcGIS.

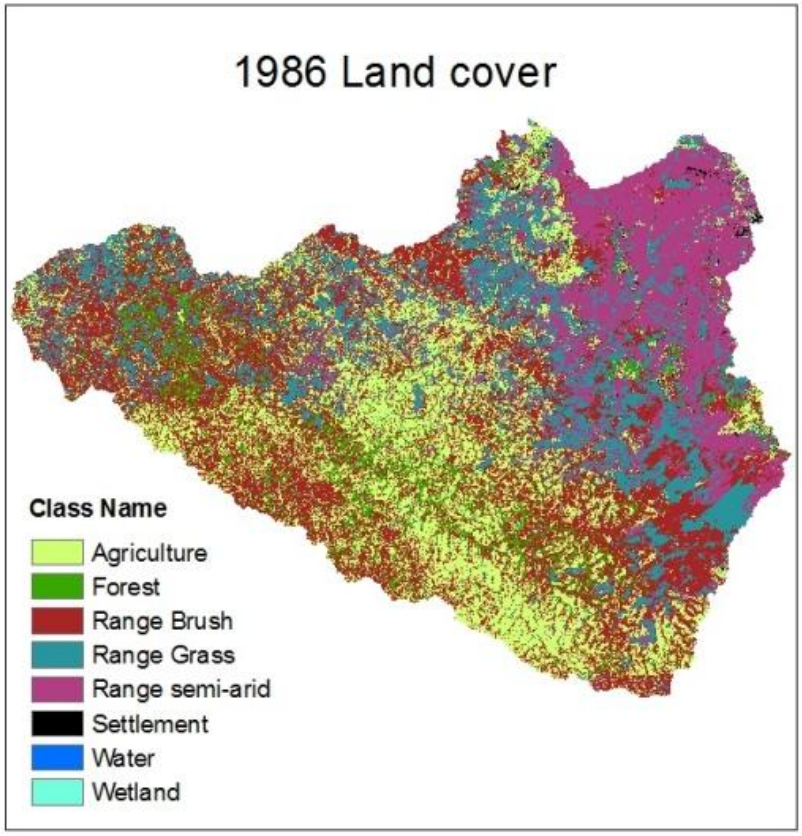

Figure 3.4: 1986 land cover maps derived using supervised classification

The analysis is presented in Table 3.5. The table shows the percentage coverage of different land use category in the different time periods (1986 and 2001) and also the percentage change in the land cover between the two periods. The results indicate a decrease in agricultural land cover by 6.4%, a decrease in forest land cover by 3.4%, an increase in settlement by 0.3% and regeneration of grass land, wetland and shrubs. The decrease in agricultural land cover, which is mainly seen in the upper north of the basin (Figure 3.2), can be attributed to the civil war, which lasted for over 20 years starting from 1986. The war caused displacement of many households to concentrated camps and farm land were lost. The agricultural activities were barely minimal, mainly along the roads and in the areas less affected by the war (southwest of the basin).

The increase in settlement can be due to the creation of the concentrated settlement together and the emergence of new town centers (e.g. Pader). Before the civil war, all settlement were scattered in small units within farmstead, which are visually difficult to recognize (Figure 3.4). The resettlement of the internally displaced persons, which started in 2008, is expected to change the agricultural land use trend far more beyond the 1986 scenario, due to many factors but mainly population increase and government incentives toward commercializing agriculture.

The decrease in forest land cover is a national concern and is due to mainly increase in demand for construction materials (timbers) and fuel. The entire population in the area derived their energy source for cooking from the forest product and this in the last few years has been the main cause of loss of forest biomass. The analysis of land use change also shows regeneration of range lands, which were part of farmland before the war, and also regeneration of wetlands. Before 1986, during the dry seasons, wetlands cultivation and grazing animals in wetland were common practices. And this could explain the different in wetland coverage between 1986 and 2001, with 2001 scenario indicating regeneration of wetlands. Wetland degradation however, still remains, with most wetland being cultivated during dry season and wetland vegetation used in craft work.

Table 3.5: Land use change between 1986 and 2001

Land cover category	Percentage coverage		Percentage change
	1986	2001	
Agriculture	23.4	17.0	-6.4
Settlement	0.3	0.6	+0.3
Forest	5.6	2.2	-3.4
Range Grass	17.8	28.1	+10.3
Range semi-arid	17.1	21.8	+4.7
Range Brush	35.3	29.2	-6.0
Wetland	0.4	1.1	+0.7
Water	0.0	0.0	0.0
(+) Increase and (–) Decrease			

3.4 Summary and conclusion

The spectral based supervised image classification techniques proved to be more superior to unsupervised image classification in classification of mixed rural land cover in Aswa basin, with accuracy of 81.48% and 70.37% and Kappa statistics of 0.7816 and 0.6609

respectively. In particularly, the spectrally based supervised image classification technique has proved to be indispensable especially where limited information is available.

In this study, the unsupervised image classification was unable to distinguish differences in phenological development of land covers in the study area, which showed high level of heterogeneity due to differences in climate and soil. In the case of supervised image classification, the application of pattern recognition in discriminating various land cover made it possible to distinguish the differences in land cover development. The land covers were clustered based on revelation of spatial and temporal pattern, which resulted into better extraction of training dataset and better classification accuracy. The same approach could therefore be applied in a similar way in other study areas where ground truth data are not easy to collect or are not easily available.

Chapter 4

4. Land use scenarios modeling. An Integrated approach of multi-criteria analysis and GIS

The objective of this chapter was to develop a GIS-Multi-criteria methodology to simulate experimental land use for use in the study of hydrologic impact of land use changes in the study area. Land use scenarios simulated were time-independent hence were not meant to prediction future land use pattern, but rather to aid spatial planning of future land use for sustainable management of land and water resources. The scenarios were developed using simplified and consistent set of assumptions based on biophysical parameters and socio-economic factors considered to be driving land use change in the study area. The GIS based multi-criteria approach was in particularly used because of its flexibility in allocating land to potential uses during planning.

4.1 Literatures reviewed

4.1.1 Modeling land use change

Land use change are characterized by the complex interaction of behavioural and structural factors associated with demand, technological capacity, and social relations, which affect both demand and environmental capacity, as well as the nature of the environment in question (Verburg et al., 2004). Numerous modeling approaches to simulate land use change pattern have been developed. Briassoulis (2000) presents an extensive review of land use theories and modeling approaches. In his review, he noted two major approaches; the top-down approach (Verburg et al., 2002) and bottom-up approach (Parker et al., 2002). The top-down approach uses an empirical, mathematical, statistical or econometric equation to describe the transitions among land use states. Different top-down land use modeling approach in literatures are: CLUE (Veldkamp and Fresco, 1996; Verburg et al., 1999), CLUE-s (Verburg et al., 2002), and Dinamica (Soares-Filho et al., 2002). The modeling approach is made up of three parts: demand change sub-model, a transition potential sub-model, and a change allocation sub-model.

The demand sub-model calculates the rate and magnitude of change, usually based on economic model, trend analysis, or scenario analysis to quantify the change (or demand). This demand is then allocated in a spatially explicit grid by the change allocation. This sub-model uses suitability (or change transition potential) maps representing the suitability/or potential for change of each cell for a given land use/or transition. This map is produced by the transition potential sub-model, given a set of input driving factors and a method to relate these maps as a multivariate statistical relation. Then, the change allocation produces a new land use map that can be used to next model iteration.

The bottom-up models describe explicitly the factors of land changes as heterogeneous and variable factors in time and space. This approach uses agent-based modeling theory, which consists of autonomous agents of an environment where the agents interact and the rules that define the relations between agents and their environment (Parker et al., 2002).

To be able to simulate land use scenarios, Parker et al., (2002) observed that these models require social-economic indicators, land use policies indicators and biophysical land use parameters. In practice however, despite being highly credible, high data requirement limits the application of these model. In Uganda, social-economic and land policies indicators are not readily available, limiting the application of complex land use change models. And yet knowing the land use change pattern is such an important aspect in planning and management of land and water resources in the country. Recently, there have been attempts to use GIS to model site suitability and use the suitability map as a guide to subsequent allocation of land to potential uses (Jones et al. 1995; Campbell et al. 1992; Carver 1991; Diamond and Wright 1988). The GIS capabilities for supporting spatial decisions (Malczweski, 1999), offers a unique opportunities to spatial land use allocation and configuration, which this study seek to explore in developing land use change pattern. GIS based land use change model also offer great flexibility to spatial configuration of land cover change, by presenting flexibility to weights assignment to different factors that control transformation of land from its state to another state.

4.1.2 GIS and Decision support

Decision-making is a process of choosing among alternative courses of action in order to attain goals and objectives. Reaching a decision ordinarily involve making trade-offs among the objectives relating to a decision (a difficult and poorly understood aspect of decision-

making, Simon, 1960). Decisions become difficult when they involve several competing objectives. The greater the number of objectives, the more complex the decision making process. In such a complex decision making environment, optimization is a typical approach to identify the best solution for a given decision problem (Wilson, et al., 1981; Thomas & Huggett, 1980). Optimization method often seeks to find the best (maximum or minimum) solution to a well-defined management problem. In the most general term, optimization model can be defined as:

- Minimize or maximize f(x) 4.1
- Subject to $x \in X$

where f(x) is the criterion function/objective function, x is a set of decision variables and X is a set of feasible alternatives. In addition, optimization problems have typically a set of constraints imposed on the decision variables. The constraints define the set of feasible solution/alternatives.

If the optimization problem involves a single criterion function, the problem is referred as a single criterion decision, however, if more than one criterion function is involved, the process is called multicriteria decision analysis.

At present, the contribution of GIS to optimization technique is largely as a method to data gathering and visualization of the results (Malczewski, 1999). However, GIS and optimization method can be fully integrated to provide a powerful tool for spatial decision support. GIS can be fully involved in decision making process according to Malczewski, (1999). Simon, (1960) introduced three phases of decision making process; intelligent phase, design phase and choice. In the intelligent phase of decision process, in which the decision environment are searched for condition that calls for decision (problem definition process), GIS offer a unique opportunity to tackle problems associated with data collection and analysis more efficiently and effectively. The data acquisition, storage, retrieval and management, convert real world decision situation to GIS database (Malczewski, 1999).

In the design phase, possible solution or alternative course of action are developed. The capabilities of GIS for generating a set of alternative decisions are based primarily on the spatial relationship, principles of connectivity, contiguity, and overlay (Malczewski, 1999). As we shall see in the next section in this chapter, GIS can be used to build the elements of

spatial multicriteria decision analysis, that is criterion maps and alternative decision and integrate the input data required for multicriteria decision making.

In making preference (choice), GIS capability is limited; however, the integration of multicriteria decision making process and GIS provides a platform for incorporating preference in to GIS procedures.

4.1.3 Multi-Criteria decision making process

Multi-Criteria Analysis (MCDM) is a decision-making tool developed for complex problems. In a situation where multiple criteria are involved confusion can arise if a logical, well-structured decision-making process is not followed. There are two types of criteria that support decision-making process, constraints and factors. These criteria represent conditions possible to be quantified and contributes to the decision making (Eastman et al., 1993). Constraints are based on the Boolean criteria (true/false), which limit the analyses to specific regions. Factors are criteria, which define some degree of suitability for all the geographic regions. They define areas or alternatives according to a continuous measure of suitability, enhancing or diminishing the importance of an alternative under consideration in the geographic space resulting after the exclusion of the areas defined by the restrictions.

MCDM problem can be structured using a number of approaches (Keeney and Raiffa, 1976; Saaty, 1980; Chankong and Haimes 1983). One such approach, which has been widely used, is the Analytic Hierarchy Process (AHP). AHP is well documented in many literatures (Mendoza 1997; Saaty 1980,1995; Kangas 1992,1993; Peterson et al. 1994; Reynolds and Holsten 1994; Pukkala and Kangas 1996) and its applications to GIS based multi-criteria analysis are reported in Banai-Kashani (1989); Eastman et al. (1992, 1993); and Xiang and Whitley (1994).

4.1.4 The Analytical Hierarchy Process (AHP) and principles

The analytic hierarchy process (AHP), developed by Saaty, (1970) allows decision makers to model a complex problem in a hierarchical structure showing the relationships of the goal, objectives (criteria), sub-objectives, and alternatives.

AHP logic hierarchical structure formulation involves six steps: (a) setting goals to be achieved, (b) decision makers creating preference, (c) formulating sets of evaluation criteria,

(d) formulating sets of decision alternatives or action variables, (e) formulating sets of uncontrollable variables or states of nature and (f) formulating sets of outcomes or consequences associated with each alternatives. Most crucial in these steps are formulating sets of evaluation criteria, decision alternative and state of nature (Figure 4.1).

The construction of judgment matrices based on pair-wise comparison of all elements in each hierarchy with respect to the higher hierarchy is done according to certain criteria of comparison within certain scales. In this study, the scales of relative importance given by (Saaty, 1983) presented in table 4.1 were used.

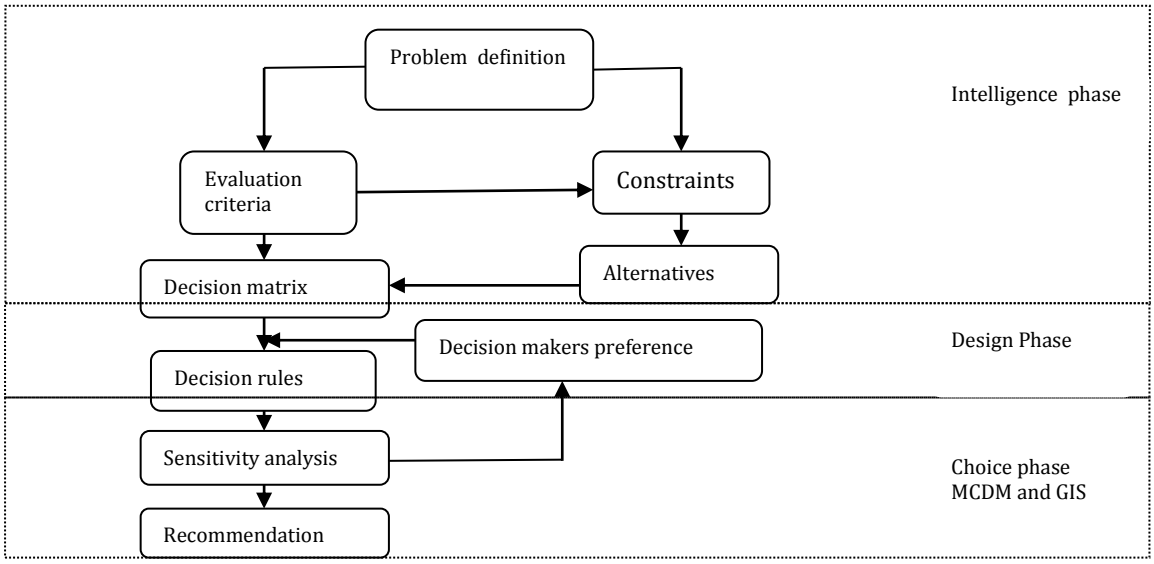

Figure 4.1: Framework for spatial Multi-criteria decision analysis, adopted from Malczewski, (1999)

Table 4.1: Scale of relative importance

Intensity of importance	Definition	Explanation
1	Equal importance	Two activities contribute equally to the objective
3	Moderate importance of one over the other	One is slightly in favour over another
5	Essential or strong	One is strongly in favour over another
7	Very strong importance	One is strongly favoured and its dominance is demonstrated in practice
9	Absolute importance	The evidence favouring one over another is of the highest possible order of affirmation
2,4,6 & 8	Intermediate values	When compromise is needed between the two adjacent judgments
Reciprocal of the above numbers	If activity *i* has one of the above numbers assigned to it when compared with activity *j* , then *j* has the reciprocal value when compared to *i*	

The principles of the AHP are based on: decomposition, comparative judgments, and hierarchic composition or synthesis of priorities (Saaty, 1994). The principle of comparative judgments is applied to construct pair-wise comparisons of all combinations of elements in a cluster. These pair-wise comparisons are used to derive priorities of the elements in a cluster with respect to the other. The principle of hierarchic composition or synthesis is applied to multiply the local priorities of elements in a cluster by the 'global' priority, producing global priorities throughout the hierarchy and then adding the global priorities for the lowest level elements (the alternatives).

There are four relatively simple axioms used in AHP used in formulation of pairwise matrix. The first axiom, the reciprocal axiom, requires that, if $^{A}/_{B}$ is a paired comparison of elements A and B, representing how many times more the element A possesses a property than does element B, then $^{B}/_{A} = \frac{1}{^{A}/_{B}}$. In other words, if A is three times larger than B, then B is one third as large as A.

The second axioms, or homogeneity axiom, states that the elements being compared should not differ by too much, else there will tend to be larger errors in judgment. When constructing a hierarchy of objectives, one should attempt to arrange elements in a cluster so that they do not differ by more than an order of magnitude. The AHP verbal scale ranges from 1 to 9 (Table 4.1), or about an order of magnitude. Judgments beyond an order of magnitude generally result in a decrease in accuracy and increase in inconsistency.

The third axiom states that judgments about, or the priorities of, the elements in a hierarchy do not depend on lower level elements. This axiom is required for the principle of hierarchic composition to apply. The axiom requires careful examination, as it is not uncommon for it to be violated. The important rule of thumb is to make judgments in a hierarchy from the bottom up, unless one is sure that there is no feedback, or one already has a good understanding of the alternatives and their tradeoffs.

The fourth axiom, introduced by Saaty, says that individuals who have reasons for their beliefs should make sure that their ideas are adequately represented for the outcome to match these expectations. While this axiom might sound a bit vague, it is very important because the generality of AHP makes it possible to apply AHP in a variety of ways and adherence to this axiom prevents applying AHP in inappropriate ways.

4.2 Methodology

4.2.1 Problem definition: - decision making on allocation of land to Agriculture and Forest

Determining suitable land for a particular use is a complex process involving multiple decisions that relates to biophysical, socio-economic and institutional organizational aspects. In general, land suitability analysis is a decision problem involving several factors. The decision problem in this study is to find the best spatial allocation of land to future agriculture and forest development, considered as the most touchy land use issues in the near future.

The overall land suitability for land use was evaluated using a set of independent biophysical land use parameters and socio-economic parameters, which limits land use potentials. The biophysical parameters used in this study are: relief, climate, vegetation cover, and water availability. And the socio-economic parameters used are accessibility and population. It was assumed that the general economic environment such as gross domestic product (GDP) share of agriculture, forestry and industrial, share in employment e.g. agriculture, forestry, industry and others and market development especially in agriculture and forestry are all influenced mainly by population, which provides for example market force and labours and by the biophysical parameters such as climate, topography, soil characteristics and water availability, which are fundamentals to land productivity. The words parameters and factors are used synonymously in this chapter.

All these parameters were presented as map layers. The map layers/criterion or the attribute maps were used as input data to the spatial multi-criteria decision analysis. Digital elevation model (DEM) derived from Shuttle Radar Topographic Mission (SRTM) at a resolution of 30 arcs second was used to prepare relief map layer. Normalized Difference Vegetation Index (NDVI) derived from Landsat 7 image of 2001, was used as the vegetation density layer. NDVI was also used as a measure of soil fertility, since the information on soil fertility was hardly available. Stream network in the study area was generated from the DEM using minimum drainage area of 4000 hectors. Distance to settlements and major roads were used as accessibility layers. Major roads and settlements were digitized from 2001 Landsat 7 image using ArcGIS onscreen digitizer. 2002 population was used to create population density map. And the rainfall map was generated using point measurements from over 40 gauges located within and outside the study area. Annual averages (using 20 years) of

rainfall records at each gauge were interpolated using Kriging interpolation technique in ArcGIS to generate rainfall map.

4.2.2 Objective setting 1: - allocation to Forest

The overall goal of land allocation to forest was considered as increase in wood production, with the objectives of providing environmental protection such as soil erosion control, soil degradation control and windbreak and to provide economic benefit such as production of timber and fuel. Factors that were used to define the degree of suitability for allocation of land to forest are: Normalized Difference Vegetation Index (NDVI), elevation, population density, rainfall, and settlement. The criteria are that, land to be allocated to forest should have minimum vegetation cover, which is in line with environmental protection; should not be in wetland or low land (elevation above 900 meters); should be in area of low population density, should be in area receiving adequate rainfall, and should not be near settlement. The constraints are; existing forest land cover cannot be allocated to forest, since it already forested, developed areas e.g. urban land cannot be allocated to forest and land covers with water cannot be allocated. The alternatives sites for allocation provide continuous measures of suitability in order of preference, with suitability 1 being most preferred allocation. To provides flexibility to land cover configuration, the study considered all alternatives generated as potentials allocation.

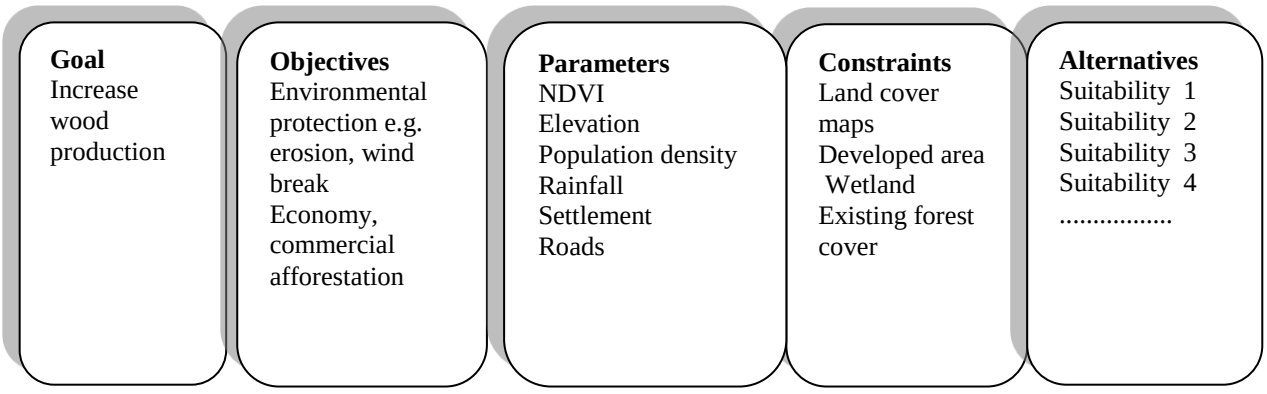

Figure 4.2: Summary of AHP structure for allocation of land to forest land use

4.2.3 Objective setting 2: - allocation to Agriculture

Maximization of agricultural production was considered the principal goal of land allocation to agriculture. The objectives are increasing productivity of land, increasing the scale of farming (commercial) and environmental protection such as controlling soil erosion

and soil degradation. Factors that were used to define the degree of suitability for allocation of land to agriculture are: Normalized Difference Vegetation Index (NDVI), population density, rainfall, settlement, road network and water sources. The criteria are: land to be allocated to agriculture should be fertile land. Due to limited information on land fertility, NDVI was used as a measure of fertility. The assumption made was that areas that are fertile will have very high NDVI. Other criteria are; land should be in area receiving adequate rainfall, should be accessible, that is close to roads and settlement and proximity to water source is highly preferred. The constraints used are; existing forest land cover cannot be allocated to agriculture, as a matter of environmental concern, developed areas e.g. urban land and wetland cannot be allocated to agriculture. The alternatives allocation provided continuous measures of suitability in order of preference, with suitability 1 being most preferred allocation. All the alternative allocations were considered during scenarios development to offer more flexibility to land cover configuration.

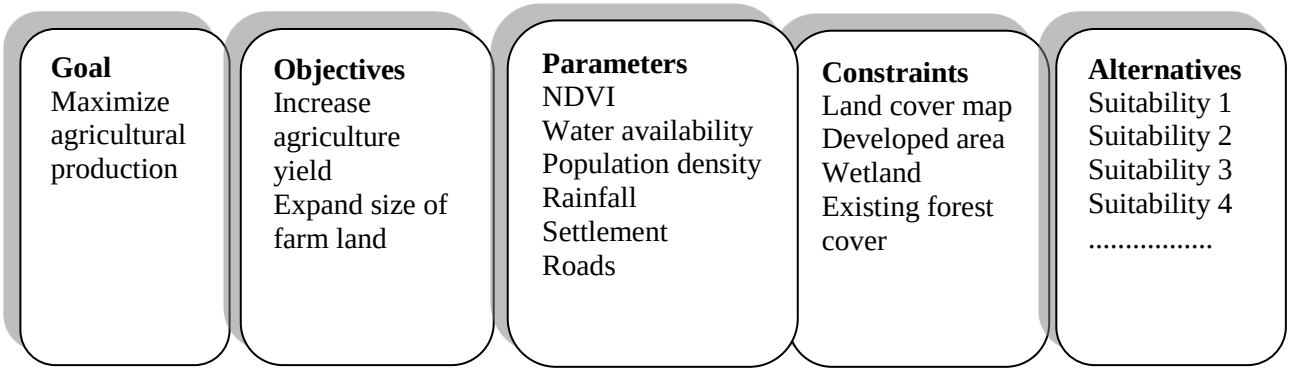

Figure 4.3: Summary of AHP structure for allocation of land to future agriculture land use

4.2.4 Criteria weighting

Central to production of land use change scenarios, is the land use related weighting factors. The weighting parameters influence the transition of a cell from one state (land use) to another state because of the proximity to the "decision cell." For example the present of a cell at a distance of 200 m from a "decision cell-road" is likely to encourage the conversion of the cell to agricultural land.

AHP methodology was used to determine the parameter weights. The scale of relative importance according to Saaty (Table 4.1) was used. The problem was decomposed by forming a pairwise comparison matrix $w_{i,j}$ with the number i_{th} row and j_{th} column giving the relative importance of the parameter F_i as compared with parameter F_j.

Typical judgment matrixes W (Figure 4.4) for the two criteria were used to derive the performance matrix; where $w_{i,j}$ is the performance value of the i^{th} alternative with respect to the j^{th}.

$$W_{i,j} = \begin{pmatrix} w_{11} & w_{12} & w_{13} & w_{14} & w_{15} & w_{16} & w_{17} \\ w_{21} & w_{22} & w_{23} & w_{24} & w_{25} & w_{26} & w_{27} \\ w_{31} & w_{32} & w_{33} & w_{34} & w_{35} & w_{36} & w_{37} \\ w_{41} & w_{42} & w_{43} & w_{44} & w_{45} & w_{46} & w_{47} \\ w_{51} & w_{52} & w_{53} & w_{54} & w_{55} & w_{56} & w_{57} \\ w_{61} & w_{62} & w_{63} & w_{64} & w_{65} & w_{66} & w_{67} \\ w_{71} & w_{72} & w_{73} & w_{74} & w_{75} & w_{76} & w_{77} \end{pmatrix}$$

Figure 4.4: The performance matrix

The scale of relative importance (1 signifying equal value to 9 signifying extreme different) was assigned to the 'pairwise parameter'. During the assignment of scale, the relationship $W_{j,i} = \frac{1}{W_{i,j}}$ was used to assign a scale to a reciprocal paired factor. The relationship means that $w_{21} = \frac{1}{W_{12}}$ and so on (Figure 4.4).

A synthesis was made on the scale by the process called 'normalisation'. The normalisation was done to obtain a 'global priorities' throughout the hierarchy. The normalisation process was achieved using equation 4.2.

$$X_{i,j} = \frac{w_{i,j}}{\sum_{i=1}^{n} w_{i,j}} \qquad 4.2$$

In Equation 4.2, the sum of the column matrix $w_{i,j}$ was used to divide each member in the column to yield normalised matrices. Through normalisation of the scale, AHP ensure that the weights are comparable for all factors.

The normalized vectors were used to compute the factor weight. The factor/parameter weight is the weight that shows the relative importance of the factor in making a decision. The factor weights were computed as the average values of each row using the expression in equation 4.3:

$$FW_{i,j} = \frac{\sum_{j=1}^{n} X_{i,j}}{n} \qquad 4.3$$

where n is the number of parameters. The resultant factor weights represent the eigenvalues of the normalized comparison matrix.

Analysis of consistency in weighting was finally carried to find if there was any inconsistency in the comparison matrix. Normally in the real world, it is hard to be perfectly consistent in the pairwise comparison. Always there must be some level of inconsistency. AHP allows inconsistency, but provides a measure of the inconsistency in each set of judgments. Saaty (1980) developed Random Inconsistency indices (RI) given in Table 4.5 and proposed the equation 4.4 as measure of consistency or degree of consistency and equation 4.5 to calculate the Consistency Ratio (CR), used as a measure of inconsistency. If the value of Consistency Ratio is smaller or equal to 10%, the inconsistency is acceptable or else the pair-wise comparison may be revised (Saaty, 1980).

Table 4.5: Random Consistency Index (RI)

N	1	2	3	4	5	6	7	8	9	10
RI	0	0	0.58	0.9	1.12	1.24	1.32	1.41	1.45	1.49

$$CI = \frac{\lambda - n}{n-1} \quad 4.4$$

$$CR = \frac{CI}{RI} \quad 4.5$$

$$\lambda_* = \sum_{i=1}^{n} X_{i,j} \times W_{i,j} \quad 4.6$$

λ is calculated by averaging the value of the Consistency Vector (λ_*)

The inconsistency was analyzed using the eigenvalues of the normalized comparison matrix, using the random consistency index (RI) and the set of equations provided in 4.4 to 4.6.

4.2.5 Integration of MCDM and GIS

GIS is a computer-based system that offers a convenient and powerful platform for performing land suitability analysis and allocation. The integration of multi-criteria methods of suitability assessments and allocation methods into a GIS system (Eastman et al., 1992 & 1993 and Xiang and Whitley, 1994) improves the spatial capabilities of GIS and the analytical power as a formal decision making tools.

The generic model of land use suitability can be conceptualised as:

$$S = f(x_1, x_2, x_3 \ldots \ldots x_n) \quad 4.7$$

where S is suitability measure and $x_1, x_2, x_3, \ldots\ldots\ldots\ldots\ldots x_n$ are factors affecting the suitability of the sites. The principal problem of suitability analysis is to measure both the individual and cumulative effects of the different factors. Integrating AHP and GIS provides a classical approach (the spatial multi-criteria decision process-MCDM) of doing this. The GIS based spatial MCDM uses weighted linear combination (WLC) to assess the suitability of grid cells by weighting and combining factor maps. WLC multiplies cell values in standardized factor maps by the corresponding factor weight, and then adds weighted values across images. WLC model according to Jiang and Eastman (2000) is described as:

$$S_k = \sum w_i x_{k,i} \qquad 4.8$$

Where, S_k is the suitability index for pixel/cell k; $x_{k,i}$ is the value criteria i for pixel k and $w_{k,i}$ is the factor weight. The factor weights $w_{k,1}\, w_{k,2} \ldots\ldots\ldots\ldots\ldots\ldots\ldots w_{k,n}$ reflect the relative importance of each criterion for a given pixel.

4.2.6 Suitability model development

The proposed integrated GIS-based model in this study provides more than site-specific and spatially explicit map of site suitability, but also uses the site suitability map to serve as a guide to subsequent allocation of land to potential uses. This allocation process was performed and implemented under a raster GIS environment. The discussion below outlines the methodology for land allocation under a raster-based GIS platform considering one land use at a time that is individual cells/pixels are allocated to a single land use given their land suitability values.

The weighted overlay tool provided in ArcGIS GIS in spatial analyst environment was used to solve equation 4.8. Before the overlay operation was done, the factor raster maps were all converted to an integer raster maps having the same 'common measurement scale'. The common measurement scale of 1 to 8 was adopted so as to match the land use map layer scale, which was classified to 8 classes. Reclassification tool was used to convert the floating raster maps to integer raster maps and to set the common measurement scale.

Each raster (parameter map) is assigned a percentage influence according to the weights derived in the MCDM procedures. In principle, the cell values of each parameter map are multiplied by their percentage influence, and the results are added together during overlay operation to create a unique output raster. Each input raster was weighted according to its

importance or its percent influence. The weight was a relative percentage, and the sum of the percentage influence weights for all the raster maps was equal to 100. By changing the "remap_assignment" evaluation scale value or the percentage influences, the results of the weighted overlay analysis changes.

Two models (output areas potentials for agricultural expansion & afforestation) were built using spatial analyst ModelBuilder to perform standardization of the factor maps (converting the floating raster to integer and setting the common measurement scale), overlay the maps and analyze the overlaid results. The structure of the model is shown in figure 4.6.

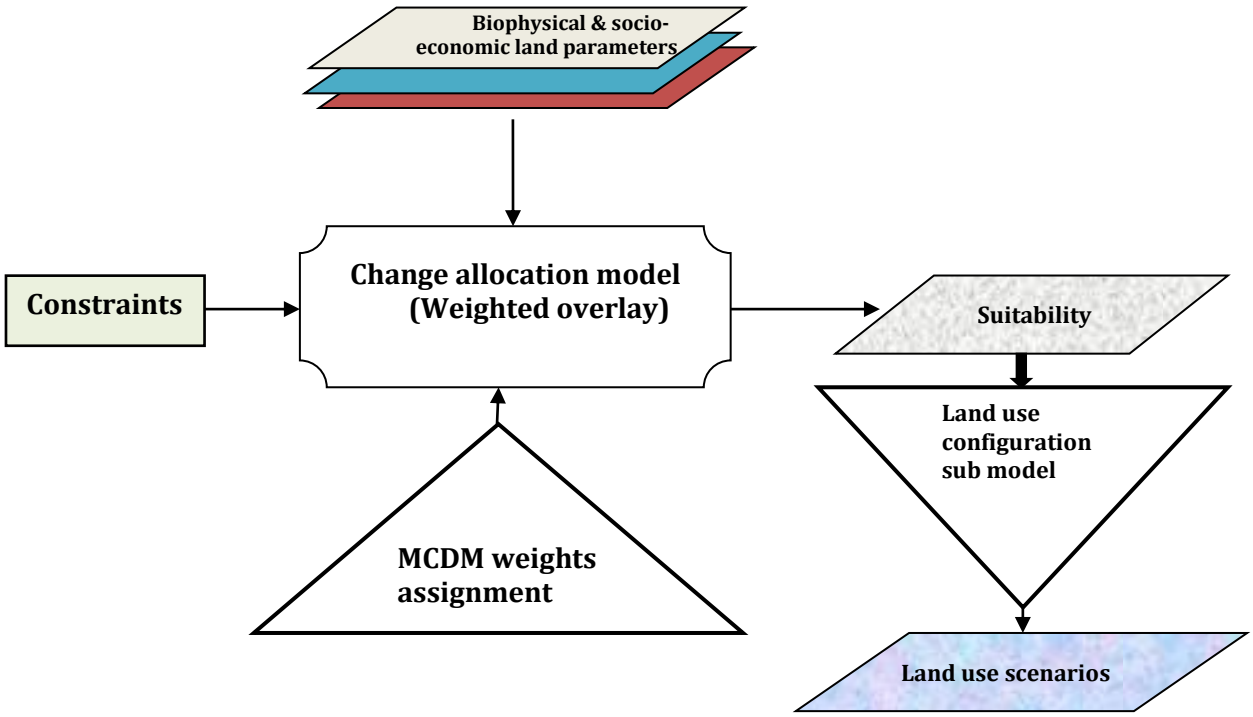

Figure 4.6: Structures of the GIS land use change model

The two models were built by stringing together inside a "ModelBiulder" windows the following sets of tools:

1. Euclidean Distance tools; was used to create Euclidean distance maps for roads, water points and settlements. Euclidean distance tool calculates for each cell the Euclidean distance to the closest source. Each distance tools was preceded by buffer tools. The buffer tool was used to create buffer polygons to a specified distance around the input feature.

2. Reclassification tools; was used to reclassify the distance map layers into the common measurement scale which was 1 to 8 and to convert the floating raster maps to integer raster maps.
3. Weighted overlay tool; was used to overlay all the input parameters as earlier described. The percentage influence derived earlier using the AHP were assigned to each raster map layers. The land use layer was used to set constraints to the suitability analysis process. Cells with values representing forest cover, developed areas and wetland were restricted for allocation by assigning NoData as the criteria for the cells.
4. Conditional tool "con" was used to de-aggregate the suitability map into "alternative suitability maps" for subsequent configuration and aggregation. The tool was used to perform the conditional if/else to evaluate input cells. Depending on the criteria, the tool extracts the cells/parcels of land that belong to particular level of suitability.

Table 4.7 summarises the allocation process. Alternative seven for agricultural allocation and six for forest allocation were excluded from the analysis. Alternative six in agricultural allocation was ignored since it was the least preferred site for allocation to agriculture, and presenting allocation extent similar to alternative three. Five alternatives from each land use experiments were finally considered in the final scenarios development (Table 4.7).

4.2.7 Spatial configuration of the suitability maps to generate a unique land use scenarios

The real problem in this study was spatial allocation of tracts of lands or sites into agricultural and forest land uses. This means, the site suitability maps generated using the overlay tools, must be aggregated together (site suitability for allocation to agriculture and forest) to obtain a unique land use scenarios. The land use suitability maps were just clustered parcels of land, with each cluster showing different level of suitability.

To capture the essence of the suitability level and the suitability alternatives on the final aggregation of the suitability maps to generate land use scenarios, table 4.7 was prepared. The table shows the configuration process during the aggregation of the alternative maps with the reference land cover maps. A1, A2 … A5, was used to denote alternative maps (parcels of land) for allocation to agriculture and F1, F2 … F5, was used to denote the alternative maps for forest allocation. The aggregation process uses simple expression; A1+F1+LC2001, executed using the Raster calculator. Where A1and F1 denotes alternative maps at suitability

level one for allocation to agriculture and forest respectively and LC2001 is the reference land cover, which was 2001 land cover map.

Table 4.7: Configuration process

Scenario I		Scenario II		Scenario III		Scenario IV		Scenario V		Scenario VI		Scenario VII		Scenario VIII		Scenario IX		Scenario X	
Alternatives	Competitive allocation	Alternatives	Competitive allocation	Alternatives	Competitive allocation	Alternatives	Competitive allocation	Alternatives	Competitive allocation	Alternatives	Competitive allocation	Alternatives	Competitive allocation	Alternatives	Competitive allocation	Alternatives	Competitive allocation	Alternatives	Competitive allocation
A1+F1	Agriculture	A1+F1	Forest	A2+F2	Agriculture	A2+F2	Forest	A3+F3	Agriculture	A3+F3	Forest	A4+F4	Agriculture	A4+F4	Forest	A5+F5	Agriculture	A5+F5	Forest

During the scenarios development, it was observed that overlapping pixels with values for agriculture, forest and the reference land cover would compete for allocation during aggregation, with the first pixel in the row overwriting the values of the other pixels. Since the main interest in the scenario development was to get all the parcels of land in each level of suitability allocated to either agriculture or forest respectively, each level of suitability were treated twice, with first treatment giving priority allocation to agriculture and second treatment giving priority allocation to forest. In the aggregation processes, unused land or land that was restricted for allocation were assigned pixels values of the reference land use. Natural forest covers were constrained from allocation as well as wetlands and settlement. Plantation forest (considered to be eucalyptus and pine) was given a new pixel value (land cover class of 9, while the native forest cover maintained the pixel value in the reference land use map.

The final land use scenarios that simultaneously consider all the individual sites suitability of mix forest and agriculture were in total ten.

4.3 Results and discussions

4.3.1 The multi-criteria analysis of the factors affecting land use allocation

The results presented in table 4.2 and 4.3 represent both the decomposition of the allocation problem (allocation to agriculture and forest) and the assignment of the scale of relative importance. The hierarchy in the tables shows the relative influence of each factor. In

allocating suitable land to forest, land use was considered as the most influential factor, and it come on top of the hierarchy while roads was considered to have the least influence and is put at the bottom (Table 4.2). In allocation of suitable land to agriculture, rainfall was considered the most influential and land use was the least influential (Table 4.3).

The values in each cell represent the scale of relative importance for the given paired factors. The diagonal has the value of 1 throughout because the diagonal represent factors being compared to itself, and the scale equal importance '1' is assigned. In the lower diagonal the values of the scale are in fractions because the factors are being paired in the reverse order and the scale of relative importance is given as the reciprocal of the upper diagonal pairwise comparisons.

Table 4.2: Weights of paired factors concerning allocation to forest

FACTOR	Land use	NDVI	Population	Rainfall	Settlement	Elevation	Road
Land use	1	3	5	7	1.5	7	9
NDVI	0.3	1	7	1.5	7	5	9
Population	0.20	0.1	1	2	1	2.5	3
Rainfall	0.14	0.7	0.50	1	5	7	9
Settlement	0.7	0.1	1	0.2	1	3	1
Elevation	0.14	0.20	0.40	0.14	0.33	1	5
Road	0.1	0.1	0.3	0.1	1.00	0.2	1
SUM	2.60	5.26	15.23	11.95	16.83	25.70	37.00

Table 4.3: Weights of paired factors concerning allocation to agriculture

CRITERIA	Rainfall	Road	Settlement	Population	Water	NDVI	Land use
Rainfall	1	9	7	5	3	2	1
Road	0.1	1	3	2	5	7	9
Settlement	0.14	0.3	1	7	1	2	9
Population	0.2	0.5	0.14	1	9	2	2
Water	0.3	0.2	1	0.1	1	1.5	7
NDVI	0.5	0.14	0.5	0.5	0.67	1	3
Land use	1	0.1	0.1	0.5	0.14	0.3	1
SUM	3.3	11.3	12.7	16.1	19.8	15.8	32

The judgment matrices for land allocation to agriculture and forest, extracted from table 4.2 and 4.3 respectively are presented as C_A and C_F.

$$C_F = \begin{pmatrix} 1 & 3 & 5 & 7 & 1.5 & 7 & 9 \\ 0.33 & 1 & 7 & 1.5 & 7 & 5 & 9 \\ 0.2 & 0.14 & 1 & 2 & 1 & 2.5 & 3 \\ 0.14 & 0.67 & 0.5 & 1 & 5 & 7 & 9 \\ 0.67 & 0.14 & 1 & 0.2 & 1 & 3 & 1 \\ 0.14 & 0.2 & 0.4 & 0.14 & 0.33 & 1 & 5 \\ 0.11 & 0.11 & 0.33 & 0.11 & 1 & 0.2 & 1 \end{pmatrix} \quad C_A = \begin{pmatrix} 1 & 9 & 7 & 5 & 3 & 2 & 1 \\ 0.1 & 1 & 3 & 2 & 5 & 7 & 9 \\ 0.14 & 0.3 & 1 & 7 & 1 & 2 & 9 \\ 0.2 & 0.5 & 0.14 & 1 & 9 & 2 & 2 \\ 0.3 & 0.2 & 1 & 0.1 & 1 & 1.5 & 7 \\ 0.5 & 0.14 & 0.5 & 0.5 & 0.67 & 1 & 3 \\ 1 & 0.1 & 0.1 & 0.5 & 0.14 & 0.3 & 1 \end{pmatrix}$$

Figure 4.5: The judgment matrices

The results of the normalized matrices are shown in matrix X_F and X_A, where X_F represent matrix for allocation to forest and X_A represent matrix for allocation to agriculture. The normalized matrix shows that there exist some inconsistencies during the decomposition and the pairwise comparison. The inconsistency is indicated by the values in the rows that are significantly larger than the rest. These values are underlined in the normalized matrix.

$$X_F = \begin{pmatrix} 0.39 & \underline{0.57} & \underline{0.33} & \underline{0.59} & 0.09 & 0.27 & 0.24 \\ 0.13 & 0.19 & \underline{0.46} & 0.13 & \underline{0.42} & 0.19 & 0.24 \\ 0.08 & 0.03 & 0.07 & 0.17 & 0.06 & 0.1 & 0.08 \\ 0.06 & 0.13 & 0.03 & 0.08 & 0.3 & 0.27 & 0.24 \\ 0.26 & 0.03 & 0.07 & 0.02 & 0.06 & 0.12 & 0.03 \\ 0.06 & 0.04 & 0.03 & 0.01 & 0.02 & 0.04 & 0.14 \\ 0.04 & 0.02 & 0.02 & 0.01 & 0.06 & 0.01 & 0.03 \end{pmatrix} \quad X_A \begin{pmatrix} 0.3 & \underline{0.8} & \underline{0.55} & 0.31 & 0.15 & 0.13 & 0.03 \\ 0.03 & 0.09 & 0.24 & 0.12 & 0.25 & \underline{0.44} & 0.28 \\ 0.04 & 0.03 & 0.08 & 0.43 & 0.05 & 0.13 & 0.28 \\ 0.06 & 0.04 & 0.01 & 0.06 & 0.45 & 0.13 & 0.06 \\ 0.1 & 0.02 & 0.08 & 0.01 & 0.05 & 0.09 & 0.22 \\ 0.15 & 0.01 & 0.04 & 0.03 & 0.03 & 0.06 & 0.09 \\ 0.3 & 0.01 & 0.01 & 0.03 & 0.01 & 0.02 & 0.03 \end{pmatrix}$$

Figure 4.6: Normalized judgment matrices

The final factor weights computed from the vector weight of the normalized matrix are shown in figure 4.7. In allocation of suitable land to forest, land use was given percentage influence of 35, followed by NDVI, with 25 percentage influence and least is road with 3 percentage influence. In the allocation of land to agriculture, rainfall had 32 percentage influence followed by roads with 21 percentage and least by land use which was given only 6 percentage influence as well as NDVI.

$$W_F = \begin{pmatrix} 35 \\ 25 \\ 8 \\ 16 \\ 8 \\ 5 \\ 3 \end{pmatrix} \begin{pmatrix} \text{Land use} \\ \text{NDVI} \\ \text{Population} \\ \text{Rainfall} \\ \text{Settlement} \\ \text{Elevation} \\ \text{Roads} \end{pmatrix} \quad W_A = \begin{pmatrix} 32 \\ 21 \\ 15 \\ 12 \\ 8 \\ 6 \\ 6 \end{pmatrix} \begin{pmatrix} \text{Rainfall} \\ \text{Road} \\ \text{Settlement} \\ \text{Population} \\ \text{Water} \\ \text{NDVI} \\ \text{Land use} \end{pmatrix}$$

Road

Figure 4.7: Factor weights

The result of the consistency analysis performed using the standardized matrix X and the factor weight W indicate that the Consistency Index (CI) for paired factors concerning allocation to forest land and agriculture were 0.006 (0.6%) and Consistency Ratio (CR) were 0.004 and 0.07 respectively, which were all smaller than 10% threshold proposed by Saaty (1980). The inconsistency made in the judgment was therefore accepted.

4.3.2 The GIS model

Figures 4.7 (a) & (b) show the model interfaces used in the modeling land use suitability for allocation to agriculture and forest respectively. The interface shown in figure 4.7(a) output areas potential for future rain-fed agriculture expansion using land use map, NDVI map, population density map, rainfall distribution map, distance to river and roads map and land use map as input.

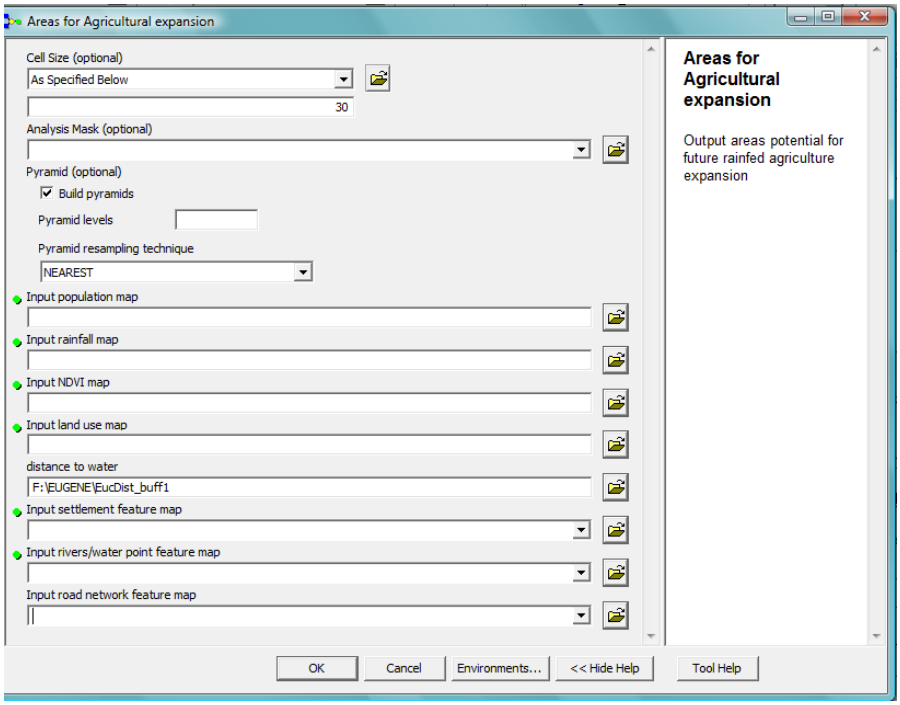

Figure 4.7 (a): Model interface for suitability analysis for allocation to agriculture

The interface shown in figure 4.7(b) output areas potential for future afforestation using land use map, NDVI map, population density map, rainfall distribution map, elevation map, distance to roads map and land use map as input.

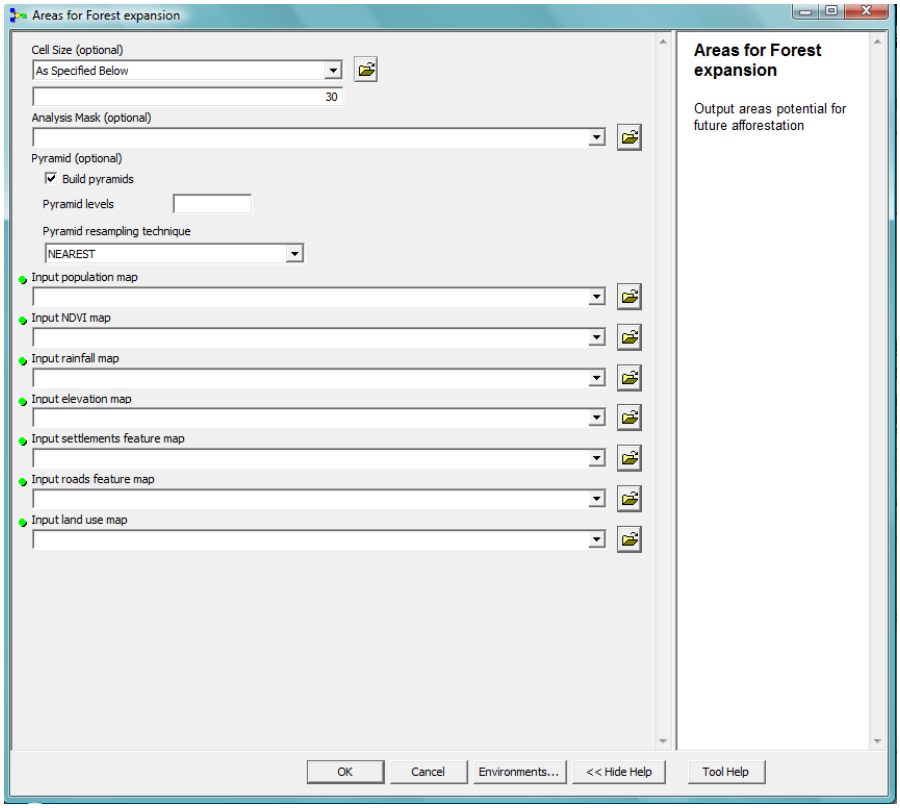

Figure 4.7 (b): Model interface for suitability analysis for allocation to forest

4.3.3 Land use scenarios

Figure 4.8 (a) & (b) shows the suitability maps generated as a result of overlaying the factor maps using the criteria and factor weights. Six alternatives spatially clustered land parcels were suitable for allocation to forest expansion (Figure 4.8(a)). Table 4.6 shows the percentage coverage of each alternative parcels of land. For example the first alternative which is the highly preferred sites for future expansion of forest was given a total allocation of 7.8% of the total basin area.

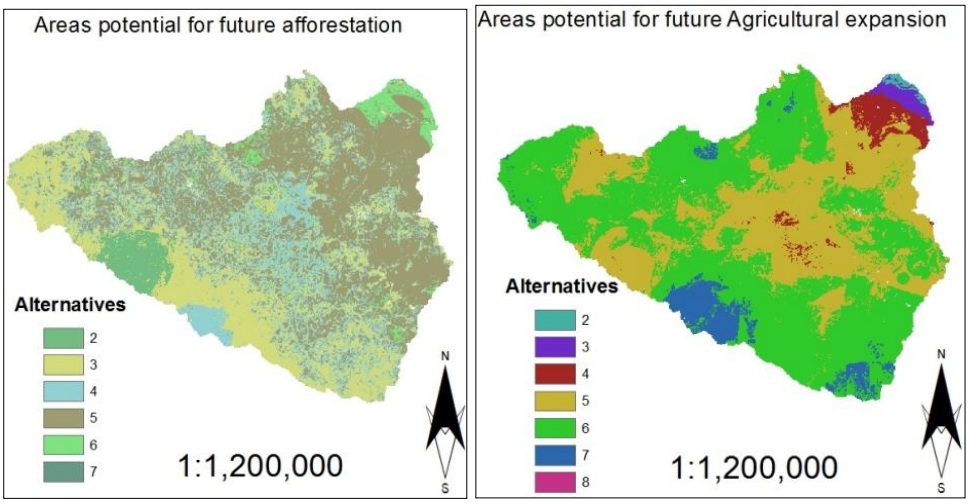

Figure 4.8: Land suitability maps

Potential areas for future agricultural expansion indicate seven alternatives. And the most preferred alternatives cover an area of 0.4% of the total basin area (Table 4.6). The seventh alternative for agricultural expansion and the sixth alternative for afforestation indicated insignificant coverage and were therefore ignored in the final analysis of the land use scenarios. Meanwhile the third alternative and sixth alternative for agricultural expansion were identical and were merged together. In general, five alternatives were considered for both agriculture and forest during the final land use scenarios aggregation.

Samples of the final land use scenarios are shown in figure 4.9. And the analysis of the percentage land cover for each of the ten scenarios is presented in table 4.8. Out of the ten scenarios formulated, six scenarios (3 and 4, 5 and 6, and 9 and 10) were identical both in space and in coverage. Table 4.9 indicates the final land use scenario chosen for analysis.

Table 4.6: Land use experiments: Areas allocated to each alternative and the allocation preference

Agriculture			Forest		
Alternative	Preference*	% land area	Alternatives	Preference*	% land area
1	2	0.4	1	2	7.8
2	3	1.1	2	3	39.1
3	4	4.0	3	4	5.7
4	5	39.7	4	5	44.7
5	6	50.3	5	6	2.7
6	7	4.5	6	7	0.0
7	8	0.0			

1. *Preference scale is in descending order, with scale 8 for agriculture and 7 for forest showing the most preferred allocation

Table 4.8: Land use scenarios generated

Scenarios	Percent land cover	
	Agriculture	Forest
1	12.4	7.5
2	12.4	7.5
3	6.2	37.5
4	6.1	37.5
5	22.5	4.6
6	20.5	5.5
7	52.0	23.2
8	32.3	42.9
9	54.2	2.1
10	53.7	2.6

Table 4.9: Land use scenarios chosen for analysis

Reference scenarios	Scenarios order	Percentage land cover	
		Agriculture	Forest
1	1	12.4	7.5
3	2	6.2	37.5
5	3	22.5	4.6
7	4	52.0	23.2
8	5	32.3	42.9
10	6	53.7	2.6

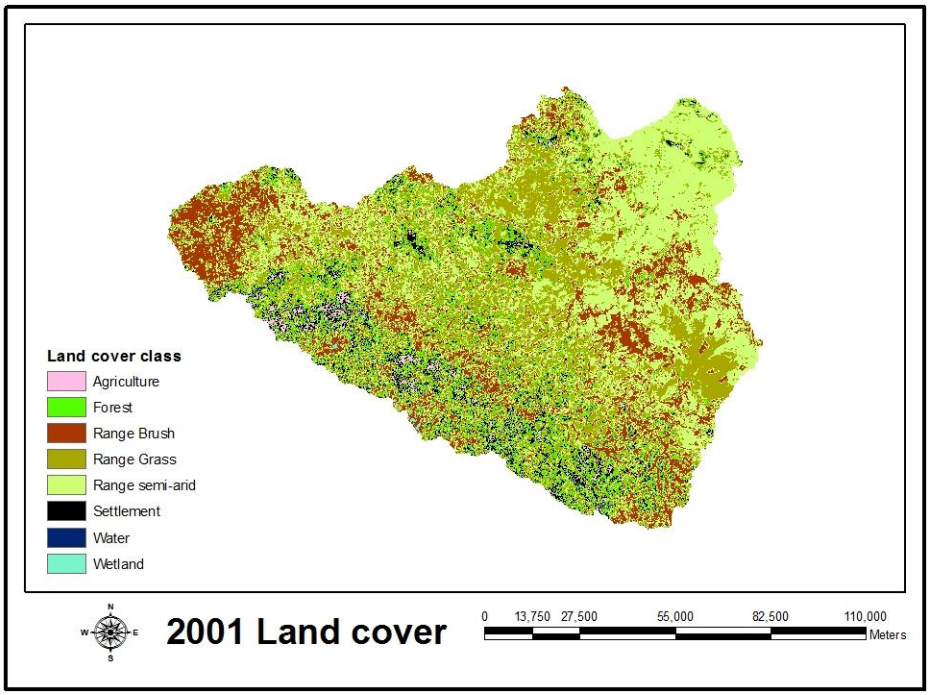

Figure 4.9a: 2001 Land use map showing reference cover covers

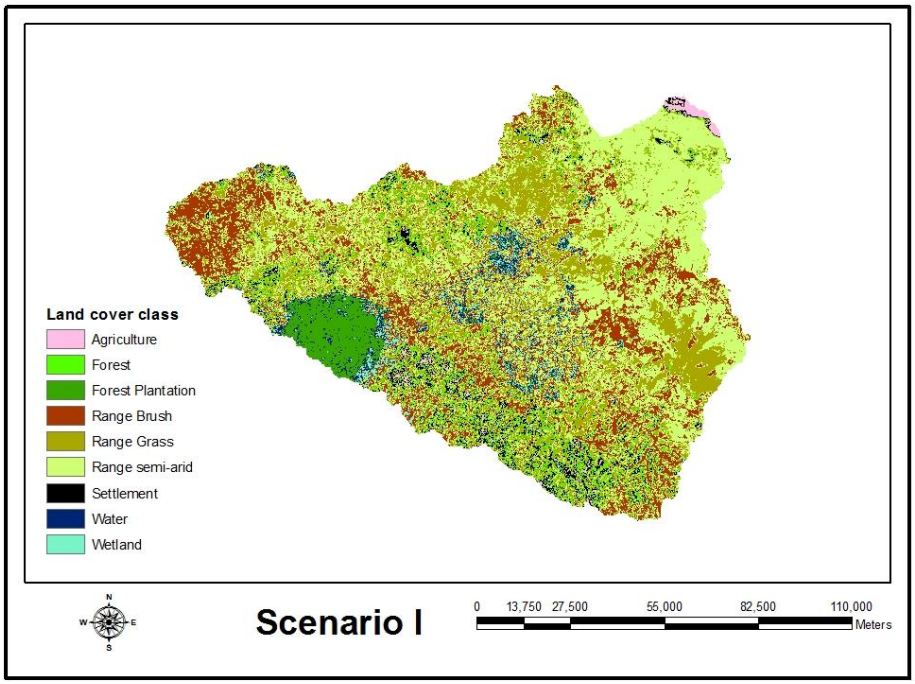

Figure 4.9b: Scenario I land use map showing spatial configuration of agriculture and plantation forest

4.4 Conclusion

The land use scenarios developed in this chapter were meant to reflect the afforestation incentives and the agricultural land use expansion in the near future. The scenarios were however time independent and did not consider "when" in the future the land use pattern may

develop. This in particular was one of the weaknesses in the GIS-Multi-criteria approach, which was noted a priori and was not considered to be a limitation in this study, which main aim was to provide avenues for planning. The land use scenarios therefore could not be validated with "actual" land use pattern; however, it relevant in testing the spatial land use polices for future land use planning was evaluated in chapter eight using the water resources optimization in the basin as the objective.

The afforestation scenarios were meant to offset the pressure on the native forest resources due to the increased demand for fuel and timber and also to contribute to the Clean Development Mechanism (CDM) campaign. The afforestation scenarios show increase in forest cover in the basin from 4.6% to 42.9% of the basin area. The afforestation extent of 37.5% and 42.9% may be considered unrealistic, since in practice, it may not be possible to realize 37.5% or 42.9% afforestation, however, the spatial pattern of the afforestation may provide crucial insight into spatial afforestation policies and it future consequences. The expansion of agricultural land use scenarios show increase from 6.2% to 53.7%. The agricultural land use expansion may be considered realistic since the expansion of farm land is primarily the main option to achieve food production increase in the near future. The effort to increase productivity of land through use of modern agricultural practices is being made, but still faces a number of limitations to be fully adopted.

In conclusion, the land use scenarios modeling using GIS based multi-criteria analysis showed high potential for use in land use planning. The major limitation noted was the lack of control on the extent of land use scenarios, which were derived independently and inability to incorporate time factor in the land use scenarios simulation (areas for new study).

Chapter 5

5. The hydrologic process model SWAT. Model set-up, calibration and validation

The application of hydrologic models in the study of hydrologic impact of land use change demands a comprehensive understanding of model structure and parameters. The basic question regarding the applicability of hydrologic model to particular conditions, with its unique environmental settings and inputs data needs to be tested prior to implementation of the model. This chapter discusses set-up, parameterisation and verification of hydrologic process model SWAT.

5.1 Data needs, data description and data generation

Data needed to implement the hydrologic process model SWAT are mainly: Digital Elevation Model (DEM), soil data (soil map indicating the soil units and the soil parameters for the different soil units), land use, the stream network (derived from the DEM), climatic data (precipitation, temperature (min. & max), solar radiation, wind speed and humidity, all in daily time step) and streamflow (used in model calibration and validation).

5.1.1 Climatic data

The meteorological data at daily or sub-daily time step is required by SWAT model. This data are precipitation (PCP), temperature (TMP) minimum and maximum, wind speed (WND), solar radiation (SLR) and humidity (HMD). The user may choose to read these data from a file or generate the values of the climatic variables using monthly average data summarized over a number of years preferably 20 or more (Niest et al., 2005).

An extensive inventory of historical data on daily precipitation, daily temperature (minimum and maximum), wind speed, and relative humidity (solar radiation missing) was obtained from FAO-NILE. The inventory of the historical data includes meteorological data from forty seven meteorological stations located within and around the basin (Figure 5.1). However, only three out of the forty seven stations had consistent dataset extending beyond 1990's. The three meteorological stations with fairly good data record on precipitation, and

temperature extending up to year 2000 are Gulu Met Station, Lira Ngetta AgroMet Station and Kitgum Centre VT. The data from the three meteorological stations (Figure 5.1) were used in this study to customize the model weather generator and run the model. The missing daily solar radiation records together with wind speed and relative humidity records were simulated using the weather generator during model simulation.

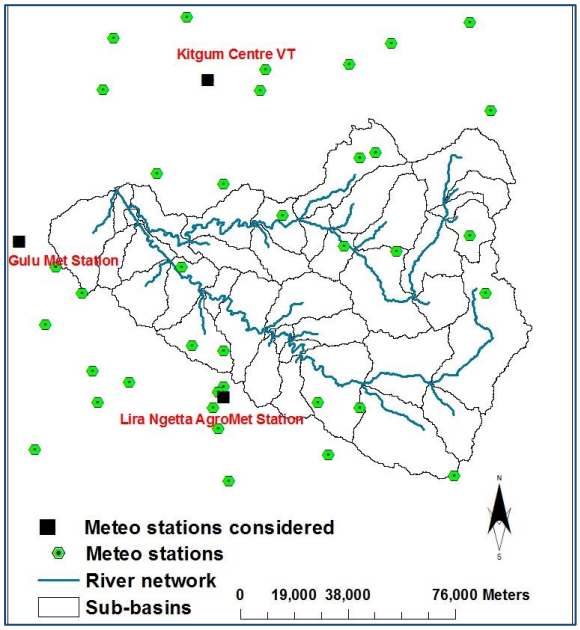

Figure 5.1: Spatial location of the meteorological station with available data

5.1.2 Solar radiation data estimation

Solar radiation is the source of energy that drives evapotranspiration processes. The most robust and recommended method for the estimation of evapotranspiration, the Penman-Monteith method (Monteith, 1965) also included in SWAT model requires data on daily solar radiation, air temperature, relative humidity and wind speed.

To be able to use this robust ET estimation method, data on daily solar radiation, air temperature, relative humidity and wind speed must be read by the model either as user input or as variable simulated by the model weather generator. As noted earlier, only air temperature and precipitation data were available as user input. Wind speed and relative humidity records were available though not covering the simulation periods of interest.

The radiation records however were completely lacking for Kitgum Center VT and Lira Ngetta AgroMet station. For Gulu Met station, monthly historical solar radiation data for seven years (1965 to 1975) were available at the Meteorological headquarters in Kampala.

Methods

The empirical equation according to Angstrom (Allen, at al., 1988) was used to estimate monthly radiation records for Gulu Met station, Lira AgroMet station and Kitgum Center VT. The proposed Angstrom equation relates solar radiation to extraterrestrial radiation as given in Equation 5.6.

$$\mathrm{Rs} = \left(\mathrm{a} + \frac{\mathrm{b}*\mathrm{n}}{\mathrm{N}}\right)\mathrm{Ra} \qquad 5.1$$

where a is regression constant, expressing the fraction of extraterrestrial (Ra) radiation reaching the earth on overcast days (n = 0), and $a + b$ fraction of extraterrestrial radiation reaching the earth on clear days (n = N). According to Allen et al., (1998), Angstrom empirical formula for radiation yields fairly good results, as there is a strong link between sunshine hours and net radiation received compared to other methods such as the one proposed by Hargreaves.

To be able to parameterise equation 5.1 using simple linear regression, a linear transformation of the equation 5.1 was performed (Equation 5.2) with parameter a representing the y-intercept and parameter b representing the gradient. The ration of the solar radiation (Rs) to the extraterrestrial radiation (Ra) was plotted against the relative sunshine duration (n/N).

$$\frac{\mathrm{R_s}}{\mathrm{R_a}} = \mathrm{a} + \mathrm{b}\left(\frac{\mathrm{n}}{\mathrm{N}}\right) \qquad 5.2$$

The extraterrestrial radiation(Ra) was estimated using the relationships;

$$Ra = \frac{24(60)}{\pi} G_{sc} d_r [\omega_s \sin(\varphi)\sin(\delta) + \cos(\varphi)\sin(\omega_s)] \qquad 5.3$$

where

(Ra) is extraterrestrial radiation ($MJm^{-2}day^{-1}$)

G_{sc} is the solar constant = 0.0820 $MJm^{-2}min^{-1}$

d_r is the inverse relative distance Earth-Sun (Equation 5.4)

ω_s is the sunset hour angle (Equation 5.6) (rad)

φ is the latitude (rad)

δ is the solar decimation (Equation 5.5)

$$d_r = 1 + 0.033\cos\left(\frac{2\pi}{365}J\right) \qquad 5.4$$

$$\delta = 0.409sin\left[\frac{2\pi}{365}J - 1.39\right] \quad 5.5$$

J is the number of the day in the year between 1 (1 January) and 365 or 366 (31 December)

$$\omega_s = arcos[-\tan(\varphi)\tan(\delta)] \quad 5.6$$

The transformed Angstrom model (Equation 5.2) was calibrated using the available monthly radiation records for Gulu Met station.

Results

The optimized values of the parameters were obtained (Figure 5.2) as $a = 0.219$ and $b = 0.4297$. The regression coefficient or coefficient of determination was 75%. Allen, (1998) however suggested that where no actual solar radiation are available and no calibration has been carried to improve a & b parameters, the values $a = 0.25$ and $b = 0.5$ are recommended. With the good coefficient of determination, the calibration of the Angstrom equation was considered adequate and the corresponding parameters a and b were used in the estimation of solar radiation.

It was not however feasible to estimate daily solar radiation for use in SWAT model using the measured sunshine hours, which was also limited. The estimated monthly solar radiation values for the three stations were used to derive custom solar radiation parameters for the SWAT weather generator.

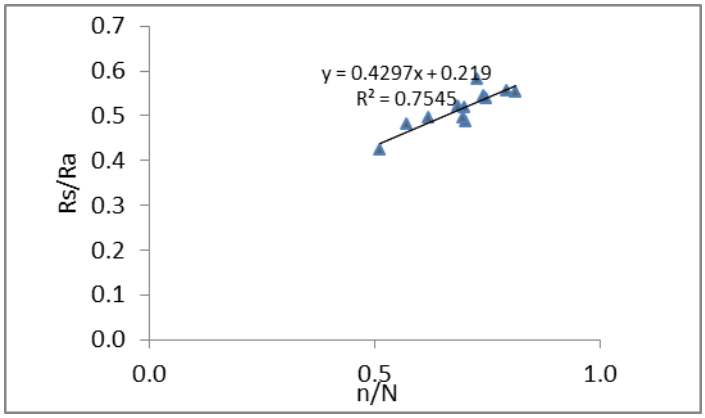

Figure 5.2: Calibration of angstrom formula

5.1.3 Customisation of the SWAT weather generator

Adoption of the SWAT weather generator developed by Sharpley and Williams, (1990), to simulate missing climatic records during simulations requires that the default parameters that come with the model be changed with the custom weather parameters.

In this study, the custom weather generator parameters were derived for the three weather stations (Gulu, Lira and Kitgum) using the historical weather records. The custom weather generator parameters derived were: latitude of the weather stations, elevation of the weather stations, average or mean daily maximum and minimum temperature for the month (12 months), standard deviation for daily maximum and minimum air temperature in the month, average or mean total monthly precipitation, standard deviation for daily precipitation in month, skew coefficient for daily precipitation in the months, probability of a wet day following a dry day in the month, probability of wet day following wet day in the month, average numbers of day of precipitation in the month, maximum 0.5 hours rainfall in the entire period of record for month, average daily solar radiation for the month, average daily dew point temperature in the month average daily wind speed in month.

The weather parameters were derived using 20 years of records except for radiation which had only few years of monthly data simulated using the calibrated Angstrom equation. The customised weather generator was used to generate the missing climatic records (wind speed, solar radiation and humidity) and to fill in the missing gaps in the measured rainfall data, and temperature data during simulation. The summary of the climatic dataset and its status in the three implementation periods (calibration, validation and scenarios simulation) is shown in table 5.1.

Table 5.1: The climatic dataset and their status in the simulation periods

Climatic variables	**Calibration period (1970-1974)**	**Validation periods (1975-1978)**	**Scenarios simulation (1978-1981; 1980-1986; 1999-2001)**
	Status	***Status***	***Status***
Precipitation	Available/input	Available/input	Available/input
Temp. (Max & Min)	Available/input	Available/input	Available/input
Wind speed	Missing/simulated*	Missing/simulated	Missing/simulated
Solar Radiation	Missing/simulated	Missing/simulated	Missing/simulated
Humidity	Missing/simulated	Missing/simulated	Missing/simulated

*Missing climatic variables were simulated using the SWAT weather generator

5.1.4 Land use data

The land use map was derived from remote sensing images using the spectrally based supervised classification of Landsat images. The land use classes were reclassified to match SWAT land cover and crop growth database. Eight land cover classes derived were, agricultural land generic, forest land cover mixed, range land brush, range land grass, range land semi-arid, wetland mixed, urban low density and water. 1986 land use dataset was used to set up SWAT model, which included calibration and validation. The SWAT land use code corresponding to the land use classes are shown in table 5.2.

Table 5.2: The reclassified land use classes according to SWAT land use/plant growth database

Land use code (SWAT land cover & crop growth database)	Custom definition
AGRL	Agriculture generic
BERM	Bermuda grass, (urban land cover)
FRST	Forest mixed cover
RNGB	Range brush land
RNGE	Range grass land
SWRN	Semi-arid range
WETL	Wetland mixed cover
FRSE*	Forest ever green*

**New land covers class considered in the land use scenarios (chapter 4)*

5.1.5 The soil data

For the purpose of modeling watershed hydrology, physical and hydraulic characteristics of soil are the most important soil attributes required by SWAT model. These soil properties are; soil hydrologic group, maximum rooting depth of soil profile, soil texture (optional), depth from the soil surface to bottom of layer, moist bulk density, available water capacity of the soil layer, saturated hydraulic conductivity, organic carbon content, percent clay, percent silt, percent sand, percent rock for each soil layer, moist soil albedo and USLE equation soil erodibility (K) factor.

The Soil and Terrain Database for north-eastern Africa (SEA), in a CD-ROM at a scale of 1:1,000,000 according to FAO, was used to derive the soil units and some soil properties. Twelve different soil units according to SEA (Table 5.3) were identified in the study area. Table 5.3 showed the different soil units and the customized soil name in the study area. The spatial arrangement of the soil unit is shown in figure 5.3.

Other information used to derive the soil properties were obtained from, harmonised world soil database (version 1.1, 2009: http://www.iiasa.ac.at/Research/LUC/External-World-soil-database/HWSD_Documentation.pdf) publication and soils of Northern Province (excluding Karamoja) published by Department of Agriculture Uganda.

Table 5.3: Soil Units in the study area

USER SOIL NAME	MUIDSHEET	MAPUNIT	SOIL UNIT NAME*
ASW1	655	ALh.ch/ALp.ch1-4ac	Haplic Alisols (chromic)
ASW2	673	ARl.or2-1ab	Luvic Arenosols (orthic)
ASW3	680	CMg.or/VRe.gl1-5ab	Gleyic Cambisols (orthic)
ASW4	691	FL1-a	Fluvisols
ASW5	731	FRh.or/FRp.um1-5ac	Haplic Ferrasols (orthic)
ASW6	760	LPe.or/LVg.ch1-be	Eutric Leptosols (orthic)
ASW7	771	LPq14-df	Lithic Leptosols
ASW8	774	LPq18-e	Lithic Leptosols
ASW9	782	LPq/LVx.fe1-5bf	Lithic Leptosols
ASW10	839	PHl.or/LPq1-4ab	Luvic Phaeozems (orthic)
ASW11	844	PTa.or1-2ab	Eutric Plinthosols (orthic)
ASW12	849	PTe.or1-3ab	Albic Plinthosols (orthic)
ASW13	861	VRe.ca12-5a	Eutric Vertisols (calcaric)

*** Soil Units in the Revised Legend of the Soil Map of the World (FAO90)**

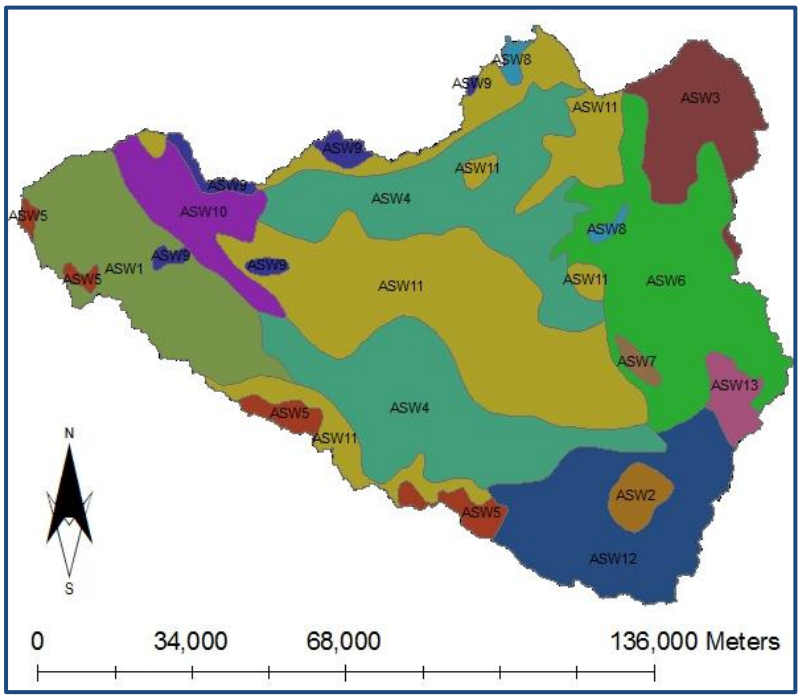

Figure 5.3: Soil map showing soil units

5.1.6 Estimation of soil parameters

1. Saturated soil hydraulic conductivity and available soil water content

Soil survey was carried out in the study area in 2007, soil samples were collected for the analysis of textural classes and organic carbon content. The analyses were carried out in the soil hydraulic laboratory at the University of Naples Federico II. This effort was aimed at getting the representative textural classes of different soil units in the study area.

Together with the information provided by SEA soil database, harmonized world soil database and the publication of soil of Northern Province, textural classes for the different soil unit were derived. The textural classes were used to extract the soil textural components indicating percentage of sand, clay and silt using table 5.4 extracted from Ahuja, Brakensiek and Shirmohammadi, (1993).

A known correlation between textural components, bulk density and organic matter developed by Saxton (Saxton, et al., 2006) was applied in the estimation of available water capacity, and saturated hydraulic conductivity.

Table 5.4: Descriptive statistics for Percentage Sand and Clay Content

	Sand				Clay			
Soil type	$\bar{x}$	*s*	CV	*n*	$\bar{x}$	*s*	CV	*n*
Clay	14.9	10.7	71.6	1177	55.2	10.9	19.7	1177
Clay loam	29.8	5.9	19.7	1317	32.6	3.7	11.4	1317
Loam	40.0	6.5	16.3	1991	19.7	5.2	26.3	1991
Loamy sand	80.9	3.8	4.6	881	6.4	3.2	50.1	881
Silt	5.8	4.5	77.2	115	9.5	2.7	28.9	115
Silt loam	16.6	11.7	70.8	3050	18.5	5.9	31.6	3050
Silty clay	6.1	4.5	73.5	1002	46.3	4.9	10.7	1002
Silty clay loam	7.6	5.3	70.7	1882	33.2	3.7	11.1	1882
Sand	92.7	3.7	4.0	803	2.9	2.0	67.1	803
Sandy caly	47.5	3.9	8.2	74	41.0	4.5	10.9	74
Sandy clay loam	54.3	7.3	13.5	610	27.4	4.0	14.6	610
Sandy loam	63.4	7.9	12.5	2835	11.1	4.8	43.2	2835

Here, $\bar{x}$ is the mean, *s,* the standard deviation; CV, coefficient of variation (percent); and *n,* the sample size

2. USLE erodibility (K) factor

The USLE erodibility (K) factor was calculated according to Williams (1995) using the textural classes derived from table 5.1. The USLE erodibility (K) factor is given by equation 5.7.

$$K_{USLE} = f_{csand} \times f_{cl-si} \times f_{org} \times f_{hisand} \quad 5.7$$

where, f_{csand} is the factor that gives low soil erodibility for soils with high coarse-sand contents and high values for soil with little sand, given by the equation (5.8)

$$f_{csand} = (0.2 + 0.3 \times \exp[-0.256 \times m_s \times (1 - \frac{m_{silt}}{100}) \quad 5.8$$

m_s is the percent sand content (0.05-2.00mm) and m_{silt} is the percent silt (0.002-0.05mm),

$$f_{cl-si} = (\frac{m_{silt}}{m_c - m_{silt}})^3 \quad 5.9$$

m_c is percent clay content (<0.002mm),

$$f_{org} = (1 - \frac{0.25 \times orgC}{orgC + \exp[3.72 - 2.95 \times orgC]}) \quad 5.10$$

orgC is the percent organic carbon content for the soil layer (%)

and

$$f_{hisand} = (1 - \frac{0.7 \times \left(1 - \frac{m_s}{100}\right)}{\left(1 - \frac{m_s}{100}\right) + \exp[-5.51 + 22.9 \times (1 - \frac{m_s}{100}]}) \quad 5.11$$

3. Moist soil albedo

The moist soil albedo (r) was estimated from Landsat 5TM image, using the reflectance corrected values for atmospheric effect (ρ_λ) and weighting coefficient ω_λ (D'Urso, 2001), using the relationship;

$$r = \sum_\lambda \omega_\lambda \rho_\lambda \quad 5.12$$

5.1.7 Digital Elevation Model (DEM)

HydroSHED DEM which is derived from Shuttle Radar Topography Mission SRTM at 3 arc-second approximately 90 meters resolution was downloaded from the SRTM website (http://srtm.csi.cgiar.org/) . The DEM was used to delineate the watershed and to derive spatial sub-basin data such as slope gradient, slope length of the terrain and stream network characteristics (channel slope, length and width).

5.1.8 Streamflow data

River flow data were available for two gauges: ASWA86201 and ASWA86202. The data were available for the period of 1960 to 1980, with missing values especially after 1978. Between 1970 and 1978, the flow data were fairly complete, with few missing flow records in 1978. The streamflow data between the periods of 1970 and 1978 were portioned into 'calibration data, using the records from 1970 to 1974' and 'validation data, using the records from 1975 to 1978. The dataset for the validation period was relatively short with very poor quality. A parallel validation of SWAT model using actual evapotranspiration derived from remote sensing techniques for the years of intent was used. This is presented in detail in the subsequent chapter.

5.2 Model construction

5.2.1 Basin delineation

The SWAT project was setup using ArcSWAT GIS interface. Watershed delineation and parameterization of stream reaches and sub-basin geomorphology was automatically done by the model interface. DEM based stream definition was used to derive flow direction and accumulation. Minimum drainage area of 16000 hectares or 160Km^2 was used to derive the stream network. Approximately 12,000 Km^2 watershed areas with a total of 40 sub-basins were delineated using a predefined watershed outlet at ASWA86202 gauge (Figure 5.4).

5.2.2 Hydrologic Response Unit analysis

When formulating and applying distributed models, the concepts of nonlinearity of hydrologic response must be taken into account (Beven, 2001). In nonlinear systems, extremes of any distribution of responses may be important in controlling the observed response. This means that hydrologic model should be described at much smaller scale in order to capture all the local heterogeneities such as infiltration rates, preferential flows, areas of first saturation and others local extremes responses (Beven, 1995).

In SWAT model, natural homogenous areas referred to as hydrologic response unit (HRU), that assumes non-variability of the data and parameters within its delineation was introduced as necessary notion in hydrologic modeling (Arnold et al., 1998). The objective of

HRU definition was to reduce the heterogeneities due to climate, soil types, topography and geology that influence hydrologic response.

In this study, the HRU definition was done using a combination of 1% land use area over sub-basin, 1% soil class over land use area and 1% slope class over soil area, after the land use and soil were imported, reclassified and overlaid with slope class. With these combinations, a total of 630 HRUs were defined.

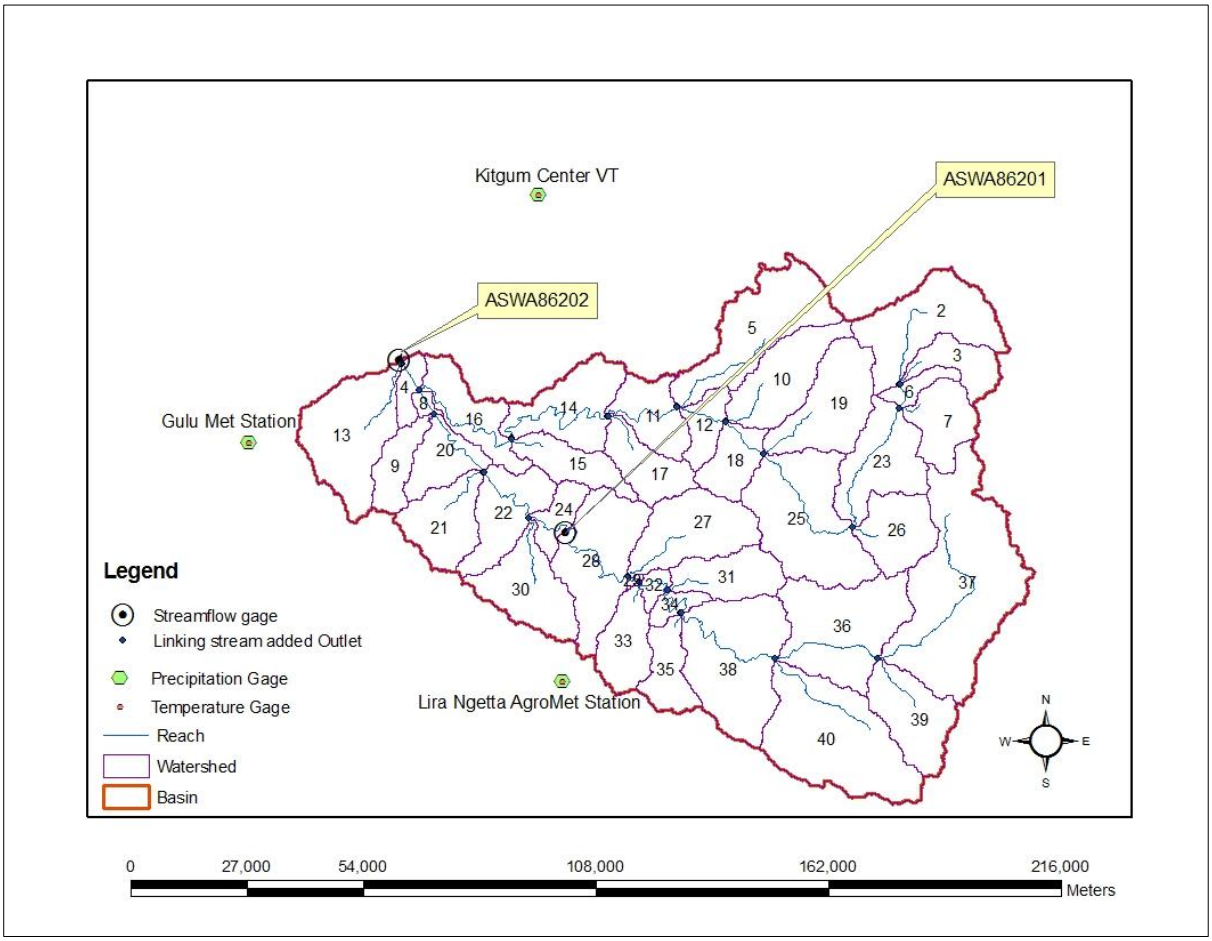

Figure 5.4: The sub-basin delineation of Aswa basin showing weather station & streamflow stations

5.3 Model configuration

SWAT model configuration is normally required before any implementation can be done. This may range from editing the model databases and restructuring the management techniques and management questions to be employed in the study. The model database written during model setup contains default values that may require modification or editing with known parameters. In this study, the crop database and management file were edited to match the land use type in the watershed, and the management techniques employed. The

development of the *LAI* (Maximum value and the pattern), was used to guide the modification of the crop growth database. Management techniques were scheduled based on the heat unit theory (Boswell, 1926; Magoon and Culpepper, 1932). The heat unit scheduling was in particular useful in this case study where land use are generic in nature (posing difficulty in determining actual operation dates) and where a distinct climatic different in the semi-arid zone exist.

5.4 Analysis of sensitivity of streamflow prediction to model parameters

Sensitivity analysis evaluates how different model parameters influence a predicted output. Sensitivity analysis enables better understanding and better estimates of values and reduces parameter uncertainty. SWAT model is a complex distributed watershed model with very many parameters. Identifying parameters that do or do not have any significant influence on the model simulation is crucial not only in reducing parameter uncertainty but also in reducing over parameterization of the model, which can destroy the physical representation of the model. Parameters identified in sensitivity analysis that influence predicted model outputs are often used in model calibration. However, (Kati and Chaubey, 2005) reported some known limitation in sensitivity analysis. They noted that due to the assumption of linearity, lack of consideration of correlations between parameters, and the lack of consideration of the different degrees of uncertainty associated with each parameter, sensitivity analysis result should treated with care.

5.4.1 Methodology

In the present study, sensitivity analysis was conducted to determine SWAT model parameters that are very sensitive to streamflow prediction. The in-built sensitivity analysis tool in the model interface ArcWAT developed by Ann van Griensven was used. The method uses dimensionless index I to express the sensitivity of a parameter. The index I is expressed by equation 5.13 which calculate the ratio between the relative changes of model output to relative change of a parameter.

$$I = \frac{x}{y}\left(\frac{y_2 - y_1}{x_2 - x_1}\right) \qquad 5.13$$

where x is the parameter and y is the predicted output, x_1, x_2 and y_1, y_2 correspond to ±10 percent of the initial parameter and corresponding output values, respectively (James and Burges, 1982). The greater the I, the more sensitive a model output variable is to that particular parameter.

5.4.2 Results

Twenty six hydrologic parameters that influence streamflow were used in the sensitivity analysis. Table 5.5 shows the model parameters and the sensitivity analysis result, ranked with most sensitive parameter in the first row. The most sensitive parameters using the objective function (of) were: soil evaporation compensation factor (ESCO), initial SCS curve number II (CN2), base-flow factors (Alpha_Bf), available soil water capacity (Sol_Awc), groundwater revap coefficient (Gw_Revap), channel effective hydraulic conductivity (Ch_K2), threshold depth of water in shallow aquifer for return flow to occur (GWQMN), surface runoff lug coefficient (Surlag), soil depth (Sol_Z) and manning's n value for main channel (CH_N2).

Three groundwater parameters; Alpha_bf, Gwqmn, and Gw-revap, one soil parameter, Sol_Awc, one evaporation parameter Esco and two runoff parameters Cn2 and Canmx were considered in model calibration (Table 5.6). The choices of the parameters were based on the processes they represent, the level of sensitivity and the expert knowledge of the hydrologic processes.

Table 5.5: Sensitivity output using ArcSWAT sensitivity tool including Parameters definition

Rank	Index	Parameter	Definition	Process
1	1.04	Esco	Soil evaporation compensation factor	Evaporation
2	0.98	Cn2	SCS curve number for moisture condition II	Runoff
3	0.74	Gwqmn	Threshold depth in shallow aquifer required for return flow	Groundwater
4	0.28	Alpha_bf	Base-flow alpha factors	Groundwater
5	0.225	Sol_Awc	Available soil water capacity	Soil
6	0.17	Sol_Z	Soil depth	Soil
7	0.09	GW_Revap	Groundwater 'revap' coefficient	Groundwater
8	0.065	Canmx	Maximum canopy index	Runoff
9	0.0588	Revapmn	Threshold depth of water in shallow aquifer for revap to occur	Groundwater
10	0.057	Ch_K2	Channel effective hydraulic conductivity	Channel
11	0.04	Blai	Leave area index for crops	Crops
12	0.024	GW_Delay	Groundwater delay	Groundwater
13	0.021	Sol_K	Soil conductivity	Soil
14	0.018	Ch_N2	Manning's n value for main channel	Channel
15	0.063	Slope	Average slope steepness	Geomorphology
16	0.0059	Epco	Plant evaporation compensation factor	Evaporation
17	0.0023	Slsubbsn	Average slope length	Geomorphology
18	0.002	Surlag	Surface runoff lag coefficient	Runoff
19	0.0016	Sol_Alb	Soil albedo	Evaporation
20	0	Biomix	Biological mixing efficiency	Soil
27	0	Smtmp	Snow melt base temperature	Snow
27	0	Smfmn	Minimum melt rate for snow during the year	Snow
27	0	Smfmx	Maximum melt rate for snow	Snow
27	0	Timp	Snow pack temperature lag factor	Snow
27	0	Tlaps	Temperature laps rate	Geomorphology

Table 5.6: Parameters changed during model calibration

	Index	**Parameter**	**Definition**	**Process**
	1.04	Esco	Soil evaporation compensation factor	Evaporation
	0.98	Cn2	SCS curve number for moisture condition II	Runoff
	0.74	Gwqmn	Threshold depth in shallow aquifer required for return flow	Groundwater
	0.28	Alpha_bf	Base-flow alpha factors	Groundwater
	0.225	Sol_Awc	Soil available water capacity	Soil
	0.09	Gw_revap	Groundwater 'revap' coefficient	Groundwater
	0.0588	Canmx	Maximum canopy index	Runoff

5.5 Calibration of the hydrologic model SWAT

5.5.1 Reviewed literatures

Hydrologic model are normally applied in particular catchment all with their own unique characteristics. Since we can never have a perfect model in practice, where unique "optimal" set of parameters exist (Beven, 1993, 1996a,b), all hydrologic models must in one way or the other undergo calibration. Model calibration is the modification of model parameter values and evaluation of the predicted output of interest to the measured data until a defined objective function is achieved (James and Burges, 1982). Calibration of distributed model normally faces problems of uniqueness, problems of equifinality, and more often problem of uncertainty.

In practice, with limited measurement available, there would most probably be a non-uniqueness problem, where by several or many different optimal parameters sets exist but measurement would not allow us to distinguish between them. Beven (1993, 1996a,b) suggested that the problem of uniqueness of places can be approach using the concept of equifinality of model structures and parameters. The concept of equifinality of model structures and parameters is that, given the limited measurements available in any application of a distributed model, it will not be possible to identify an "optimal model." Rather, we would accept that there may be many different model *structures* and *parameter sets* that will be accepted in simulating the available data.

Beven (2001) noted that in dealing with the problem of equifinality, it is important to note that it is "parameter set" that is important in giving a good fit to the observation. And that it is very rarely the case that the simulations are so sensitive to a particular parameter.

The problem of model uncertainty stem from the fact that errors in input data and errors in model structures, all of which may be very difficult to assess a priori and which affect the modeling process are real. Recognition of these problems (equifinality and uncertainty) has resulted into development of number of optimization algorithm (Beven and Binley, 1992; & Duan et al., 1992). The objective function for most of these optimization algorithms consists of a statistical test, such as minimization of relative error (RE), minimization of average error (AE), or optimization of the Nash-Sutcliffe Coefficient (NS) (Santhi et al., 2001a; Grizzetti et al., 2003).

5.5.2 Manual verse automatic calibration

Distributed hydrologic model can be calibrated either manually or automatically, using some kind of optimization algorithm. Manual calibration is a trial-and-error process of parameter adjustment. After each parameter adjustment is made, the simulated and observed watershed behaviour is visually compared to see if the match between them is improved. The logic by which the parameters should be adjusted in manual calibration to improve the match is difficult to determine (due to the compensating effects which the model parameters usually have on the model output). This may make manual calibration very difficult exercise. The main weakness in manual calibration is however lack of generally accepted objective measures of comparison, which makes it difficult to know when the manual calibration process should be terminated.

Automatic optimisation procedures on the other hand uses mathematical search algorithms that seek to minimize differences between selected features of modelled and observed behaviours by systematic trial alterations (iterations) in the values of the model parameters. The objective function, which is the quantitative measure of the fit of modelled behaviour to the observed, is calculated after parameter iteration. Successful iterations are those which cause a reduction in the value of the objective function (for direct search method). During the search only the parameter set associated with the current least objective function value is retained, which, at the end of a search, is regarded as the optimal parameter set.

Despite being very robust, automatic calibration still require user expertise and are typically used in conjunction with a manual procedure.

5.5.3 Methodology

Hydrologic model SWAT was calibrated using the historical monthly streamflow recorded at the gauges ASWA86202. The streamflow recorded in the year 1970 to 1974 were used in the calibration.

Manual calibration was chosen despite several optimization algorithms available. The reason for the choice of the manual calibration was mainly due to the flexibility the method offers with respect to the choice of parameter to be optimized and the parameter bound and requiring less expertise. During the manual calibration, the “sensitive parameters” to adjust

were determined through visual analysis of the simulated and measured streamflow hydrograph and the successful value of the parameter within a given parameter bound was that which optimise the Nash and Sutcliffe coefficient and the coefficient of determination (R^2). In this way, parameter bound are put under control and over-parameterisation is control by discarding parameters that are insensitive to the objective function. Table 5.6 gives the parameters that were manually adjusted during the calibration.

The performance of the model in predicting the streamflow during manual calibration was evaluated using both statistical and graphical methods. In particularly, the graphical techniques (streamflow hydrograph), was used to provides a visual comparison of the simulated and measured data, identify model bias, identify the differences in timing and the magnitude of peak flows and shapes of recess curves (Moriasi et al., 2007). In this way, it was possible to identify the next parameter to optimize, to improve on the predicted streamflow using visual analysis of the streamflow hydrograph.

The standard regression with slope and y-intercept of the best fit regression line was used to provide the statistical measure of the convergence of the calibration process. In this approach, the slope is used to indicate the relative relationship between simulated and measured values, and the y-intercept to indicate the presence of lag or lead between model prediction and measured data. As the slope approaches 1 and y-intercept approaches 0 the calibration process may be considered to have converged to an optimal parameter set. The statistical coefficient of determination (R^2) describing the proportion of the variance in the measured data explained by the model was also used. The value of R^2 ranges from 0 to 1, with higher values indicating less error variance, and typical values greater than 0.5 considered acceptable (Santhi et al., 2001a, Van Liew et al., 2003).

The last statistical method employed was the Nash-Sutcliffe efficiency (NSE), which is the normalized statistic that determines the relative magnitude of the residual variance ("noise") to the measured data variance ("information") (Nash and Sutcliffe, 1970). The NSE indicates how well the plot of the observed data versus the simulated data fits the 1:1 line. Using one observation, the NSE is computed as

$$g = 1 - \frac{\sum_{i=1}^{n}(Q_m - Q_s)^2}{\sum_{i=1}^{n}(Q_m - \overline{Q_m})^2} \qquad 5.14$$

where, Q_m = measured discharge, Q_s = simulated discharge

Using all these criteria, calibration of the model was considered successful after no significant improvement could be realised in any of the above indicators through adjusting the model parameters.

5.5.4 Results and discussion

Six of the most sensitive parameters were included in the manual calibration procedure (Table 5.7). The results of the calibration are shown in Figures 5.5 &5.6.

Table 5.7: Parameters optimized during manual calibration

Parameter	Definition	Unit	Default values	Changed values
Esco	Soil evaporation compensation factor		0	1 (replacement)
Cn2	SCS curve number for moisture condition II	-	Relative to soil hydrologic group and land cover	-15 (add)
Gwqmn	Threshold depth in shallow aquifer required for return flow	mm	0	0.95 (replacement)
Alpha_bf	Base-flow alpha factors	-	0.048	0.65 (replacement)
Sol_AWC	Soil available water capacity	mm	Relative to soil type	X 1.2 (relative)
Canmx	Maximum canopy index	mm	0	10 (replacement)
GW_REVAP	Groundwater 'revap' coefficient	-	0.02	0.2 (replacement)

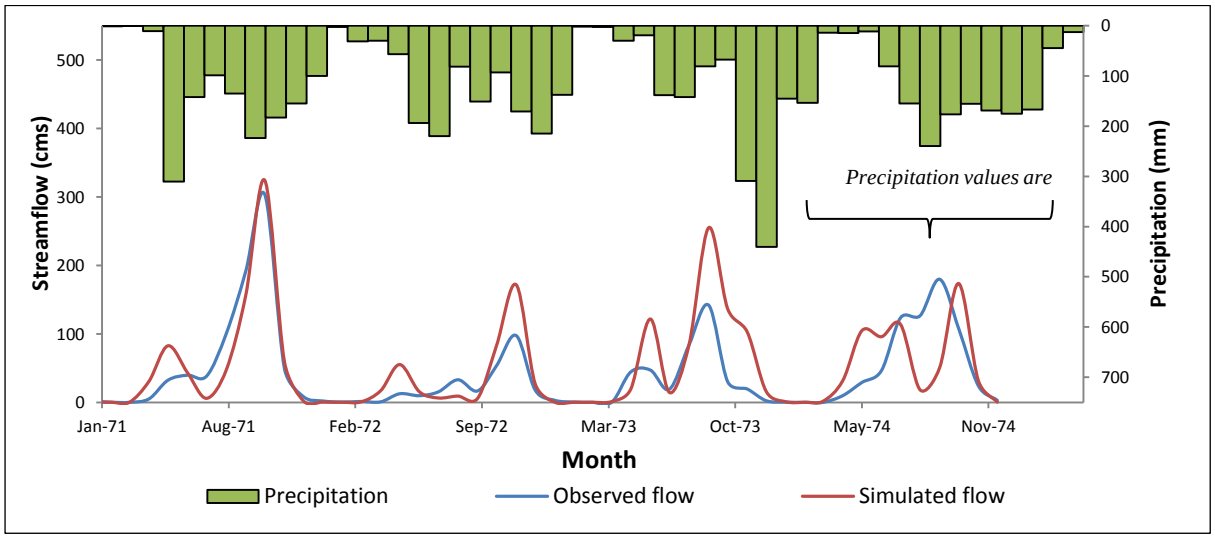

Figure 5.5 Hydrograph of observed and simulated monthly streamflow after model calibration

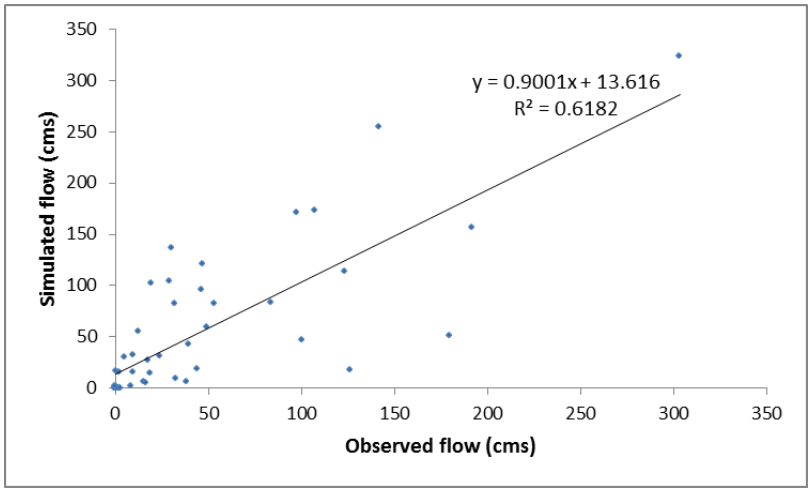

Figure 5.6: Regression correlation of observed and simulated monthly streamflow

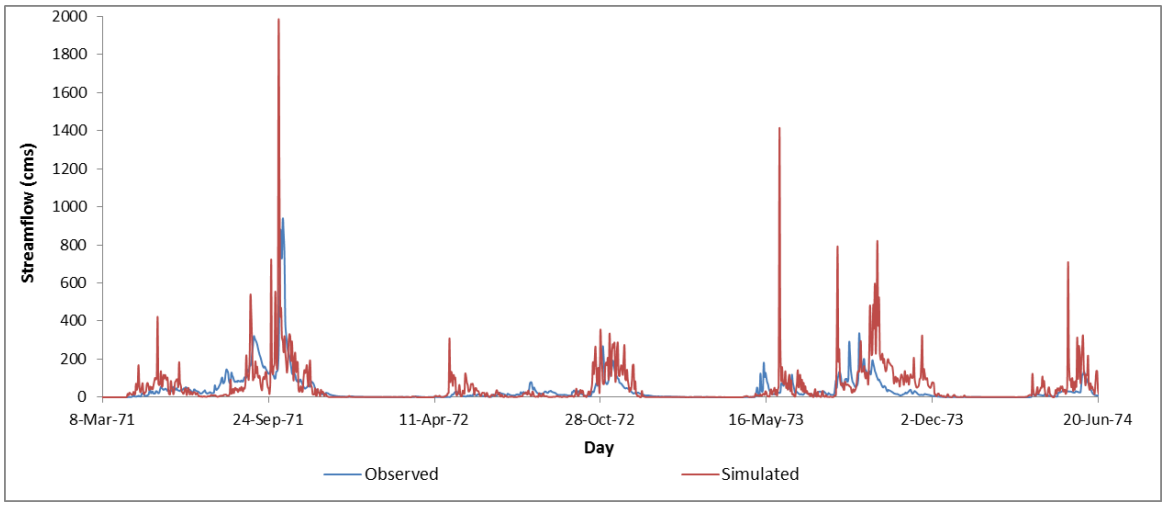

Figure 5.7 Hydrograph of observed and simulated daily streamflow after model calibration

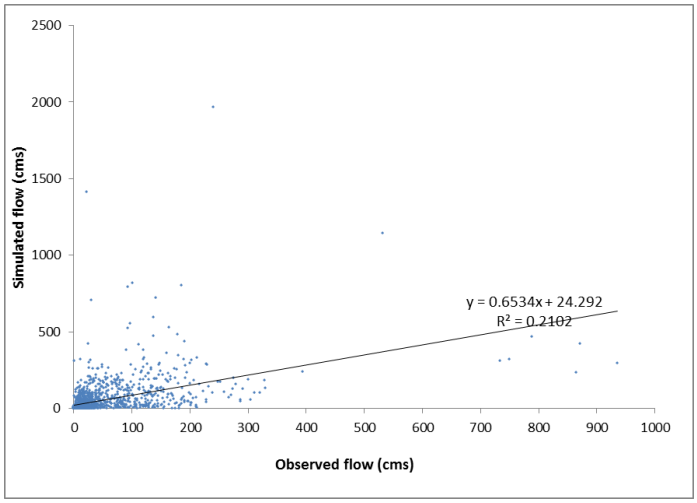

Figure 5.8: Regression correlation of observed and simulated daily streamflow

Visual analysis of the monthly and daily streamflow hydrograph (Figure 5.5 & 5.7) indicates that the calibrated model slightly overestimate the peak runoff. The hydrograph also showed that the rainfall data between May 1974 and November 1974 are not representative.

Standard regression plot (Figure 5.6) evaluates the calibrated model performance with slope of 0.9 indicating a good relative relationship between simulated and measured streamflow and y-intercept of the best fit regression line of +13.616 indicating the presence of lag between model prediction and measured streamflow.

The coefficient of determination (R^2) describing the proportion of the variance in the measured data explained by the model was obtained as 0.618. The value of R^2 ranges from 0 to 1, with higher values indicating less error variance. The reported performance rating for R^2 (Santhi et al., 2001a, Van Liew et al., 2003), indicate that typical values of R^2 greater than 0.5 is considered acceptable. The Nash-Sutcliffe efficiency (NSE) of 0.47 was obtained for monthly calibration. The performance rating of NSE for SWAT model calibration in the ranges of 0.54 to 0.65 was reported as adequate. However, considering that the measured data, (streamflow and climatic data) are highly uncertain, the performance of the calibrated model can be considered good if the rating of NSE is relaxed (Moriasi et al., 2007).

5.5.5 SWAT model calibration issues

The calibration of the hydrologic model SWAT was faced with a number of model uncertainty issues. Most notably was the model inputs uncertainty. The uncertainty in precipitation and streamflow data is reflected in the streamflow hydrograph, in which case the model failed to simulate observed streamflow peaks between May and November 1974. The input precipitation between these periods was not representatives and had significant missing values.

Analysis of parameter uncertainty however was not performed, but looking at the streamflow hydrograph, it become clear that there was a missing parameter(s) required to regulate peak flow the knowledge of which was not clear (unknown). It seems that not all processes were being model in the basin, especially the processes related to the land use categories regulating the runoff and evaporation losses. The model seems to be underestimating evapotranspiration losses and over estimating runoff. This could in part be attributed to the accuracy of land use category prediction, which has two issues. The first

issue was to do with the time lag between the streamflow records being used in calibration (1970 to 1974) and the land cover dataset used (1986). A considerable land use change could have occurred in the ten years different. In the validation periods (1975-1978) however, the model performance (NSE = 0.64) was much better, this could be due to the representativeness of the hydrologic processes in validation periods (much closer to the 1986) with the 1986 processes. The second issue in land use category prediction was to do with matching the land use categories in the study area with SWAT land use categories. In the modeling area, most of the land use categories were generic in nature, and the determination of the individual land use parameter were not done.

The underestimation of the evapotranspiration could also be attributed to the inadequate water available to meet the evapotranspiration demand. The real caused was probably underestimation of precipitation. To increase the water available for evapotranspiration, the Gw_ravap coefficient, which controls the water movement from the shallow aquifer into unsaturated layer, was set to maximum values of 0.2. This means, on a given day the maximum amount of water leaving shallow aquifer via *revap* to the unsaturated zone is 0.2 x potential evapotranspiration for the day (Neitsch et al., 2005), which is quite a significant water lost from shallow aquifer.

5.6 SWAT model validation

Testing/verification/validation of a model after the parameter values are estimated is required to determine whether the calibrated model provides adequate information for answering the question facing the decision-makers. Calibrated model may fail the verification test on some occasions. Reasons may be due to: 1) errors in the data used in calibration, both the data used as input to the model and the data used to check model output should be checked very carefully (data with large errors should not be used for calibration and), 2) use of a period of record that does not contain enough events of the physical processes needed to calibrate key parameters, 3) inadequate and or miss-representation by the model of hydrological processes found in the catchment, model results should be compared visually with the recorded data series to look for consistent variations.

Validation procedures are similar to calibration procedures in that predicted and measured values are compared to determine if the objective function is met. However, a dataset of measured watershed response selected for validation preferably should be different from the

one used for model calibration, and the model parameters are not adjusted during validation. Validation provides a test of whether the model was calibrated to a particular dataset or the system it is to represent. If the objective function is not achieved for the validation dataset, calibration and/or model assumptions may be revisited.

The model validation was conducted using climatic data set for the period of 1975 to 1978. Evaluations of model performance during validation are presented in Figures 5.9 and 5.10. The hydrograph (Figure 5.10) indicates that the model consistently predicts the measured streamflow, but with some lags. The visual evaluation of the hydrograph plot showed fairly good model match in validation period.

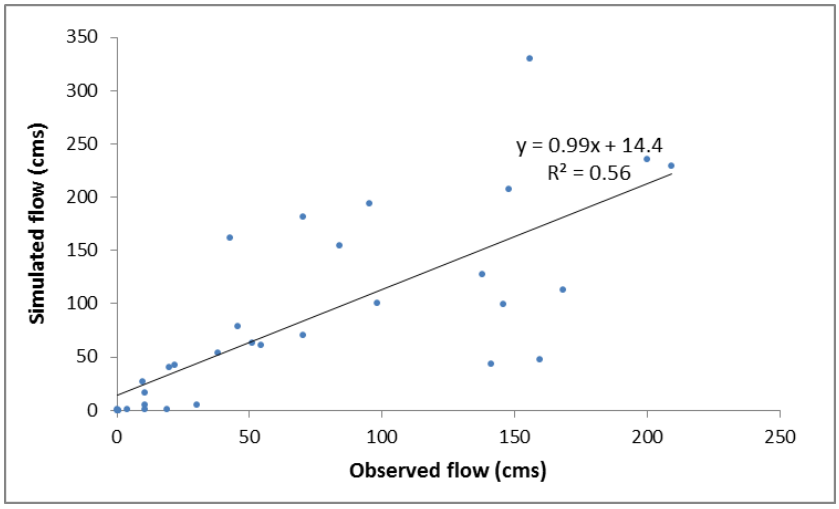

Figure 5.9: Regression correlation of observed and simulated monthly streamflow during validation

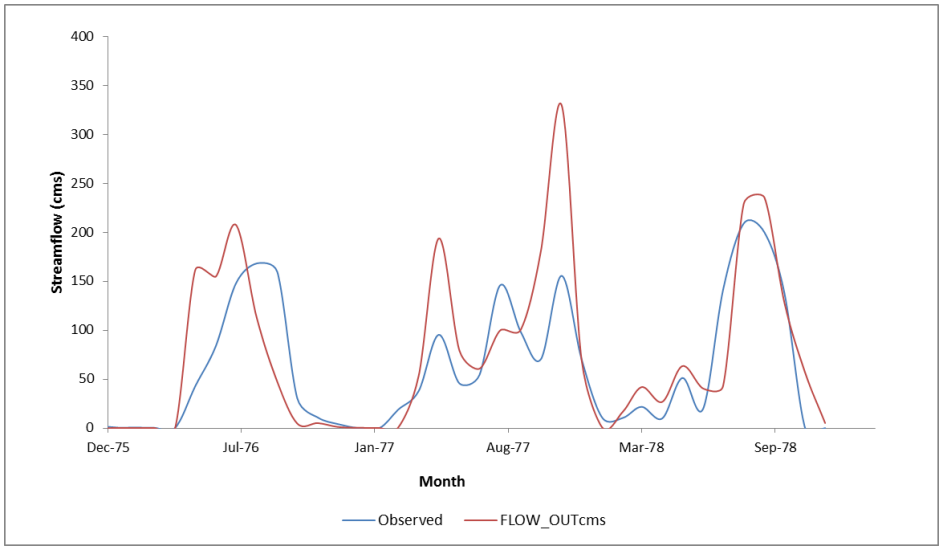

Figure 5.10: Hydrograph of observed and simulated monthly streamflow after model validation

Statistical evaluation of model performance during validation using standard regression plot (Figure 5.6) indicates a good relationship between simulated and measured streamflow with the slope of 0.99 and the y-intercept of the best fit regression line of +14.4, which indicate lag between model prediction and measured streamflow. The values of R^2 of 0.56 obtained indicate a good model fit during validation. Above all, the objective function, the Nash-Sutcliffe efficiency (NSE) of 0.64 indicates that the model performance during validation is satisfactory.

5.7 Conclusion

The analysis of sensitivity of model parameters to streamflow prediction showed groundwater parameters dominating and ranked among the most sensitive parameters. Out of the seven parameters considered in model calibration, three were groundwater parameters; the baseflow recession constant (Alpha_bf), the threshold hold depth for water in shallow aquifer required for return flow (Gwqmn) and the coefficient that allows for water in the shallow aquifer to rise up in the unsaturated zone to meet the unavailable water required by plant (Gw_revap).

Calibration of the model using the seven parameters showed that the most sensitive parameters ESCO, was adjusted to provide no compensation for the soil evaporative demand by the lower soil layer. Meanwhile, maximum amount of water was allowed to rise into the unsaturated zone from the shallow aquifer to compensate for the unavailable water for transpiration. This was logical in low land areas were groundwater table are shallow and in areas with deep rooted vegetation. The baseflow recession constant value of 0.65 used in calibration indicates an average (moderate) groundwater flow response to change in recharge, which seems to be a realistic value considering that the streamflow in the period of no recharge is always low. The groundwater parameters, ESCO and maximum canopy index (canmx) were treated as lumped parameters.

The statistic evaluation of the model during calibration and validation showed a considerable acceptance, with NSE of 0.47 and 0.64 respectively. The low level of model performance during calibration and validation were mainly due to input uncertainty and accuracy of the land use categories used.

Chapter 6

6. Implementation of the calibrated hydrologic model SWAT for the reference year 2001

6.1 The hydrologic process simulations

6.1.1 Methods

The hydrologic process simulations using the hydrologic model SWAT were carried out to quantify the hydrologic processes in the year 2001, considered as the reference year for scenarios analyses. The simulation used the 1999 to 2001 climatic records. The short simulation period was due to climatic data inconsistency in the records before 1999. Two years simulation was used as initialization periods and the hydrologic processes analyses were based on 2001 simulation.

6.1.2 Results

The summary of the monthly water balance in 2001 is presented table 6.1 and figure 6.1. Table 6.1 includes in the last two columns the values of the change in storage based on the available soil water. The values in the water balance column was based on equation 2.3, which is represent the conceptual pathways water takes within the hydrologic systems. The values in the water balance column and change in storage column shows that the SWAT water balance closes with some little variation (<3%), which could be attributed mainly to the numeric error in the modeling process. The values in the water balance column shows seven moths (January, February, May, June, August, November and December) in 2001 had water deficit.

In figure 6.1, the monthly variation in water balance shows that maximum water yield in the year was achieved in the month of November, with January, February, March, June and September getting very low water yield. Basin water yield is modeled in SWAT as the sum of lateral flow, baseflow and surface runoff. Surface runoff contribution to basin water yield is more seen in the months of April, October and November, while in the rest of the month, surface runoff contribution was very minimal. The dominant process that contributes to water yield in the basin was baseflow with 78.4% contribution and least was lateral flow with just

7.5%. The soil water (SW) showed insignificant monthly variation. The actual ET has the peak in August and the monthly variation between April and October was very minimal.

Table 6.1: 2001 Monthly water balance (values in mm of H_2O)

Month	Precipitation	Surface runoff	Lateral flow	Percolation	ET_a	Soil water storage	Water balance	Change in storage
Jan	51.96	0.06	0.53	11.65	39.94	74.55	-0.22	-
Feb	27.83	0.01	0.24	0.16	48.34	53.7	-20.92	-20.85
Mar	139.84	0.87	0.97	26.48	81.66	83.4	29.86	29.7
Apr	190.03	4.66	1.63	71	102.75	93.07	9.99	9.67
May	133.1	1.14	1.42	46.26	106.68	71.02	-22.4	-22.05
Jun	109.28	0.02	0.68	7.72	103.54	68.37	-2.68	-2.65
Jul	175.53	0.59	1.39	41.82	108.11	91.86	23.62	23.49
Aug	144.4	1.03	1.25	36.22	121.45	76.34	-15.55	-15.52
Sep	120.71	0.06	0.89	13.89	100.59	81.53	5.28	5.19
Oct	184.89	6.04	1.8	68.91	101.65	87.89	6.49	6.36
Nov	175.42	10.88	2.05	95.91	80.16	74.49	-13.58	-13.4
Dec	35.03	0.02	0.45	1.75	40.92	66.55	-8.11	-7.94
TOTAL	**1488.02**	**25.38**	**13.3**	**421.77**	**1035.79**	**922.77**	**-8.22**	

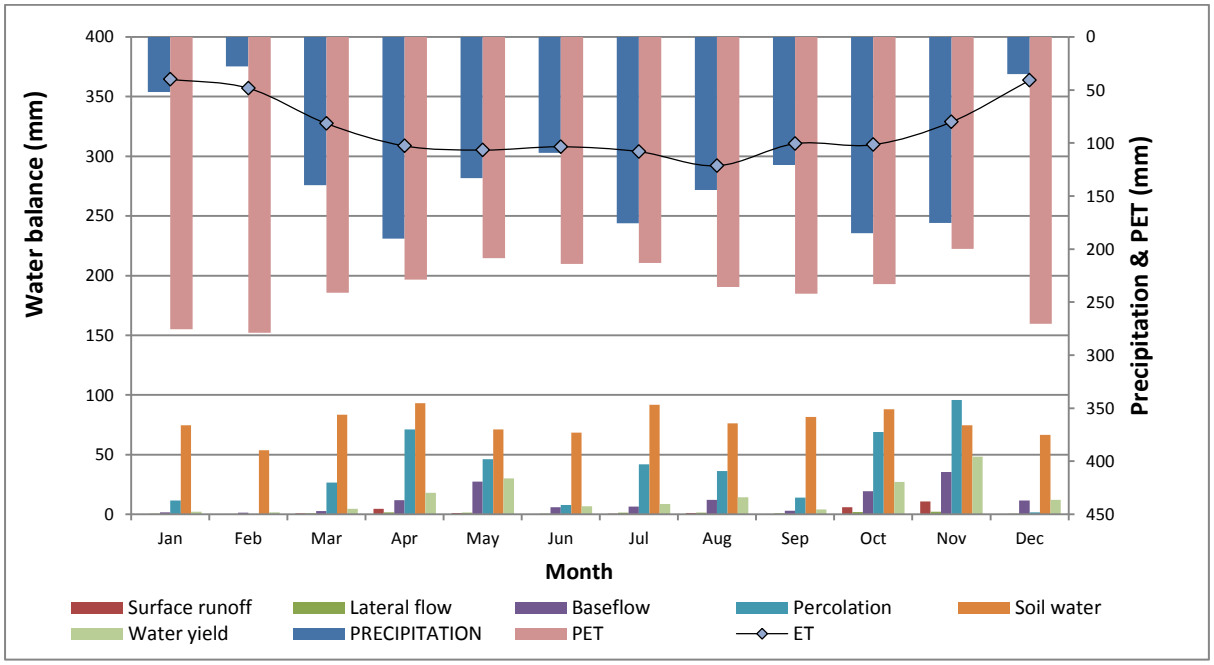

Figure 6.1: The monthly water balance summary for 2001

6.2 Validation of the hydrologic process simulations in 2001 using SSEB

Temporal transfers of parameters estimates can lower the performance of hydrologic model. There are some known issues associated with the application of the hydrologic model SWAT to predict the futures conditions which are outside the model conditions. These issues are mainly associated with the physical hydrologic parameters which often changes with time. In chapter V, the hydrologic model SWAT was calibrated by using streamflow data for the period 1970 to 1974; subsequently, the model was conditioned to simulate the hydrologic processes in the calibration and validation periods. The question now is can the optimal parameters set obtained in chapter V be transferred to properly simulate the hydrologic processes in 2001 and land use scenarios?

To answer this question, the performance of the hydrologic model SWAT in 2001 was validated using the actual evapotranspiration estimate from the satellite images based on the Simple energy balance approach (SSEB) according to Senay et al., 2007. The available observed streamflow data were very limited covering the periods between 1960 and 1980 and were used in the calibration and validation periods.

6.2.1 Actual ET and the energy balance approach

Immerzeel, and Droogers (2007), demonstrated that the hydrologic model SWAT can be successfully calibrated using the actual evapotranspiration estimates based on satellite observation. In their approach, the Surface Energy Balance Algorithm (SEBAL) formulated by Bastiaanssen et al., 1998 was used to derive the actual ET using the MODIS thermal images on a bi-weekly basis. This breakthrough has given a new hope of using distributed hydrologic model in areas where streamflow records are lucking.

The success of the energy balance approach in estimation of the actual ET however still relies heavily on the quality of the data and the skill used in processing the data, which limits the adoption of the use of actual ET in calibration and validation of hydrologic models. With the more advancement being made in the use of energy balance to estimate actual evapotranspiration from satellite observation (Senay et al., 2007), the problem of data limitation and expertise in data preparation may soon become a non-issues.

The actual evapotranspiration in energy balance approach is calculated as the residual of the difference between the net radiation and losses due to the sensible heat flux and the ground heat flux, represented in equation 6.1.

$$\lambda ET = R_n - G - H \qquad 6.1$$

where λET is the latent heat flux, R_n is the net radiation flux at the surface, G is the soil heat flux, and H is sensible heat flux, units in W/m^2. The concept behind the energy balance approach in the estimation of actual ET is based on the assumption that the temperature difference between the land surface and the near-surface (air) varies linearly with the land surface temperature. The linearity relationship derived using two anchor pixels named by Bastiaanssen et al., 1998 as the "hot" and the "cold" pixels, which are used to infer known fluxes i.e. respectively $\lambda ET = 0$ and H=0. The "hot" and "cold" pixels theory is now being used in several energy balance approach. Senay et al. (2007) developed the simplified surface energy balance approach (SSEB) to estimate actual evapotranspiration, using the similar assumption of the "cold" and the "hot" pixel but without solving the energy balance equation 6.1. They validated the SSEB and found it to be in good agreement with the energy balance approach SEBAL according to Bastiaanssen et al., 1998 and METRIC according to Allen et al., 2005, which uses energy balance equation 6.1.

The SSEB according to Senay et al., (2007) is based on the assumption that, the latent heat flux (actual ET) varies linearly between the two extremes conditions; no latent heat flux, associated to "hot" pixel and maximum latent heat flux associated to "cold" pixels. They further extended the assumption that the surface temperature difference is only caused by the differences in moisture availability and water use. Based on these assumptions, the SSEB approach uses simple ratio between the pixel temperature difference from the no ETa condition and the amplitude to calculate the proportional fraction (ET_f) of the ETa (Equation 6.2):

$$ET_f = \frac{TH-TX}{TH-TC} \qquad 6.2$$

where: TH is the land surface temperature at the "hot" pixel, TC is the land surface temperature at the "cold" pixel and TX is the land surface temperature value at any given pixel.

In this chapter the SSEB approach was used to estimate the actual ET index (fraction) and compare with the value of the ration between actual and reference ET obtained in the SWAT model for the simulation of the hydrologic processes for the year 2001. To achieve this task, the Land Surface Temperature product derived from MODIS (MOD11A2, http://mrtweb.cr.usgs.gov/) was used.

6.2.2 Data set characteristics

Land surface temperature products (LST) derived from MODIS senor on-board Terra satellite were used to derived the actual ET fraction (index) according to equation 6.2. The MODIS LST data are created as a sequence of products beginning with a scene and progressing, through spatial and temporal transformations, to daily and eight-day global gridded products. There are seven series of the LST data products available. In this study, the fourth product, MOD11A2, which is an eight-day LST product obtained by averaging from two to eight days of the MOD11A1 product was used. The temperatures are extracted in degree kelvin with a rescaling factor of 0.02.

6.2.3 Analysis

An average of the "hot" and "cold" pixels, identified with the aid of MODIS NDVI for each of the 8-day composite scene were used to derived the actual ET fraction. For each given composite scene, the "cold" pixels were taken from well vegetated areas assumed to have maximum actual ET and the NDVI>0.60 was considered to represent the cold pixels. Likewise, the "hot" pixels were taken from the areas with NDVI<0.3. At least three LST values for the "hot" and "cold" pixels were taken for each image and the averages used in equation 6.2.

A model was built in ERDAS Imagine to compute ET_f (equation 6.2), for each composite 8-day image using the corresponding average values for the "hot" and "cold" pixels. The per-pixels ET_f values were then aggregated for each sub-basin using the "zonal attributes" utility in ERDAS and compared with the corresponding SWAT ET fraction. The sub-basin SWAT ET fraction was computed as the ratio of the actual ET and potential ET in the sub-basin SWAT output.

6.2.4 Results and discussions

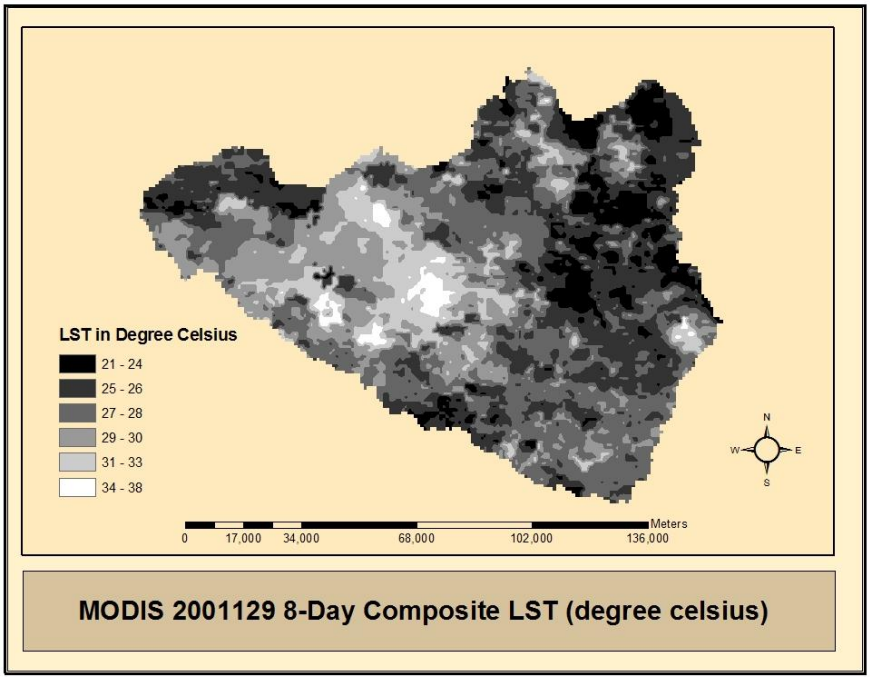

Figure 6.3: MODIS LST 8-day composite for May 9/16 2001

The LST for May 9/16 (DOY 129) is shown in figure 6.3. The minimum surface temperature for the composite scene was 21 to 24 degree Celsius and the maximum surface temperature was between 34 and 38 degree Celsius. More "hot" surfaces were found in the central and extreme "cold" surface were located mainly in the north-east of the basin.

The time series plot of the "hot" and "cold" pixels temperatures extracted is shown in figure 6.4. In May 9/16 composite scene, the "cold" pixel temperature deviates by 13.6 degree Celsius from the "hot" pixel temperature. For all the composite scenes, the "cold" pixels temperature deviates by 8 degree Celsius from the "hot" pixels temperature. There seems to be non-convergence between the "cold" and the "hot" pixels temperatures at the beginning and the end of the year. Actually the "cold" pixel temperature deviates by 16.6 degree Celsius from the "hot" pixel temperature in the beginning and the end of the year. The existence of such high deviation could be explained by the influence of the wetland vegetation, which have high actual ET (low surface temperature) compared to grassland, which would be wilting and having minimal actual ET (high surface temperature) in the dry periods of January and December. The high discrepancy in the "hot" pixel temperature and the "cold" pixel temperature variation during the dry seasons affected the estimation of the actual ET fraction using the SSEB in the beginning of the season and end of the season

(Figure 6.6). Better estimation in these periods would be achieved by zoning the study area into more homogenous land use categories. This was however, not within the scope of this study.

In the month of May to August when most vegetation have attained full development, and the variance in "hot" and "cold" pixels temperature reduces, the SSEB estimate of the actual ET fraction closely resembled the SWAT actual ET fraction (Figure 6.7). The analysis of the spatial and temporal correlation between the SWA ET fraction and the SSEB ET fraction is given in the table 6.2 and 6.3. The analysis shows that the spatial correlation between the SWAT ET fraction and SSEB ET fraction is better than the temporal correlation. The reasons could be due to the high deviation between the "hot" and "cold" pixels with time, explained earlier.

Table 6.2: Spatial correlation coefficient between the SSEB ETa fraction and the SWAT ETa fraction

R^2	Slope	Intercept
0.447	0.915	0.095

Table 6.3: Temporal correlation coefficient between the SSEB ETa fraction and the SWAT ETa fraction

R^2	Slope	Intercept
0.370	0.431	0.322

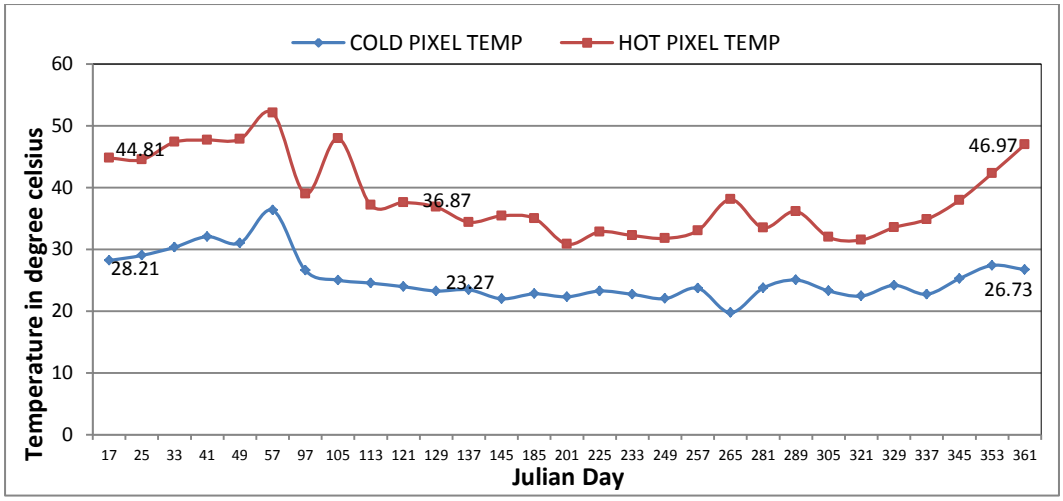

Figure 6.4: Temporal variation of the "hot" and "cold" pixels temperature derived from MODIS LST product MOD11A2 (8-days composite) for the Aswa basin (year 2001).

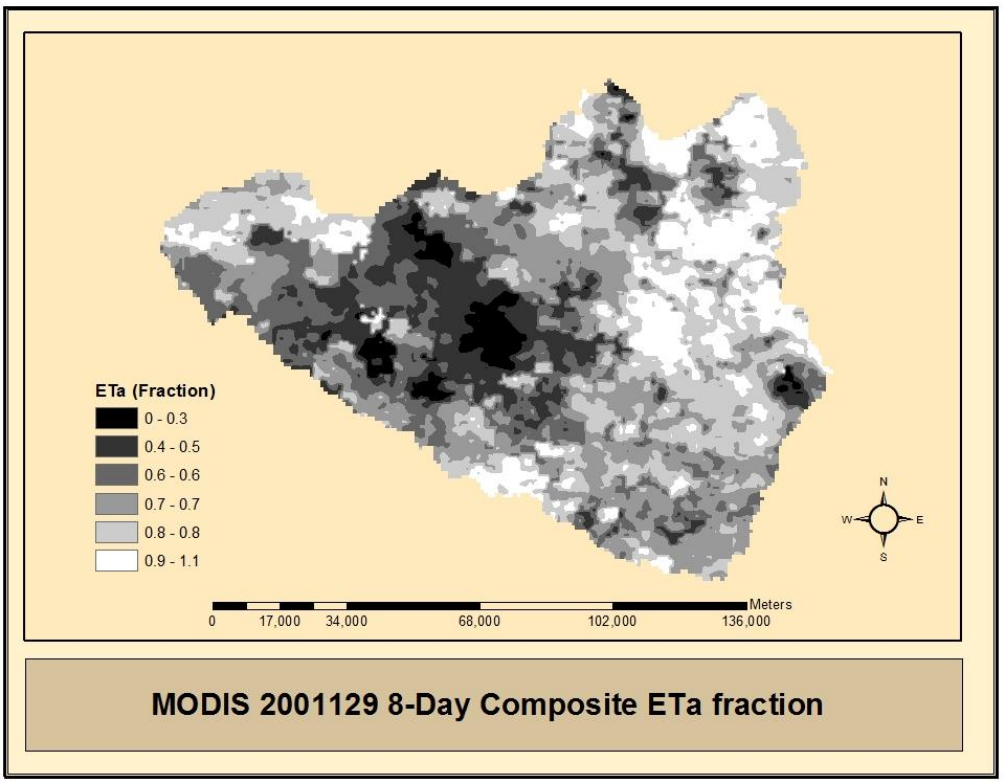

Figure 6.5: Temporal per-pixel actual ET fraction for May 9/16 2001 (DOY 129)

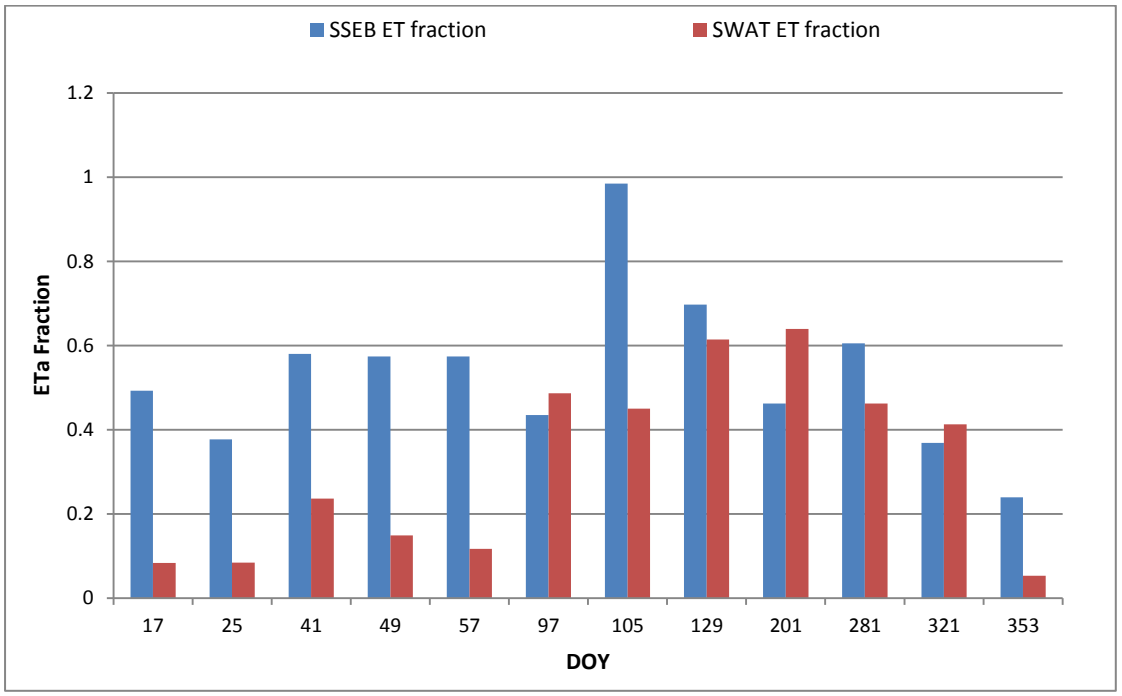

Figure 6.6: Temporal variation of ETA fraction for SSEB and SWAT for May 9/16 2001 (DOY 129) in sub-basin 1

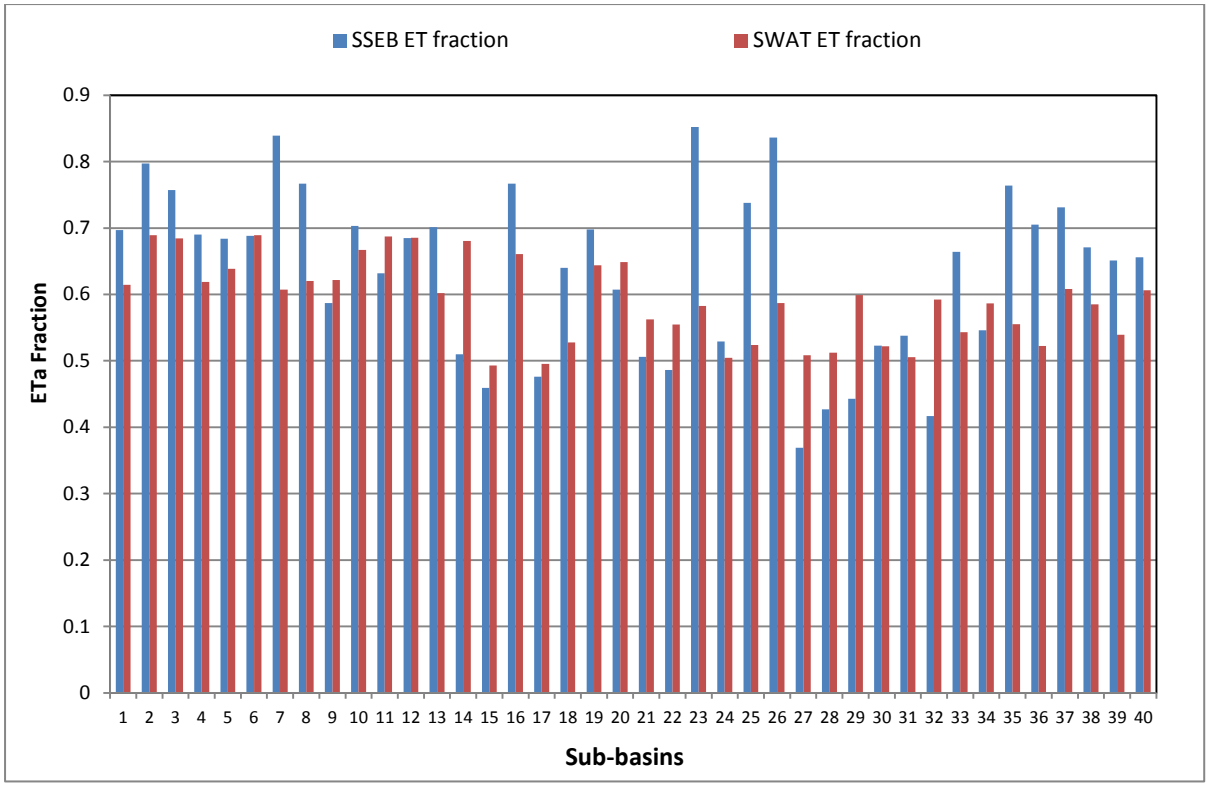

Figure 6.7: Spatial variation of ETa fraction for SSEB and SWAT for May 9/16 2001 (DOY 129)

6.3 Conclusions

The question to whether the optimized SWAT parameters can be transferred to simulate the hydrologic processes in 2001 was answered. The application of the calibrated hydrologic model SWAT in simulation of the hydrologic processes in 2001 was considered acceptable, with the spatial and temporal variable of ET_a index estimated using SSEB and SWAT showing fairly good agreement, with SSEB ET_a fraction always greater than the SWAT ET_a fraction. The under estimation of the SWAT ET fraction could be due to inadequate water available required to meet the ET demand, explained earlier in the SWAT calibration issues. Meanwhile, the reason for the overestimation of the SSEB ET fraction was not very clear. It could be issues to do with aggregation of the ET_f or the wrong assumption used in identifying the "hot" and "cold" pixels values.

However, the use of surface energy balance models based on the analysis of MODIS LST products still proves to be quite potential for the validation of distributed hydrological models, especially in those studies focusing on mapping the evapotranspiration processes for resources management. The application of more complex surface energy balance models other than the SSEB algorithm applied here may prove to be difficult in areas with limited

data availability. Nevertheless, the comparison between spatial and temporal variability of the ET_f derived from SSEB and ET output of distributed hydrological model opens new perspectives for validation purposes.

Chapter 7

7. The hydrologic impact of land use change between 1986 and 2001

In chapter III, land cover maps for 1986 and 2001 were produced and changes in land cover quantified. In this chapter, the hydrologic model SWAT was applied to analyses the impact of changes in the land use on water resources availability.

7.1 Materials and methods

7.1.1 The land use change characteristics

The assessment of the land cover changes between 1986 and 2001 are shown Figure 7.1. The most significant land cover changes in the periods were reduction in agricultural land by about 6% reduction in forest cover by about 3%, regeneration of range lands by about 9% (range grass, range semi-arid and range brush) and increase in area under settlement by 0.3% (Figure 7.1). How the changes in land cover affect the hydrologic processes are discussed in the next sections of this chapter.

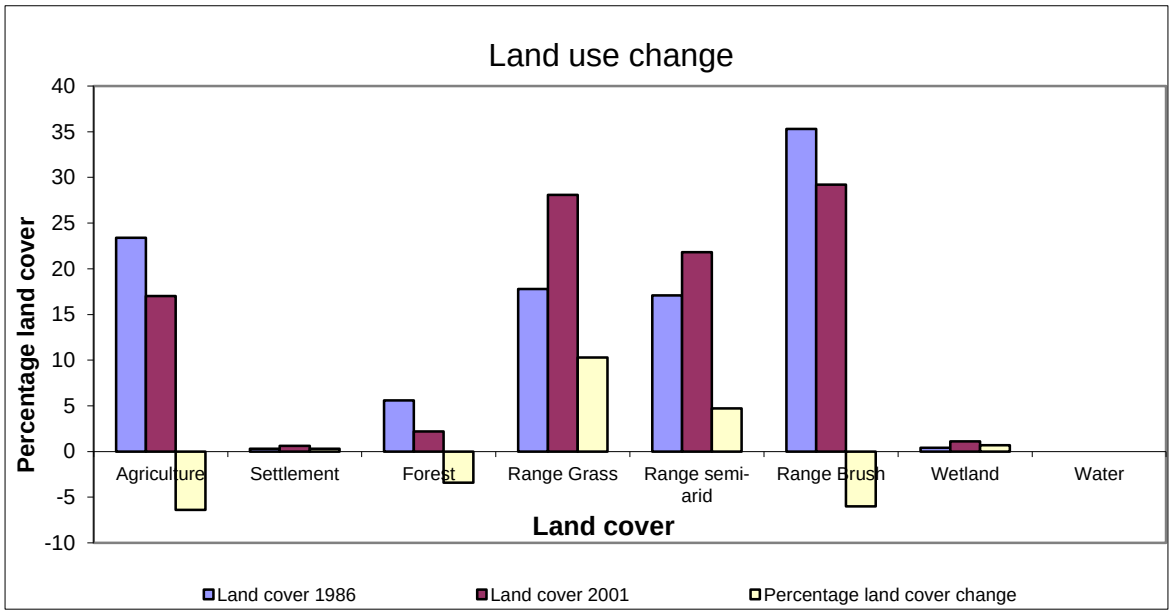

Figure 7.1: Percentage land cover and land cover change between 1986 and 2001

7.1.2 The climatic characteristics

1. Spatial variability

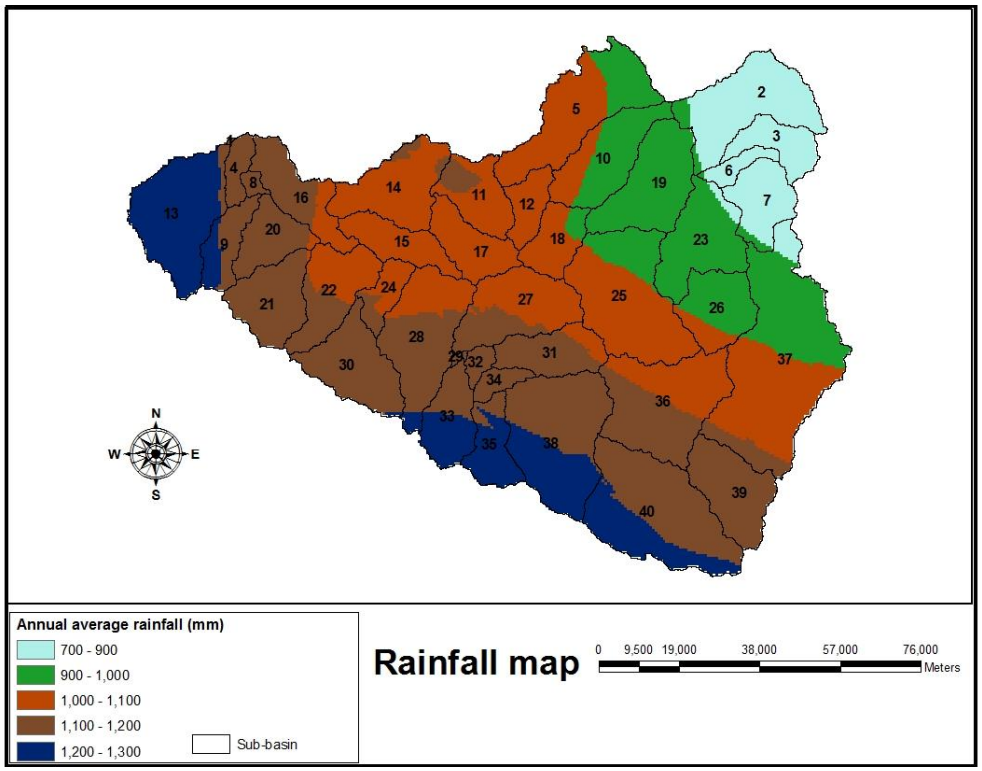

Figure 7.2: Annual rainfall distributions

The annual rainfall distribution map (Figure 7.2) prepared using 20 years of historical annual averages shows the spatial rainfall distribution in the study area. The rainfall distribution map was used to define five climatic zones that were considered in assessing the effect of spatial location of the land cover, with respect to climatic variations on the hydrologic processes. The definitions of the climatic zones are given in Table 7.1.

Table 7.1: Climatic zones in the study area

Climate	**Annual average precipitation (mm)**
Very Dry	< 900
Dry	900 – 1,000
Moderately Wet	1,000 – 1,100
Wet	1,100 – 1,200
Very Wet	> 1,200

2. Temporal variability

The temporal variation in annual average basin precipitation for thirteen years is shown in Figure 7.3. The basin average values of the annual precipitation were derived using records from the three meteorological stations (Gulu, Lira and Kitgum). The statistical analyses of the

annual average records (Table 7.2) indicate a small variation (155.26 mm) of the annual average precipitation from the mean.

Table 7.2: Statistic for the annual average basin precipitation records

STD	MEAN	MAX	MIN
155.26	1465.30	1780.12	1194.54

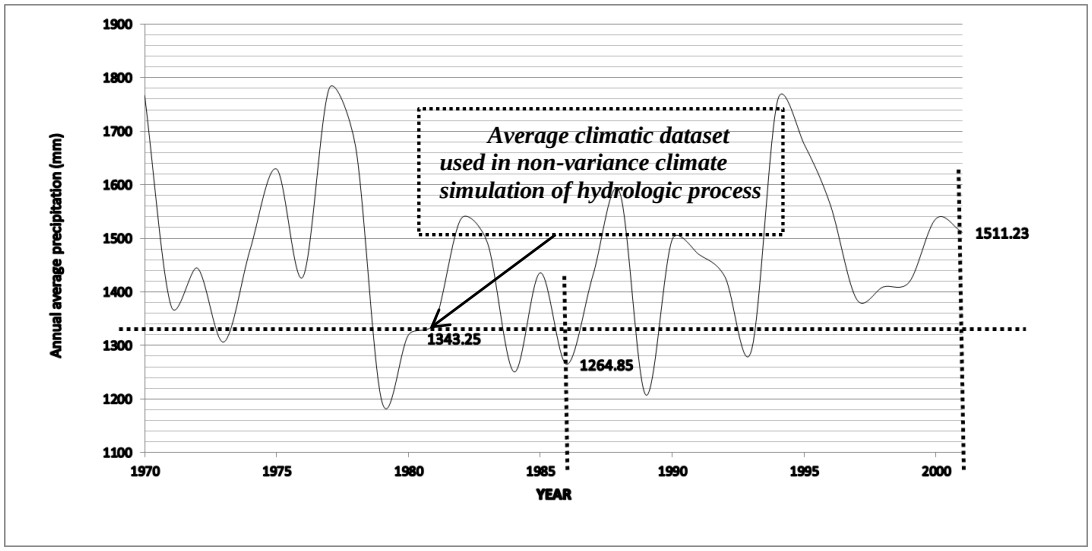

Figure 7.3: Annual average basin precipitation variation

Similarly, monthly analysis of the precipitation variation for the year 1986 and 2001 (Figure 7.4) indicates some significant variation in the monthly average precipitation in the months of Jan, March, May, August and December. In the rest of the months, precipitation variations were insignificant. The significant difference in precipitation suggests that the variance in the hydrologic processes in the study area would be due to mix response of land use changes and difference in precipitation.

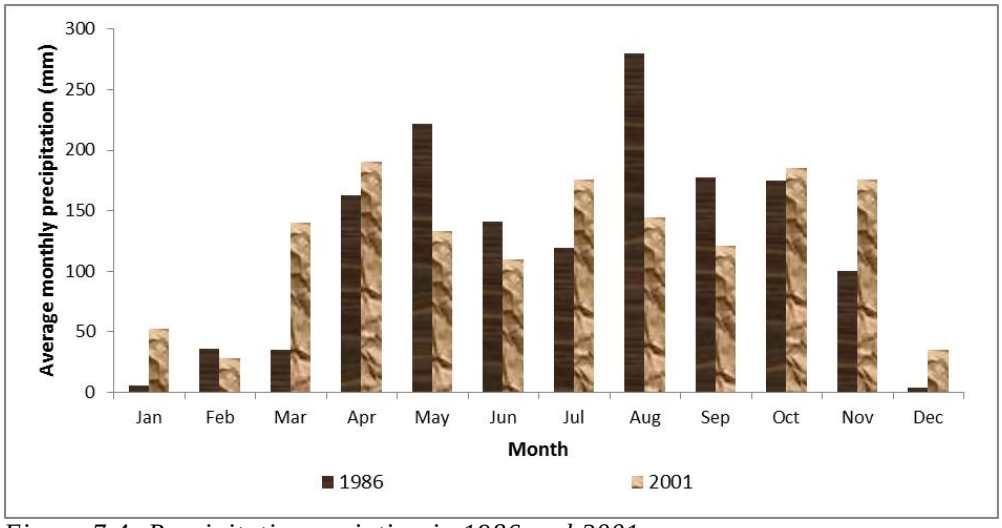

Figure 7.4: Precipitation variation in 1986 and 2001

7.1.3 Hydrologic impact of land use change

The assessments of the hydrologic impact of land use change were carried out with two objectives. The first objective was to consider the impact of land use change in the actual situation, when both climatic variation and land use change are considered. The second objective was to consider only the variation in the land use and keep the climatic dataset constant. The second objective was meant to isolate the effect of climatic variation on the hydrologic processes from the effect of land use changes. The second objective was extended in chapter eight where hydrologic impacts of the experimental land use change scenarios were simulated.

In the first objective, 1986 hydrologic processes were simulated using the climatic dataset for 1980 to 1986, and 2001 hydrologic processes were simulated using the 1999 to 2001 climatic dataset. The analyses of the hydrologic processes were based on 1986 simulation and 2001 simulation respectively. In 1986 simulation, a six years "warm up" period was used to initialize the model and in 2001 simulation, two years "warm up" period was used. In the second objective, the hydrologic processes for both years were simulated using a kind of average climatic dataset for 1986 and 2001, corresponding to 1981 (Figure 7.3). Three years of initialization was considered, hence the climatic dataset used in the second objective including the initialization periods was from 1978 to 1981.

7.2 Results and discussion

7.2.1 The hydrologic impact of land use change in actual situation

In 1986, the summaries of the annual water balance are shown in Figure 7.5. The water balance analyses indicate that the net basin water yield was 168.26 mm. Out of which, 116.11 mm was contributed by baseflow, representing 69% of the water yield and surface runoff contribution was 39.44 mm equivalent to 23.4% of the water yield. The remaining portion (7.6%) was contributed by the lateral flow.

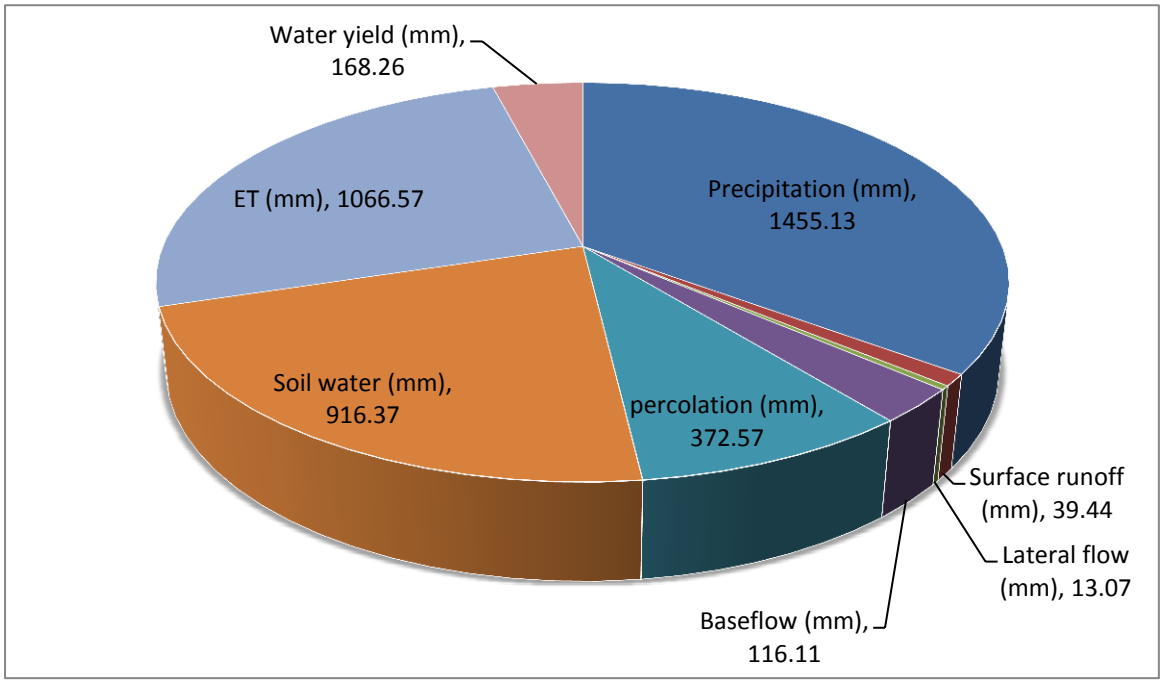

Figure 7.5: The annual average water balance summary, 1986

In 2001, the summaries of the annual water balance shown in figure 7.6 showed that the net water yield of the basin in the year was 177.46 mm. The details analysis shows surface runoff contributing 25.38 mm of water to the net basin water yield, which was equivalent to 14.3%. The surface runoff contribution in 2001 was therefore less than 1986 surface runoff by 14.06 mm. The baseflow was the most dominant hydrologic process in 2001 contributing up to 78.4% (139.17 mm) to the net water yield.

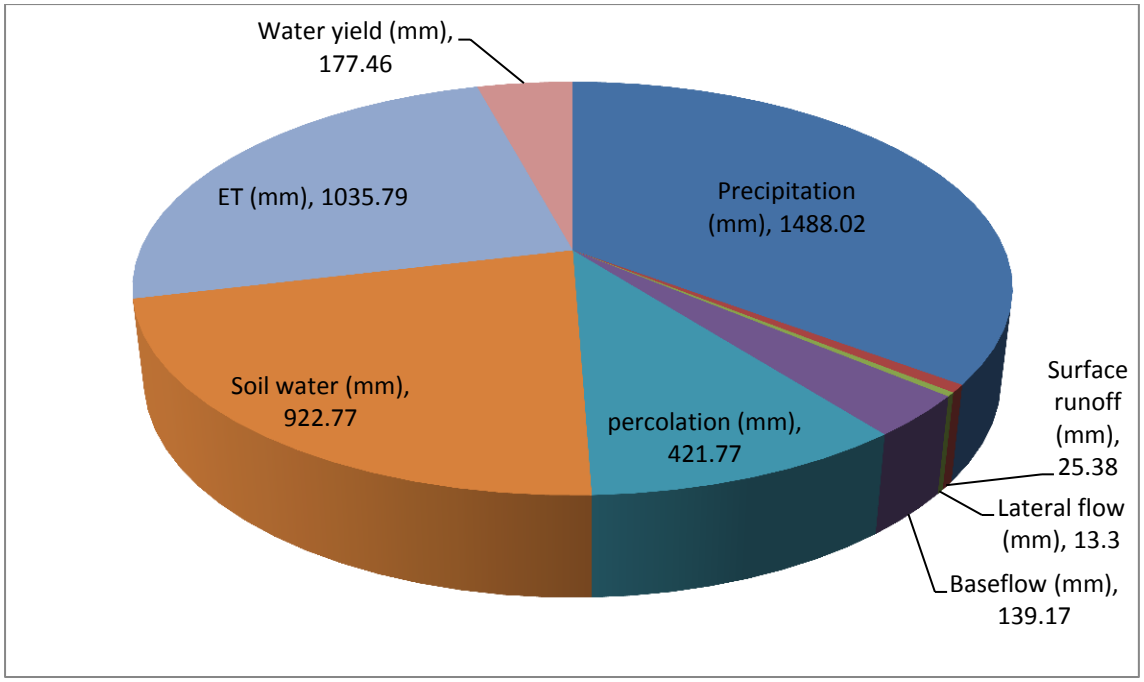

Figure 7.6: The annual average water balance summary, 2001

The analysis of variation in water balance in 1986 and 2001 are shown in figure 7.7 indicates that the year 2001 was relatively wetter, with annual average precipitation difference of 32.89 mm. The net water yield in 2001 was also more by 9.2 mm, equivalent to $112.10^6 m^3$ compared to the year 1986. The difference in the annual water yield could in part be attributed to the differences in wetness. However, the difference in actual evapotranspiration, which is 30.78 mm more in 1986 than in 2001, cannot be explained by the difference in annual precipitation received alone. Actual ET is a function of vegetation types, moisture condition, aerodynamic and surface resistance and available energy. In this analysis, moisture availability is ruled out because 2001 was wetter and therefore should have more ET. Considering that the variability in solar radiation and wind speed are minimal on average, the contribution of vegetation change in actual ET variation becomes significant.

The differences in baseflow contribution also indicate a significant effect of land use change on the hydrologic process. In general, increase in baseflow in the year 2001 may be associated with reduction in deep rooted vegetation. The analysis of land use change indicated that there was a decrease in forest cover by up to 3 % and this is in support of more baseflow generation.

The surface runoff generation processes in the two years showed a decrease by 14.06%. Runoff process is promoted in landscape covered with less dense vegetation. In 1986, more agriculture land covers were probably the main source of surface runoff. However, in 2001,

the agricultural land covers were decreased and more rangelands were regenerated. The reduction in agricultural land cover and regeneration of rangelands could explain the general change in surface runoff contribution.

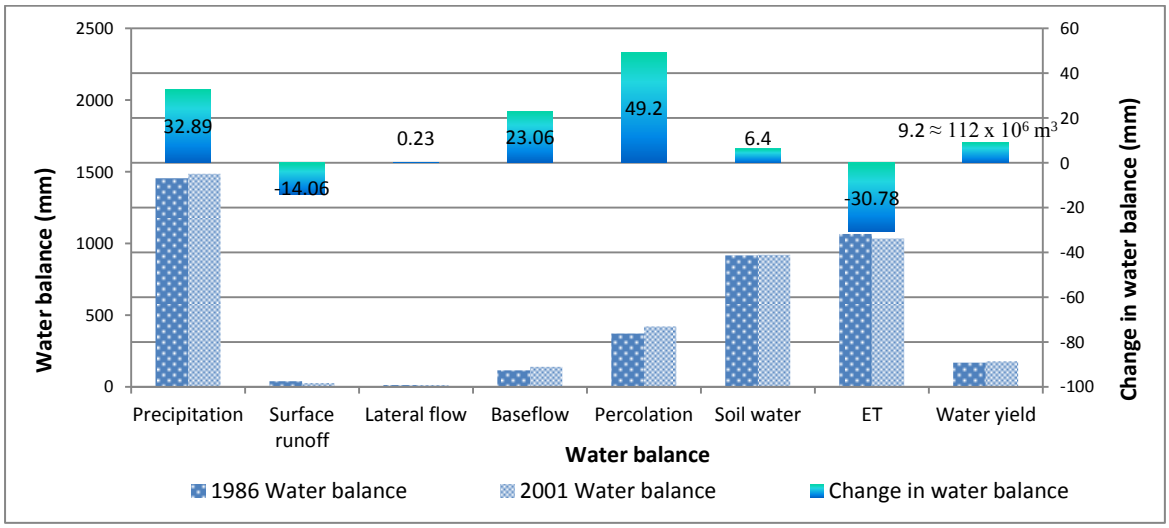

Figure 7.7: Water balance variation in 1986 and 2001, variable climate

7.2.2 The hydrologic impact of land use change under non-variance climate

In Figure 7.8, the net water yield in 2001 after subtracting the effect of precipitation and climatic variables increases by 2.52 mm equivalent to $30.10^6 m^3$ compared to 9.2 mm ($112.10^6 m^3$), when climatic records were allowed to vary. The analysis also showed a decrease in actual ET, which is a manifestation of lost in forest cover. However, the baseflow in non-variance climate simulation showed a slight increase of 1.52 mm, compared to 23.06 mm using variable climate. The increase in baseflow using non-variance climate simulation still confirms the effect of deforestation in the year 2001 on the hydrologic process, although the effect was rather small. The significant water gained (30 million cubic meters) in 2001 due to deforestation could be beneficially used in supplemental irrigation to boost the agricultural production.

In general, analyses using non-variance climate simulation indicated that land use changes had significant impact on the hydrologic process in the two years; however, some influence especially baseflow was mainly due to difference in precipitation.

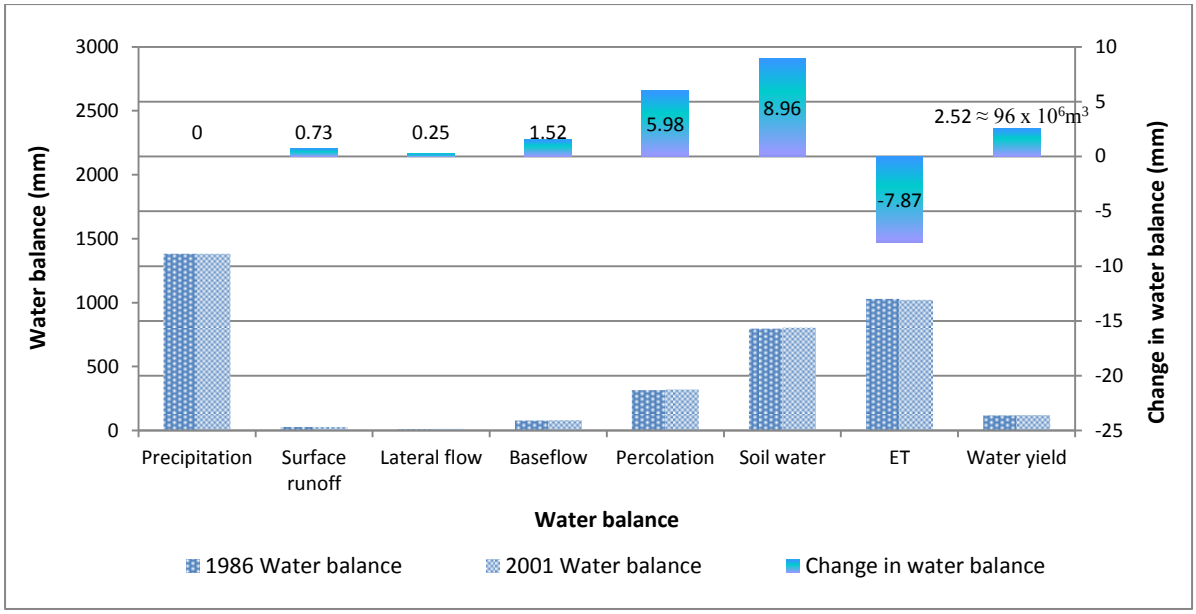

Figure 7.8: The effect of land use change on hydrologic processes in reference years, non-variable climate

7.3 Conclusion

The hydrologic process simulations were performed to quantify the available water resources in Aswa basin as it was before 1986 and as it is at present after 2001. The analyses indicated that more water was available in 2001 than in 1986. It was shown that this increase was due to mainly two factors. The first factor was changes in land use and second was precipitation difference. The aggregated effect of land use change and precipitation difference had a net increase in water yield by 9.2 mm equivalent to $112.10^6 m^3$ of water. Subtracting the effect of precipitation variation, using single (non-variable) climate simulation, land use change influence showed an increase in water yield by 2.52 mm equivalent to $30.10^6 m^3$ of water. In general, the analysis provided in this chapter reinforces the following conclusions:

1. Reduction in forest cover (deforestation) increases contribution of groundwater to streamflow, and the net water yield. This is in general agreement with published literatures.
2. Regeneration of rangelands and reduction of agricultural land cover decreases surface runoff contribution to streamflow.
3. Precipitation rates and amount is the key driver to hydrologic processes. In this respect, using non-variance climate may be valuable in assessing the effect of land use changes alone on the hydrologic processes.

Chapter 8

8. Hydrologic impact of experimental land use scenarios

8.1 Technical background

The recent government incentives towards afforestation and commercialization of agriculture, provides both opportunity and constrain to water resource management. Noting from the previous discussions, environmental benefits of afforestation may include among others, reduced peak flows and reduced sediment and nutrient loads of rivers. However, the afforestation project can also consequently reduce water yield. It has been suggested that a well-chosen spatial planning of afforestation can enlarge the beneficial environmental impact of afforestation (Brooks et al., 2003). For example, afforestation of steep terrain or near-stream areas is usually assumed to have a relatively larger effect on the streamflow regime. Little however, is known about the potential consequences of agricultural expansion on water yield. But from the water quality point of view, agricultural land covers are potential non-point pollutant source. In the case where fertilizer application is minimal, this threat is not substantial to water quality management. However, the replacement of the dense grassland, with agricultural land cover may affect runoff generation and consequent sedimentation.

To have an effective planning and management of land and water resources, the environmental benefits a particular land use change pattern must be known in advance. However, the spatial planning of land use with the objective of optimizing environmental benefits such as sediment and nutrient loads, streamflow and groundwater yield, is still far to be achieved due to the complexity of the process involved. Most of the attempts in land use change impact assessments, using hypothetical land use scenarios offer more of a solution to particular land use change problem than opportunity to manage future land use change impact.

In this chapter, the emphasis was to support the operational decisions concerning future land use change (afforestation and agricultural land use policies) in the study area using six experimental land cover scenarios generated using different spatial policies concerning possible afforestation and agricultural land use pattern that can arise in the near future. The specific objectives of this chapter were to examine the spatial variation in hydrologic

response that can arise as a result of spatial policies concerning future land use change and assess the relationship between the spatial location of land use, extent of the land use and type of land use (in this case forest and agricultural land cover) on water yield generation.

8.2 The climatic conditions

The climatic conditions are discussed in the previous chapter. In this chapter, spatial analyses of the hydrologic response were made with reference to the local climatic condition and to the land cover change. In the reviewed literatures in the previous chapter, precipitation was acknowledged as the key driver to hydrologic processes. In this chapter, effort was made to explore the effect of the spatial variability in precipitation on the hydrologic processes and how this affects the type and extent of land use in a given climatic zone. For simplicity, the climate zoning in this chapter was aggregated into three, defined as dry (Very dry and dry), wet (moderate and wet), very wet (see chapter VI for detail description).

8.3 Land use scenarios analyses

Six experimental land use scenarios, showing different land cover extend and location as derived in chapter IV were used in this chapter in the simulation of hydrologic impact of land use change. The land use scenarios were not time dependence hence were not a prediction of the future. The analyses of the land use scenarios at basin scale and sub-basin scale are provided in the following sub-sections.

8.3.1 Basin scale analyses of land use scenarios

The extent of the six experimental land use scenarios is shown in Figure 8.1. In the first scenario, agricultural expansion takes 12.4 % of the basin area, while plantation forest takes 7.5 % of the basin area. In the second and fifth scenarios, the allocation to plantation forest is high and may be considered unrealistic at basin scale. However, for the purpose of testing spatial policies, the second and the fifth scenarios present crucial afforestation policies in terms of spatial location and extent.

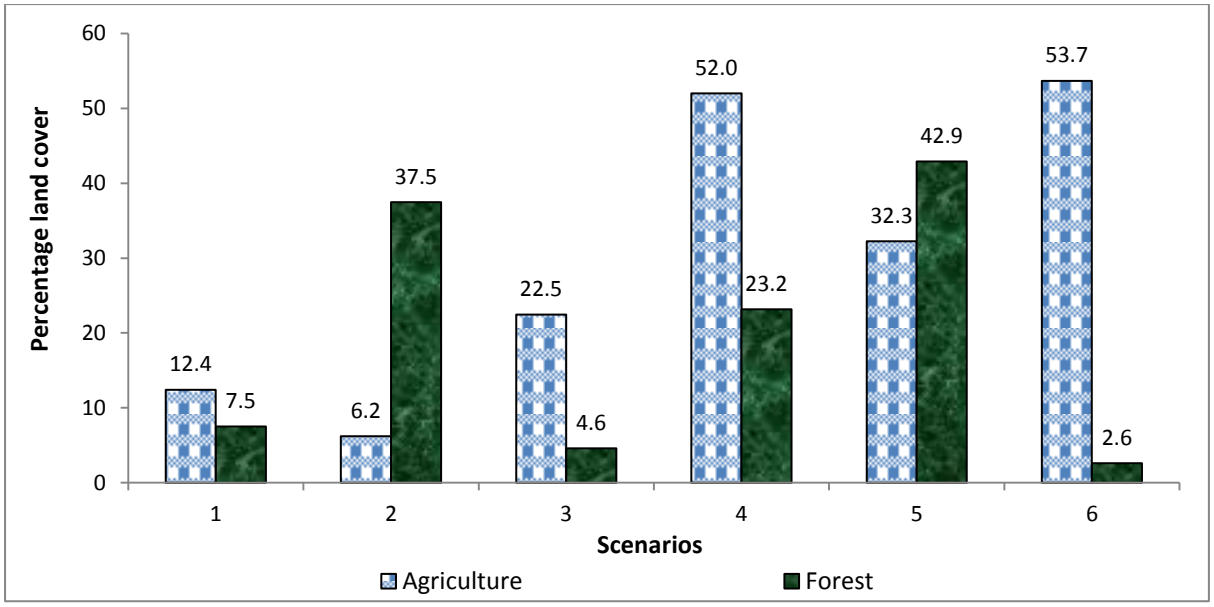

Figure 8.1: Experimental land use coverage at basin scale

8.3.2 Sub-basin scale analyses of land use scenarios

The sub-basin scale (spatial) representations of scenarios were used to show land cover location (spatial arrangement) in the basin. The spatial arrangement of the six experimental land use scenarios were analysed in this section.

a) Scenario I

Figure 8.2 and 8.3 shows the graphical and map representation of the spatial arrangement of forest and agricultural land use scenarios. The graphical representation indicates that the new plantation forests were mainly allocated in very wet region of the basin (sub-basins 30, 21, 22, 18, 25, 27, 28, 36 and 38).

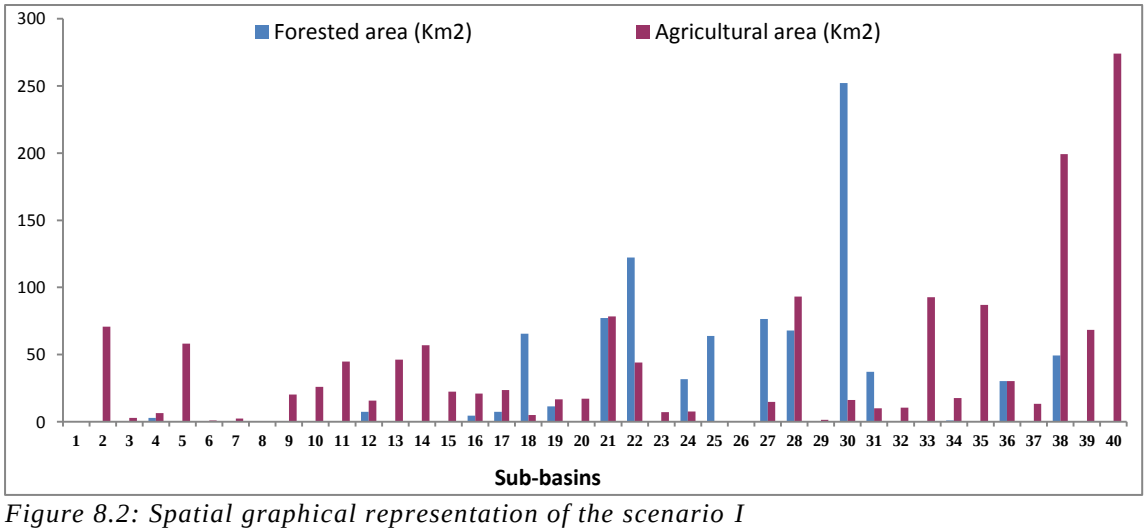

Figure 8.2: Spatial graphical representation of the scenario I

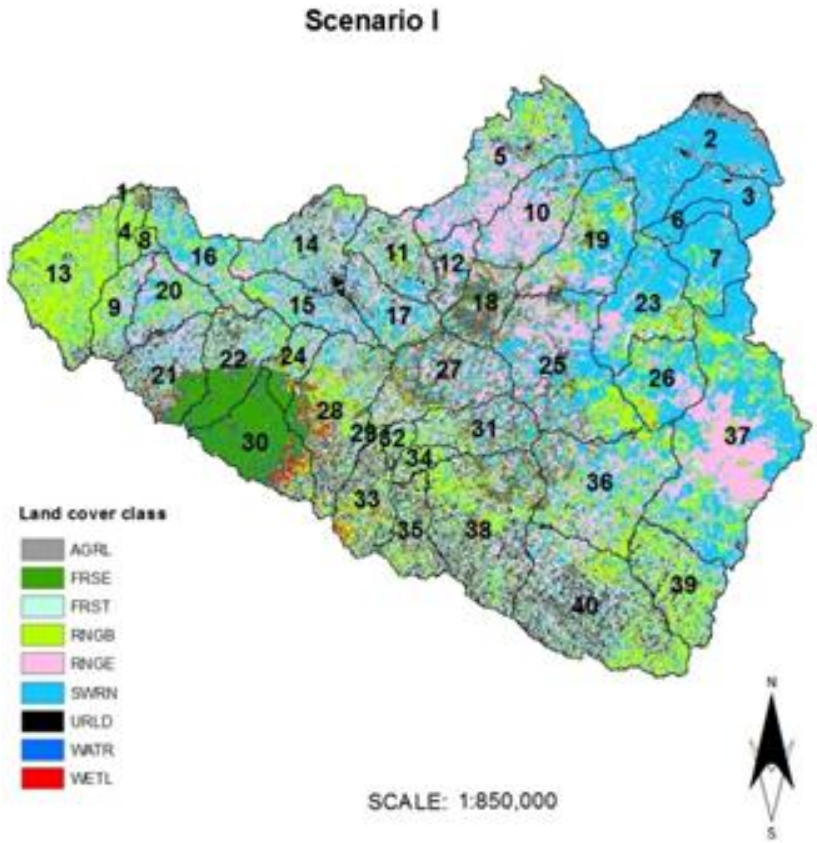

Figure 8.3: Spatial representation of experimental land use scenario I

b) **Scenario II**

The analyses of the land cover extent and location in the second scenario is shown in Figure 8.4 & 8.5. The graphical and map representation shows that agriculture and forest land cover scenarios were spread all over the basin with different coverage (extent) in the sub-basins. The map representation of the second scenario indicates a skewed distribution of afforestation toward the southern and wetter regions of the basin (sub-basins 40, 38, 35, 33, 13, 39) and to lesser extent in the central and northern part, the less wet region (Figure 8.2). The extent of the forested land cover in each sub-basin is shown in Figure 8.4. At least all sub-basins were afforested in this scenario, with sub-basins 34 and 13 having the largest forest cover >80%, which may seems to be unrealistic allocation, except if the sub-basin represent the gazetted areas for afforestation.

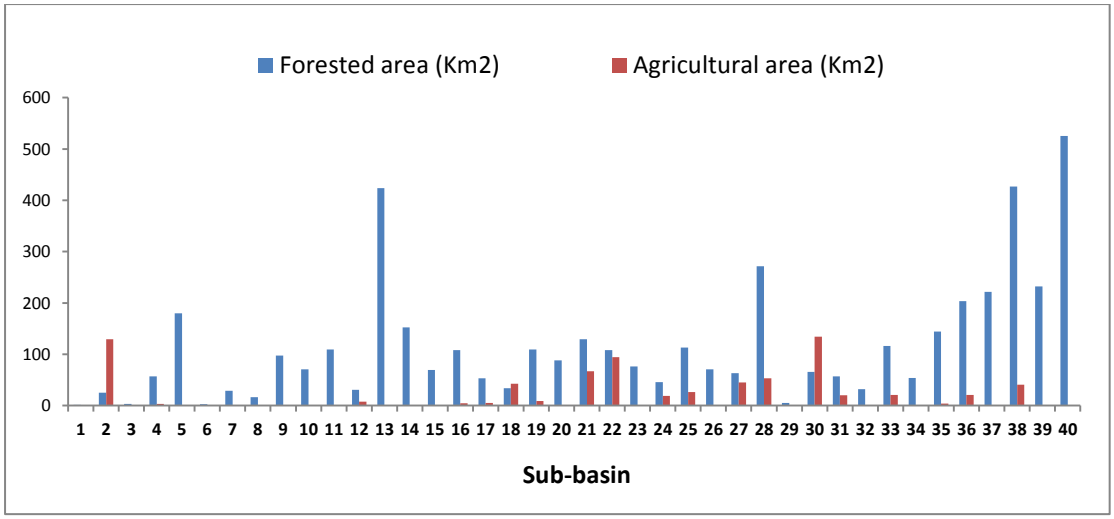

Figure 8.4: Spatial graphical representation of the scenario II

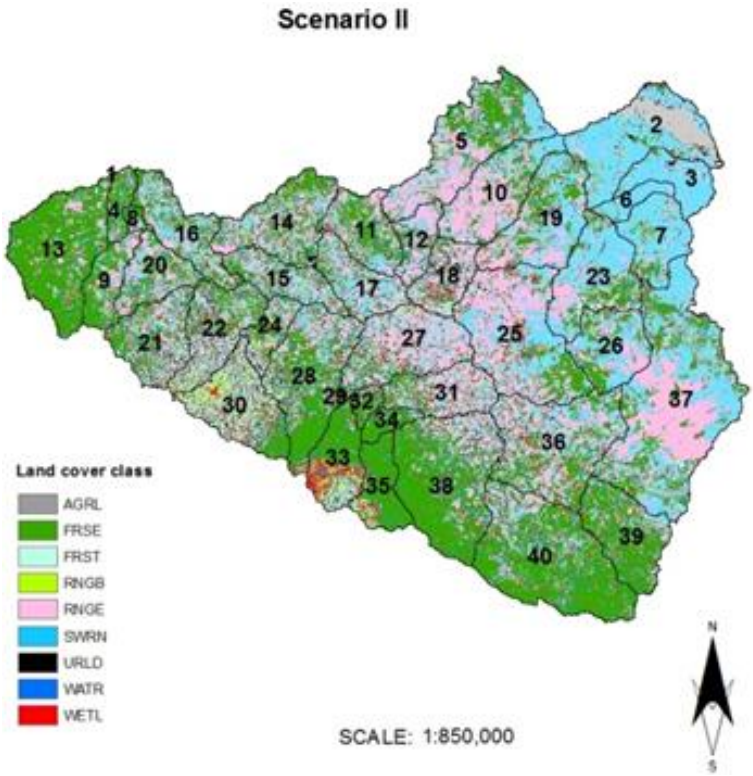

Figure 8.5: Spatial map representation of scenario II

c) Scenario III

The analyses of the afforestation and agricultural land use extent and location in the third scenario are represented in figure 8.6 and 8.7. The scenario represents medium growth in agriculture and low growth in forest development. The forest development is mainly in the central sub-basins (27, 18, 31 and 25) and to lesser extent in sub-basins 5, 10 and 19 in the

dry region and sub-basins 17, 24, 29 and 35 in the wetest region of the basin. The agricultural land cover was however extensively increased in sub-basin 40, 38 and 2.

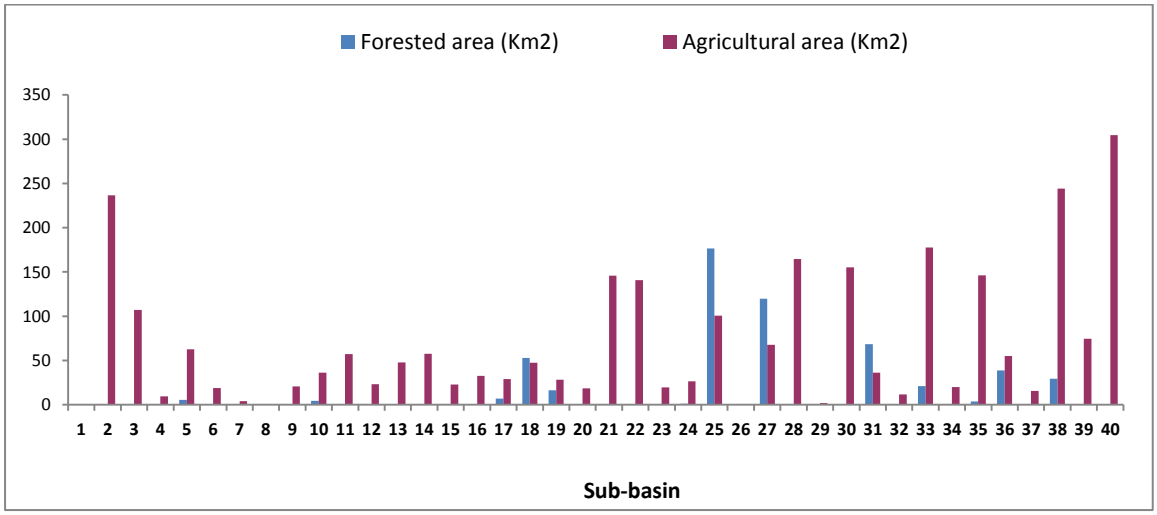

Figure 8.6: Spatial graphical representation of the scenario III

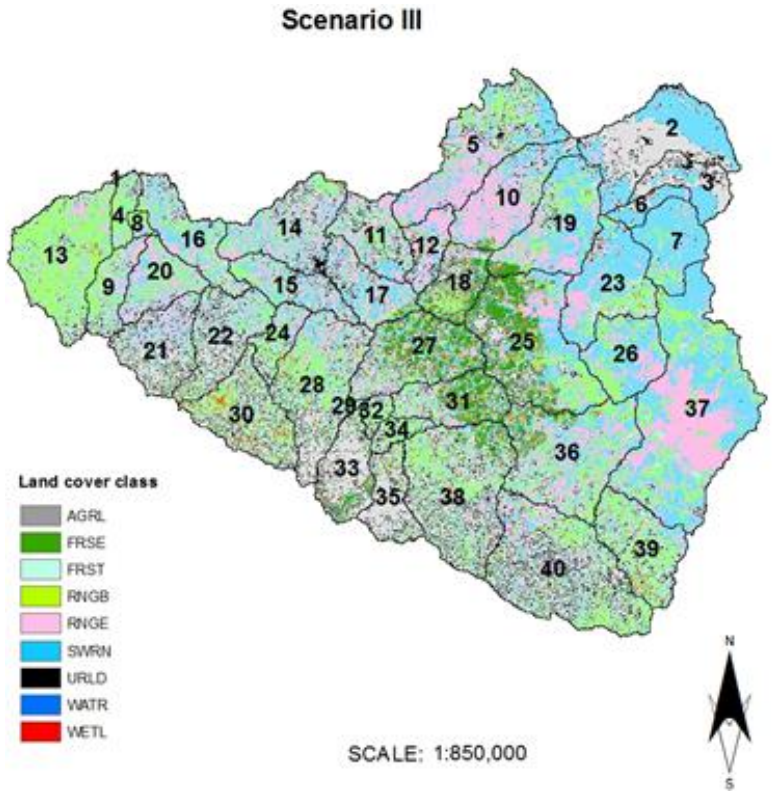

Figure 8.7: Spatial map representation of scenario III

d) Scenario IV

The analyses of the afforestation and agricultural land use extent and location in fourth scenario, represented in figures 8.8 and 8.9 shows high growth in agriculture and medium

growth in forest development. The scenario represents 52.0% increase in agricultural land and 23.2% increase in forest development. The forest land use change covered almost all the sub-basins (Figure 8.8 & 8.9) except sub-basins 30 and 35. In this scenario, sub-basins in the dry region (Figure 7.2) received significant amount of afforestation.

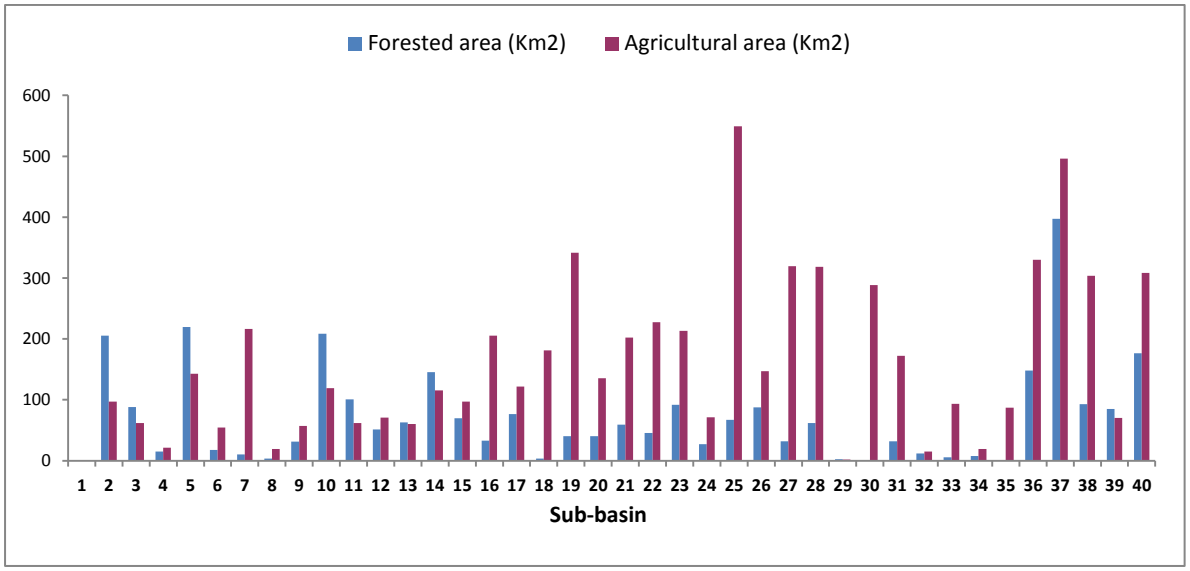

Figure 8.8: Spatial graphical representation of the scenario IV

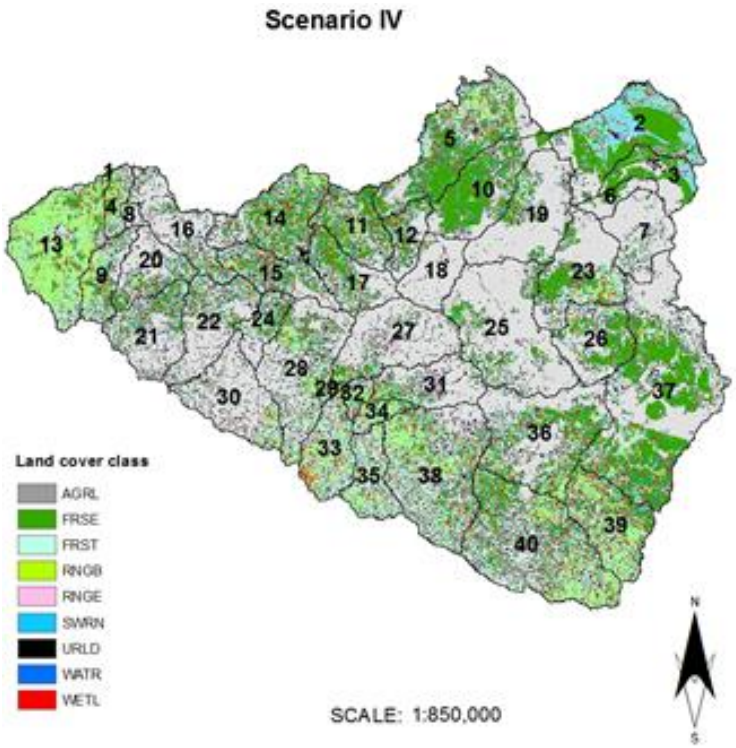

Figure 8.9: Spatial map representation of scenario IV

e) Scenario V

The fifth scenario (Figure 8.10 & 8.11) represents high growth in agriculture and high growth in forest development, similar to scenario IV. The scenario represents 32.3% growth in agricultural land and 42.9% growth in forest development. Forest land cover change was concentrated mainly in the dry regions of the basin, with over 50 % of the sub-basin's area in the arid region covered by forest.

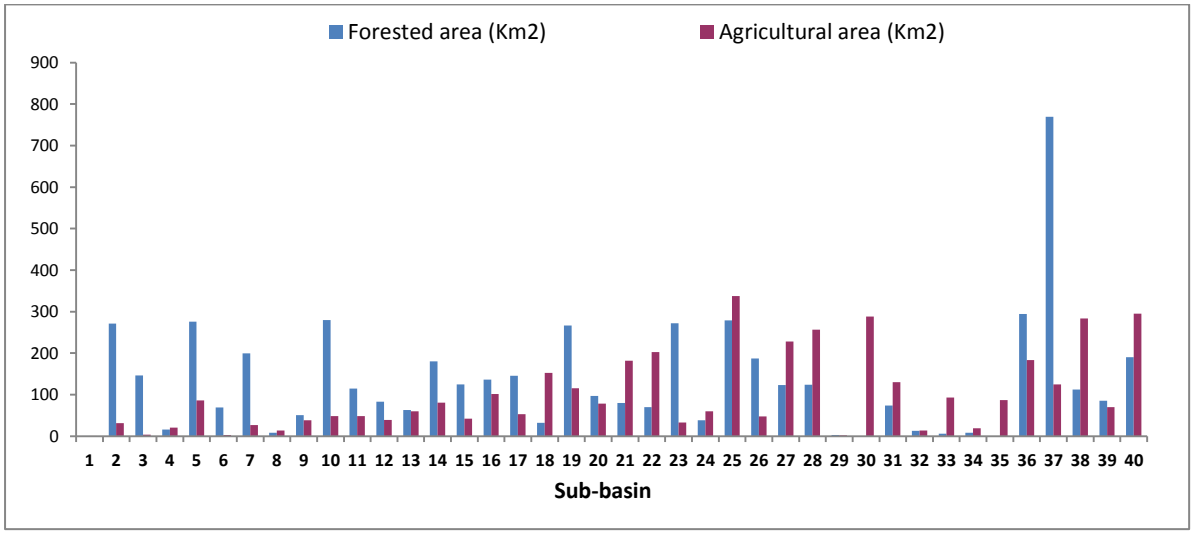

Figure 8.10: Spatial graphical representation of the scenario V

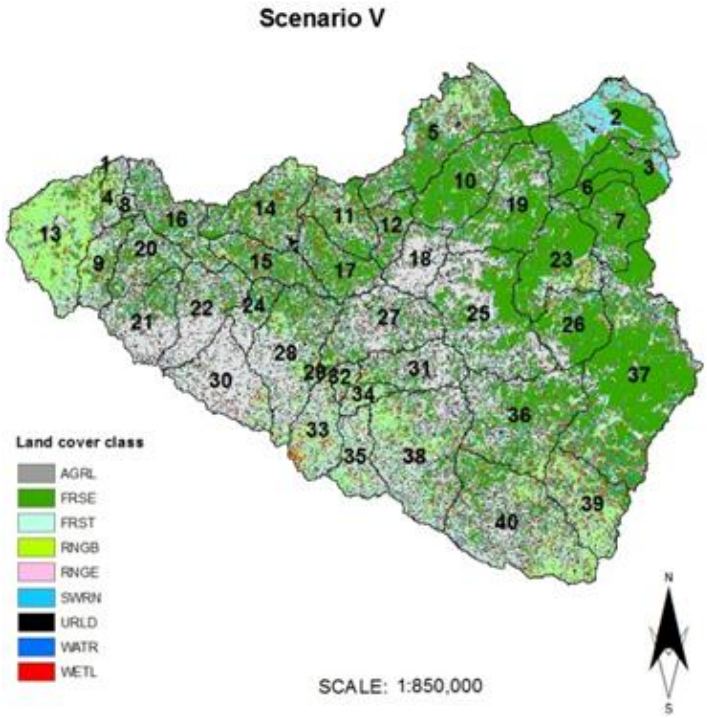

Figure 8.11: Spatial map representation of scenario V

f) Scenario VI

The sixth scenario represents high growth in agriculture and very low growth in forest development mainly in the dry region of the basin. The scenario represents 53.7% growth in agricultural land and 2.6% growth in forest development (Figures 8.12 & 8.13). The extents of the forested areas are shown in Figure 8.12.

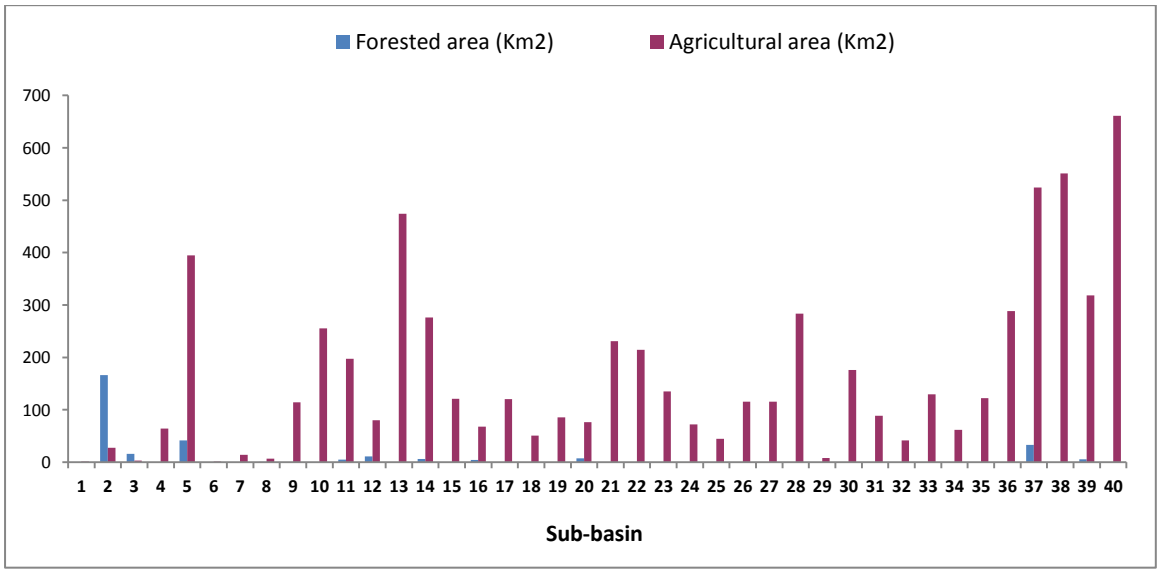

Figure 8.12: Spatial graphical representation of the scenario VI

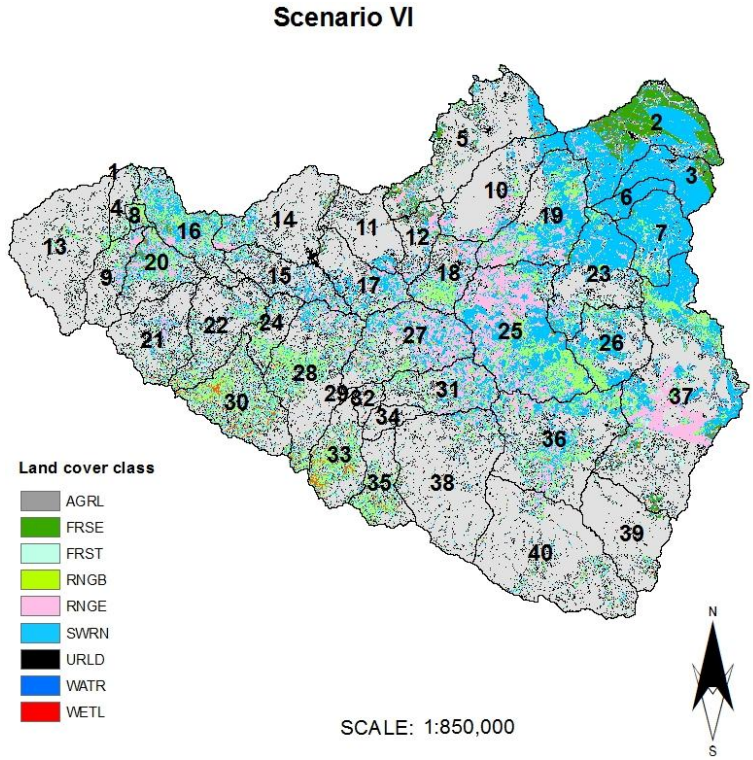

Figure 8.13: Spatial map representation of scenario VI

8.4 Hydrologic impact simulation

The hydrologic process model SWAT was used to simulate the hydrologic impact of the experimental land use changes. The hydrologic model was calibrated and validated in chapter V. The transfer of the calibrated parameters to simulate the hydrologic processes in the experimental land use scenarios was considered to have no consistent impact on the predicted change in water yield relative to baseline conditions, since the analyses in this chapter was a relative comparison. The results are therefore considered independent of the model efficiency and accuracy in prediction of water balance variables.

The simulations of the hydrologic impact were made using a single simulation periods of 1999 to 2001 for all the scenarios. In this simulation, 1999 and 2000 were used as initialization periods. The analyses of the hydrologic impact of the experimental land use change were then based on 2001 simulation.

Surface runoff contribution to streamflow was used as the hydrologic indicator in analysing and discussing the hydrologic response at sub-basins and basin scale. Surface runoff generation was considered to be more sensitive to land use change, because of its quick response and sensitivity to land surface cover. Groundwater processes (baseflow, shallow aquifer recharge and deep aquifer recharge) were also discussed at sub-basins and basin scale.

8.4.1 Water use estimates in different land cover

Analyses of actual monthly average evapotranspiration for different land cover in the study area (Figure 8.14) was made to give an insight to how much water on average is demanded by the different land cover per month and how these different in water demand affect the replacement of the land cover with another land cover. The result showed that agriculture is second smallest water user in the basin after settlement land cover. The analyses also indicate that the different in water requirement between forest evergreen (plantation forest) and semi-arid range, the dominant land cover in the dry climates was just 11.8 mm of water monthly. Similarly, semi-arid range demands 4.7 mm of water more than agriculture monthly. Generally, it can be proposed that land use “succession order”, defined here as the substitution of the existing land cover with the new land cover of interest plays a crucial role in the net impact of a particular land use change on hydrologic processes.

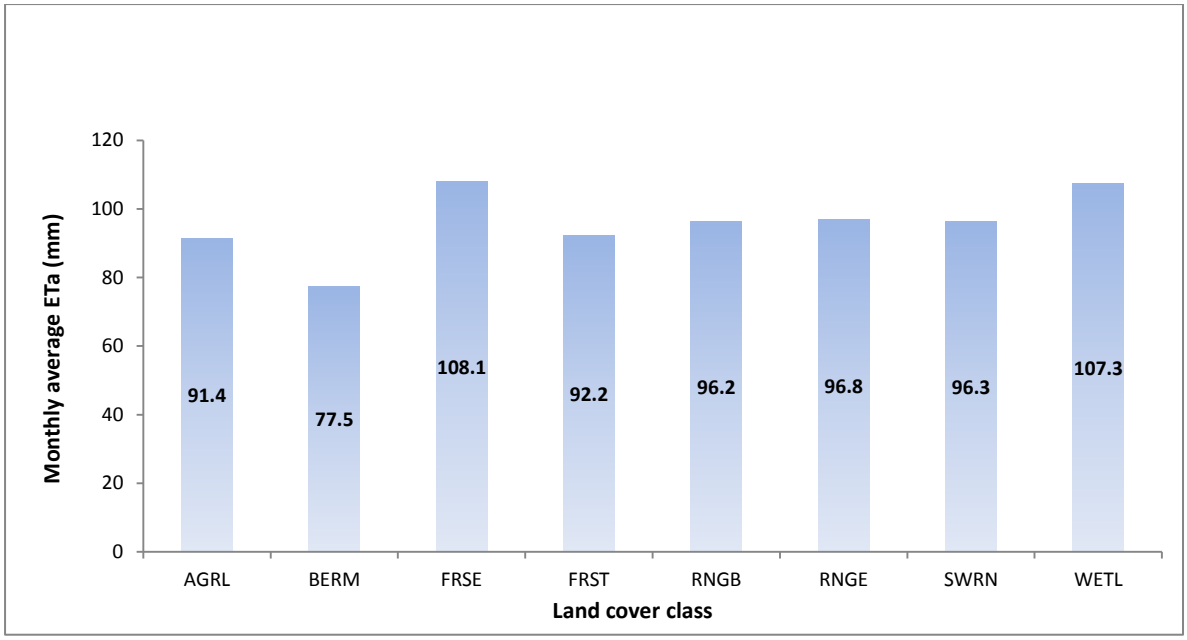

Figure 8.14: Estimated contribution of ET for each land cover in the study area

8.4.2 Hydrologic impact of experimental land use scenario I

The analysis of the hydrologic impact of land use change in scenarios I is shown in Figure 8.15. The analyses showed that the impact of increasing forest land cover in the sub-basins was a decrease in surface runoff generation. In sub-basins 12 and 19 located in dry region the impact of afforestation on surface runoff generation were less pronounced. In other words, increase in forest land cover did not show any significant change in surface runoff generation. The reduction in surface runoff in sub-basin 12, which cannot be visually seen in Figure 8.15, was about 0.018 mm corresponding to 5.5% increase in forest land cover. In sub-basin 17, located in wet zone, the impact of 3.3% increase in forest land cover was a reduction in surface runoff by 0.24 mm.

Similar impact of forest land cover change to surface runoff generation can be seen in sub-basin 24 and 25, with small increase in forest land cover producing significant reduction in surface runoff contribution to streamflow.

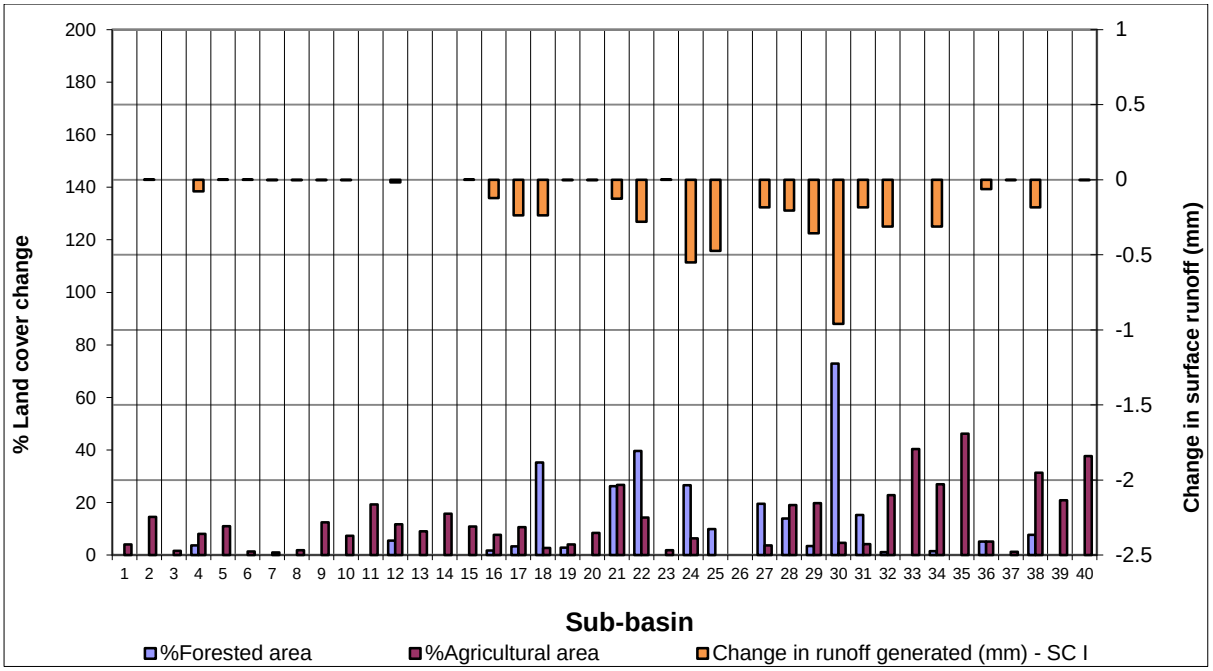

Figure 8.15: Surface runoff generation response to land cover change in scenario I (SC I)

There seems to be an interesting correlation between afforestation and surface runoff generation in scenario one. The regression analysis indicates a negative correlation with correlation coefficient of -0.6012 (Figure 8.16).

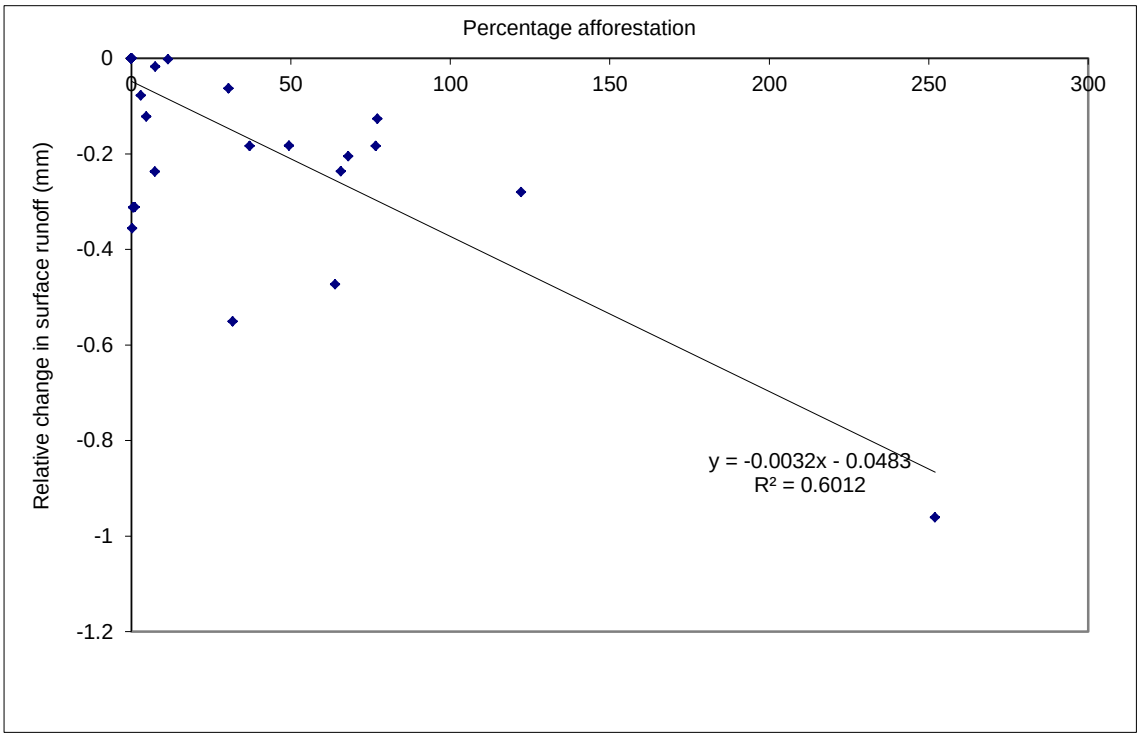

Figure 8.16: Regression plot afforestation and surface runoff generation scenario I

At basin scale, scenario I produces a notable change in surface runoff generation (Figure 8.17). The surface runoff was reduced by 2.79 mm, which is equivalent to 15.5% of the baseline surface runoff generation. Groundwater contribution to streamflow was also significantly decreased by 7.54 mm of water, which is equivalent to 5.7% of the baseline condition. The net water yield of the basin was reduced by 9.98 mm of water corresponding to about 6% of the baseline. The actual ET was increased by 10.8 mm, which is equivalent to 0.89% of the baseline scenario.

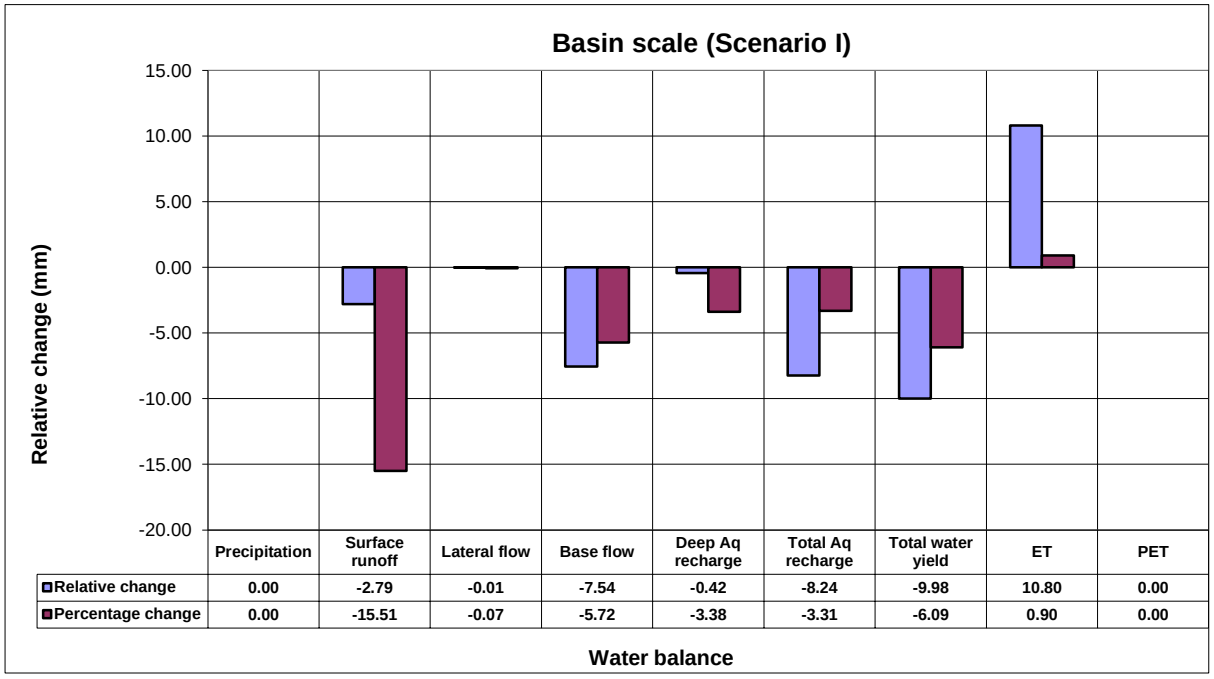

	Precipitation	Surface runoff	Lateral flow	Base flow	Deep Aq recharge	Total Aq recharge	Total water yield	ET	PET
Relative change	0.00	-2.79	-0.01	-7.54	-0.42	-8.24	-9.98	10.80	0.00
Percentage change	0.00	-15.51	-0.07	-5.72	-3.38	-3.31	-6.09	0.90	0.00

Figure 8.17: Basin scale relative change in water balance, scenario I

8.4.3 Hydrologic impact of experimental land use scenario II

The impact of increasing agricultural and forest land cover on hydrologic processes in scenario II is shown in Figure 8.18. The impact of land use change to surface runoff generation in sub-basins 2, 3, 5, 14 and 19 found in the dry region were less manifested as earlier on noted in scenario I. In sub-basins 5, 14 and 19 in particular, the impact of afforestation on surface runoff generation was insignificant increase (<0.05mm). The increase in runoff due to afforestation seems to disagree with the rest of the sub-basins in the study area and with proven knowledge (Bosch and Hewlett, 1982). However, Croke et al., (2004) observed that hydrologic system is subject to different kind of weather pattern and spatial complexity, and is dynamic and random in nature.

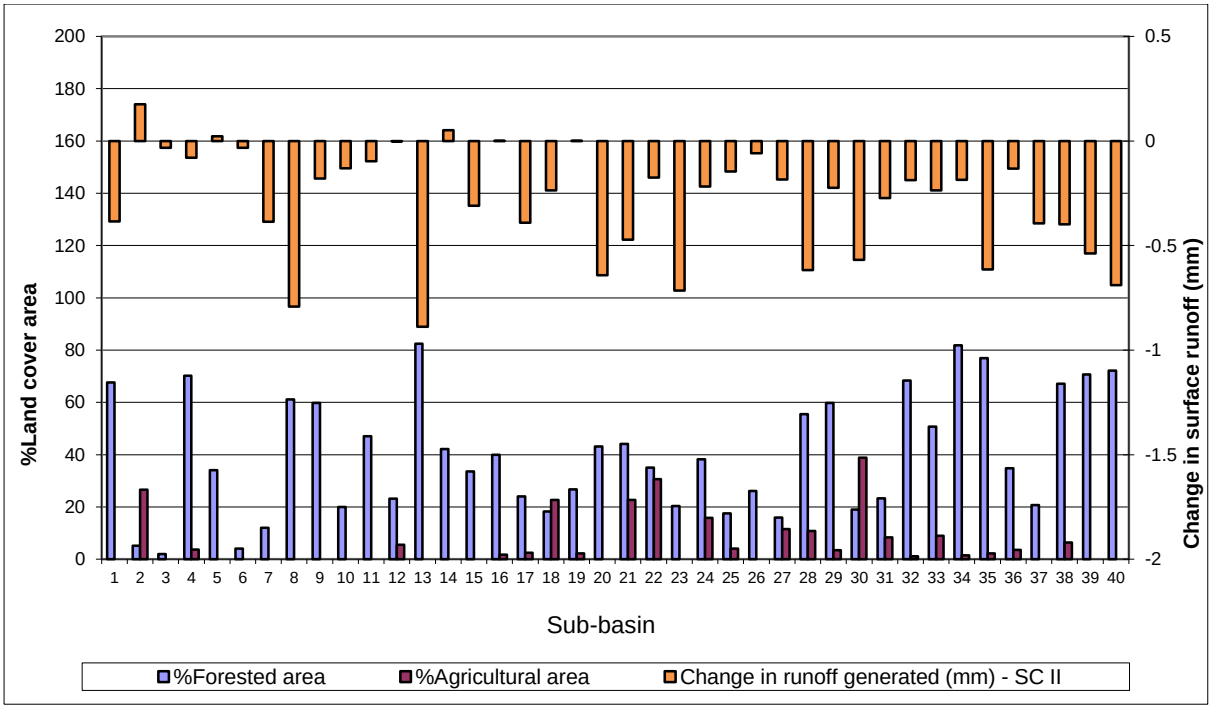

Figure 8.18: Surface runoff generation response to land cover change in scenario II (SC II)

At basin scale, the hydrologic impact of afforestation and agricultural land expansion in second scenario was summarised in Figure 8.19. The results showed a significant reduction in net water yield by 25.98 mm, which is equivalent to 15.85% of the baseline. Surface runoff was decreased by 6.42 mm equivalent to 35.69% of the baseline scenario and baseflow was reduced by 19.62 mm (14.89% of the baseline). The net actual ET of the basin was increased by 28.30 mm (2.35% of the baseline scenario) more than in scenario I.

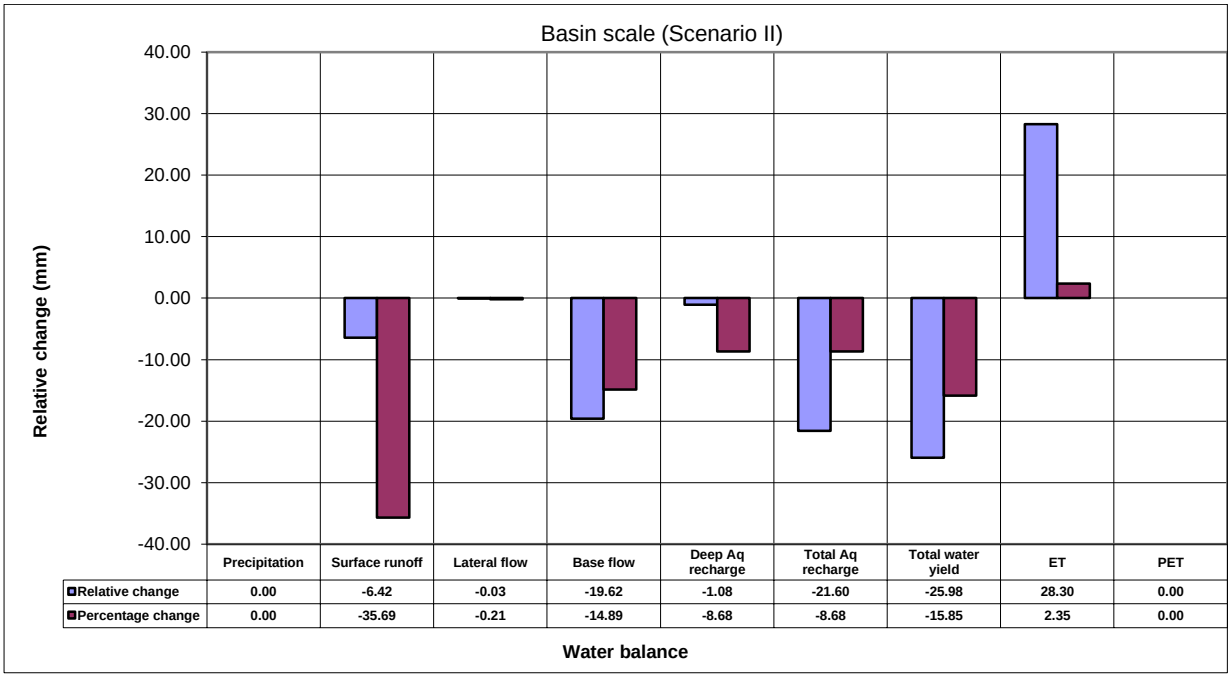

	Precipitation	Surface runoff	Lateral flow	Base flow	Deep Aq recharge	Total Aq recharge	Total water yield	ET	PET
Relative change	0.00	-6.42	-0.03	-19.62	-1.08	-21.60	-25.98	28.30	0.00
Percentage change	0.00	-35.69	-0.21	-14.89	-8.68	-8.68	-15.85	2.35	0.00

Figure 8.19: Basin scale water balance change, scenario II

The scatter plot of afforestation and relative change in surface runoff contribution to streamflow shows a weak correlation (Figure 8.20) compared to scenario I. This could mainly be due to the influence of agriculture land cover, which was more extensive in the second scenario compared to the first scenario.

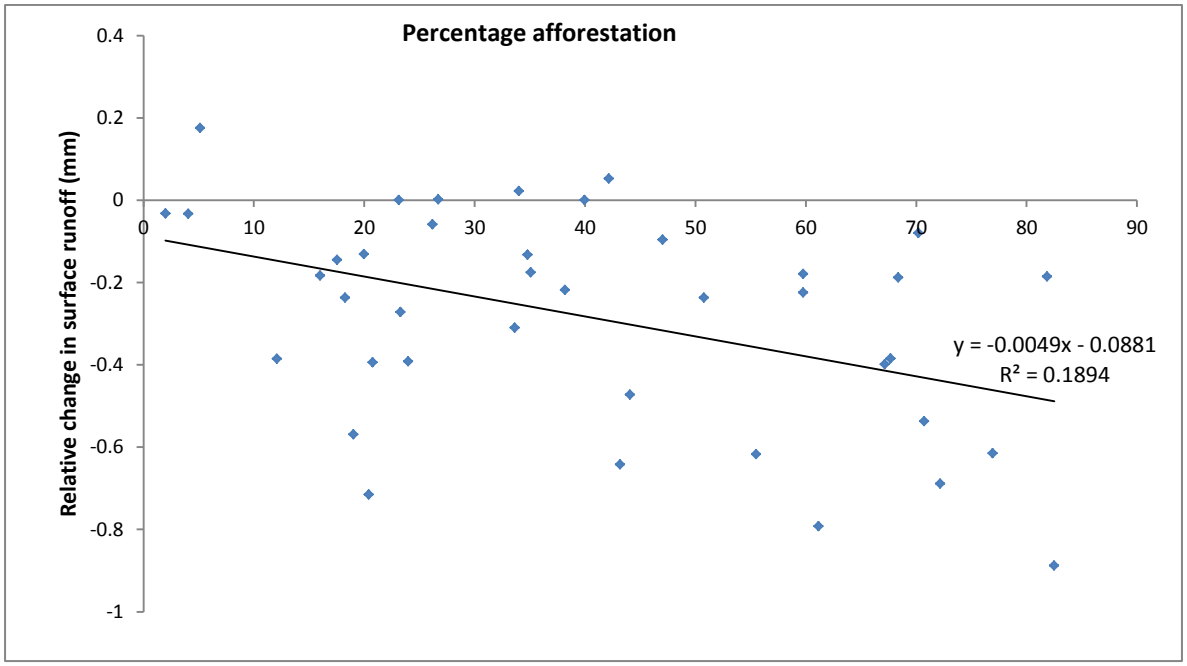

Figure 8.20: Regression plot of afforestation and surface runoff generation scenario II

8.4.4 Hydrologic impact of experimental land use scenario III

The hydrologic impact of agricultural and forest land cover change presented in the third scenario (scenario III) is shown in Figure 8.22 & 8.23. Scenario III represents medium growth in agriculture and low growth in forest development. The agricultural land cover was more extensively increased in sub-basin 40, 38 and 2, considered to be very wet.

The hydrologic responses due to the land cover changes were unique. In most sub-basins with agricultural land expansions, surface runoff generation were decreased. In scenario I and II, increase in agricultural land area responded with increase in surface runoff and afforestation reduces runoff generation except for a unique sub-basin 5, 14 and 19 in scenario II, where afforestation had small increase in runoff generation. The unique hydrologic response to agricultural land expansion in scenario III can be attributed to "succession order" in the land use change. In other words, replacement of land covers with significant difference in water demand and vegetation density e.g. semi-arid range with agriculture.

In general, the third scenario showed little spatial variation in surface runoff contribution to streamflow. The hydrologic response at basin scale, indicate increase in surface runoff by 7.45 %, baseflow by 1.82 % and net water yield by 2.26 % and actual ET was decreased by 0.42 %. The spatial location and configuration of the land covers and the succession orders of the land covers in scenario III could explain the mixed hydrologic response.

There was no statistical relationship between the forest land use change and the hydrologic response in the third scenario (Figure 8.21).

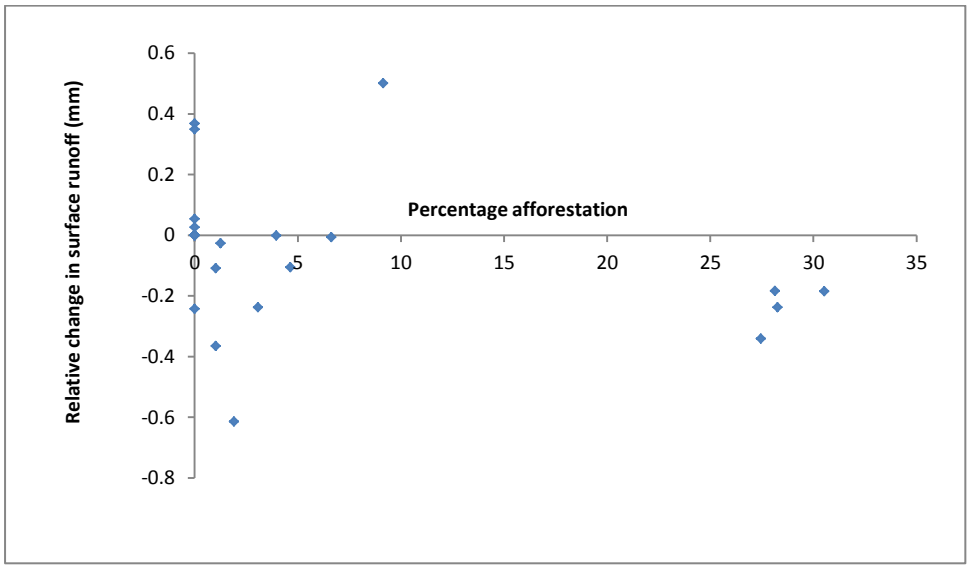

Figure 8.21: Regression plot of afforestation and surface runoff generation scenario III

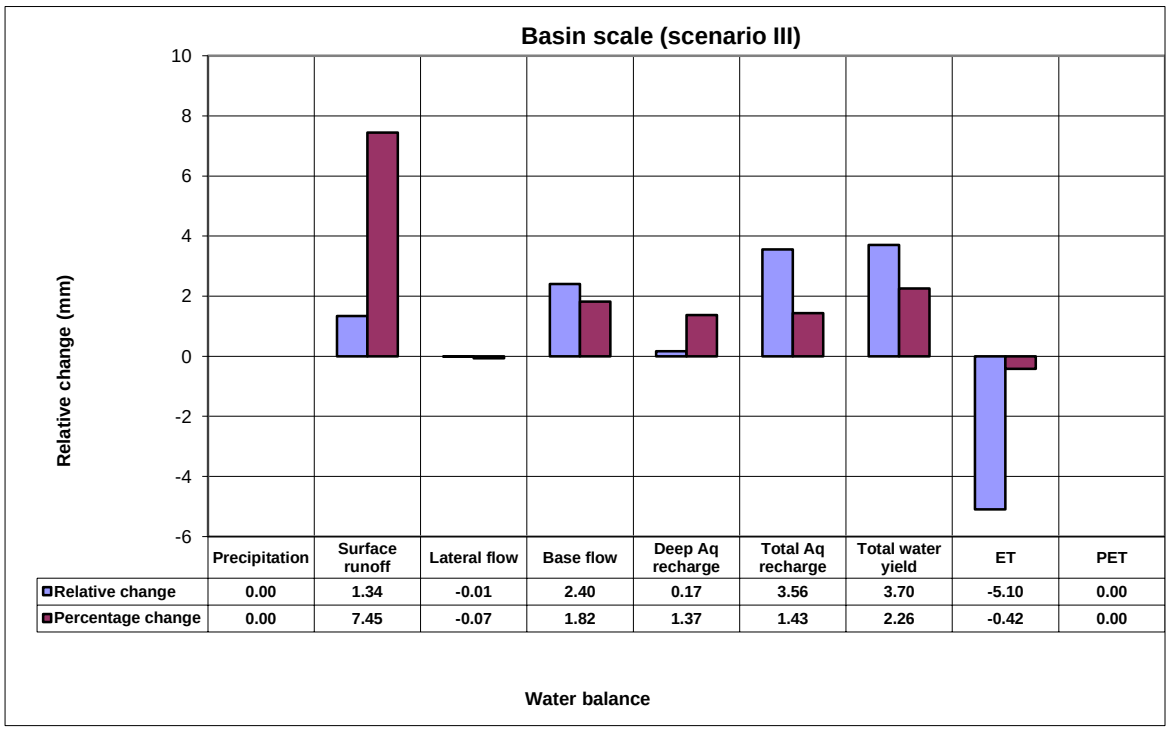

	Precipitation	Surface runoff	Lateral flow	Base flow	Deep Aq recharge	Total Aq recharge	Total water yield	ET	PET
Relative change	0.00	1.34	-0.01	2.40	0.17	3.56	3.70	-5.10	0.00
Percentage change	0.00	7.45	-0.07	1.82	1.37	1.43	2.26	-0.42	0.00

Figure 8.22: Basin scale water balance change, scenario III

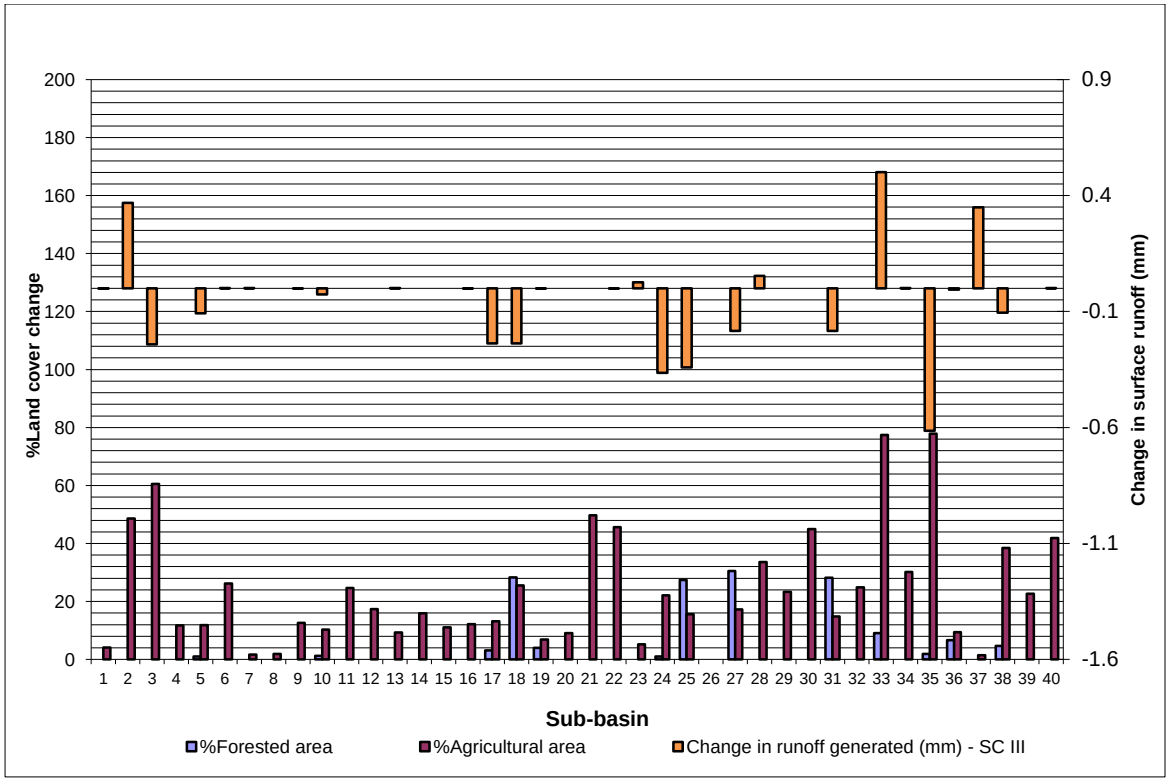

Figure 8.23: Surface runoff generation response to land cover change in scenario III

8.4.5 Hydrologic impact of experimental land use scenario IV

The hydrologic impact of afforestation and agricultural land expansion in scenario IV presented in Figures 8.24 & 8.25 showed highly mixed response at sub-basin scale. In the dry zone, afforestation produces consistence response, as noted in previous discussion. The response in wet and very wet sub-basins, however were highly variable. In sub-basin 26, surface runoff was increased by 0.87 mm against 32.58 % afforestation and 54.69 % agricultural land cover expansion. The increase in surface runoff in sub-basin 26 can be attributed mainly to agricultural land expansion, considering that in the previous analyses, afforestation in most sub-basin responded with reduction in surface runoff. In sub-basins 29, however, surface runoff was decreased by 0.25 mm against 22.5% increase in agricultural land cover and 26.2% afforestation. The hydrologic response in sub-basin 26 and 29 showed that the impact of afforestation on surface runoff generation is more significant when the two land covers are equitably increased in a sub-basin. However, in sub-basin 24, the impact of afforestation on surface runoff was dominant despite 26.2% afforestation and 59.5% expansion in agricultural land. Both sub-basins 24, 26 and 29 are located in the same climatic zone. It can be suggested that the decrease in surface in sub-basin 24, given the configuration

of 26.2% afforestation and 59.5% agriculture, was due to "succession order", with forest land cover replacing land cover with very low water demanding.

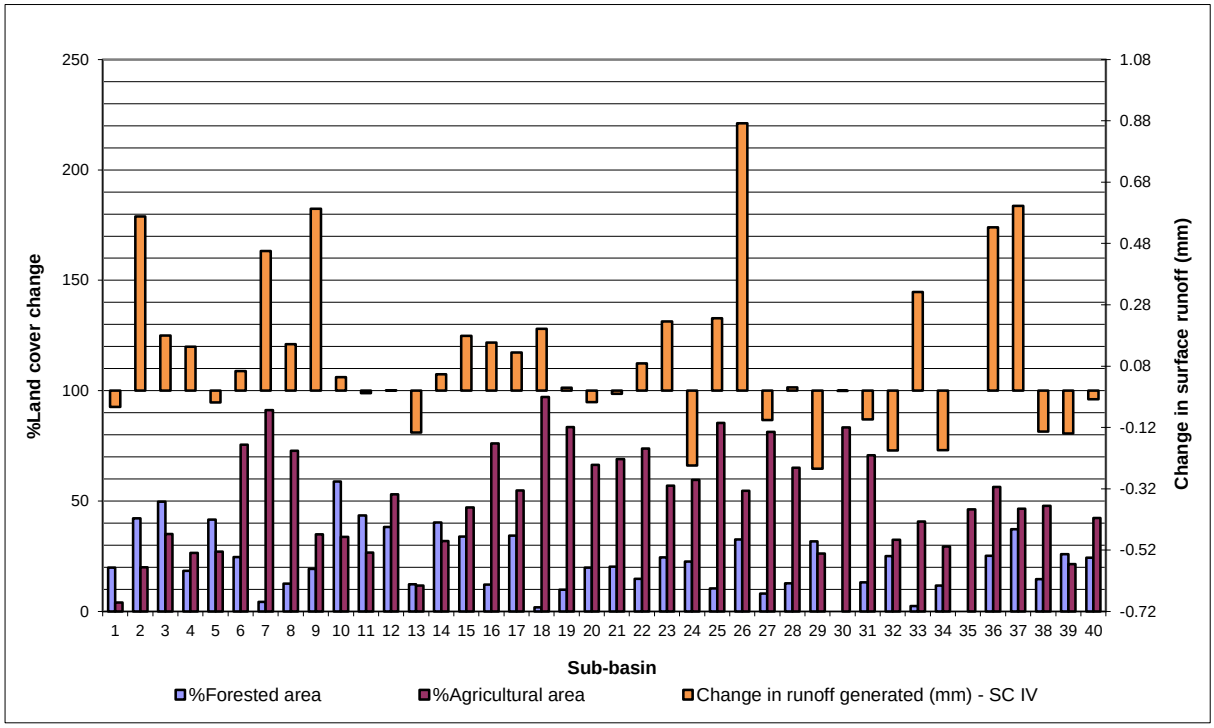

Figure 8.24: Surface runoff generation response to land cover change in scenario IV

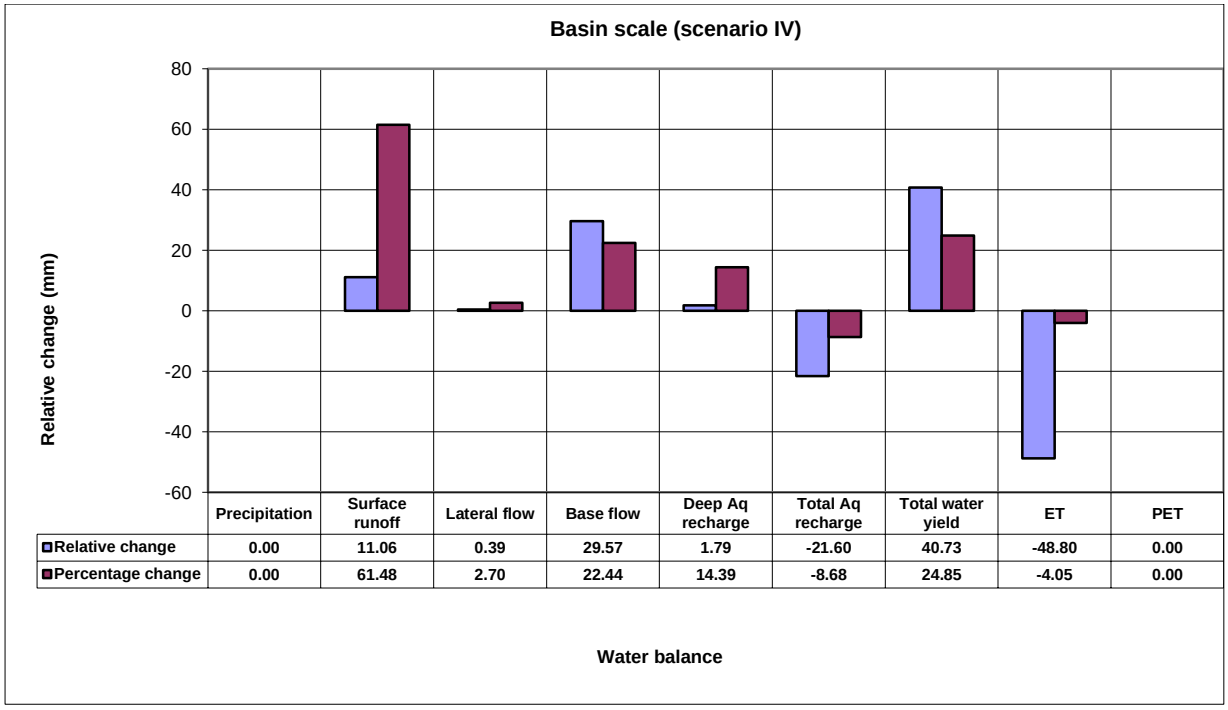

	Precipitation	Surface runoff	Lateral flow	Base flow	Deep Aq recharge	Total Aq recharge	Total water yield	ET	PET
Relative change	0.00	11.06	0.39	29.57	1.79	-21.60	40.73	-48.80	0.00
Percentage change	0.00	61.48	2.70	22.44	14.39	-8.68	24.85	-4.05	0.00

Figure 8.25: Basin scale water balance change, scenario IV

At basin scale, the analyses of the hydrologic impact of afforestation and agricultural land expansion showed an increase in surface runoff contribution by up to 61.48 % of the baseline, baseflow increased by 22.44% and total water yield increased by 24.85 %. Scenarios IV represent typical agro-forestry scenarios in the basin.

8.4. 6 Hydrologic impact of experimental land use scenario V

The analyses of hydrologic impact of afforestation and agricultural land expansion presented in scenario V are shown in figures 8.26 and 8.27. Like in the previous discussion, the hydrologic impact of the afforestation and agricultural land increase were quite mixed. In sub-basin 26 for example 69.66 % afforestation and 17.60% increase in agricultural land cover responded with 0.69 mm increase in surface runoff. This response is however quite unique and disagree with previous findings. The reasons for increase in surface runoff against afforestation in sub-basin 26 located in wet zones could be associated to an inherent model uncertainty and to land use succession order, discussed previously. In the dry regions, surface runoff was increased with afforestation. In particular, sub-basin 3 had 0.37 mm increase in surface runoff against 82.69 % afforestation and 2.01 % increase in agricultural land.

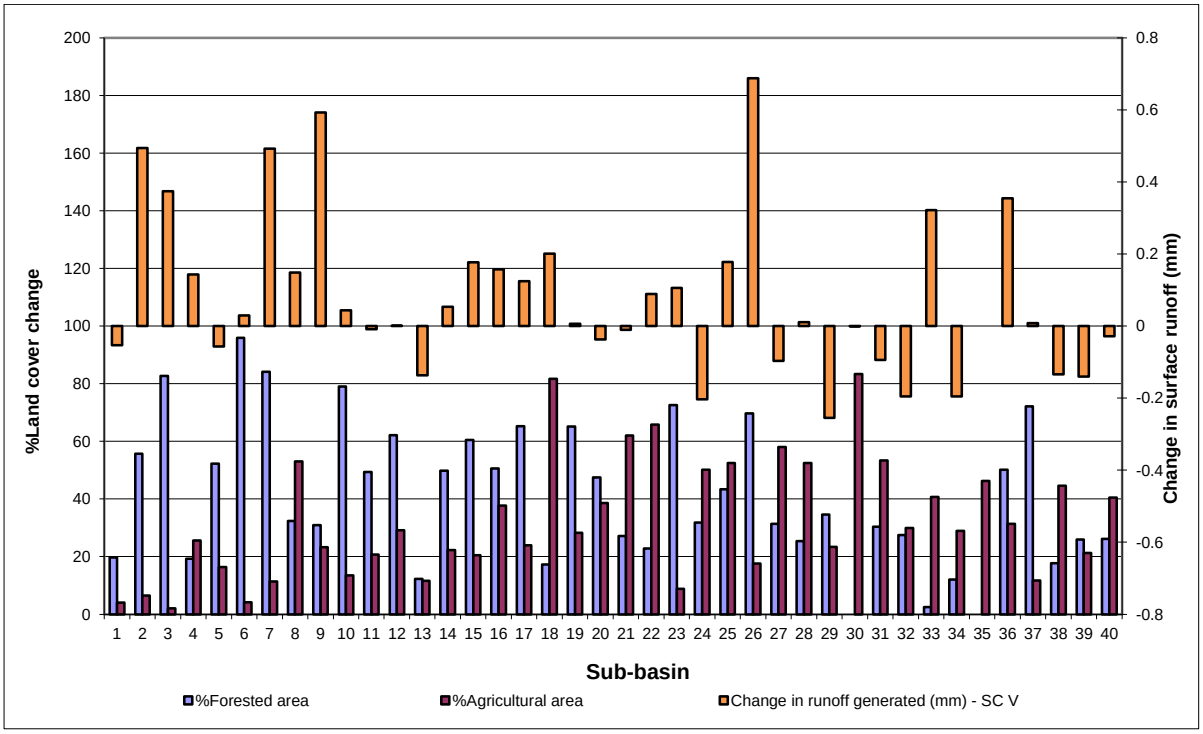

Figure 8.26: Surface runoff generation response to land cover change in scenario V

At basin scale, the fifth scenario indicates moderate change in water balance. Surface runoff was increased by 14.95 %, total water yield by 5.7 %, baseflow by 5.03 %, total

aquifer recharge by 3.79 % and actual ET was decreased by 1.05 %. The fifth scenario presents the most compromised scenario, with positive change in water balance.

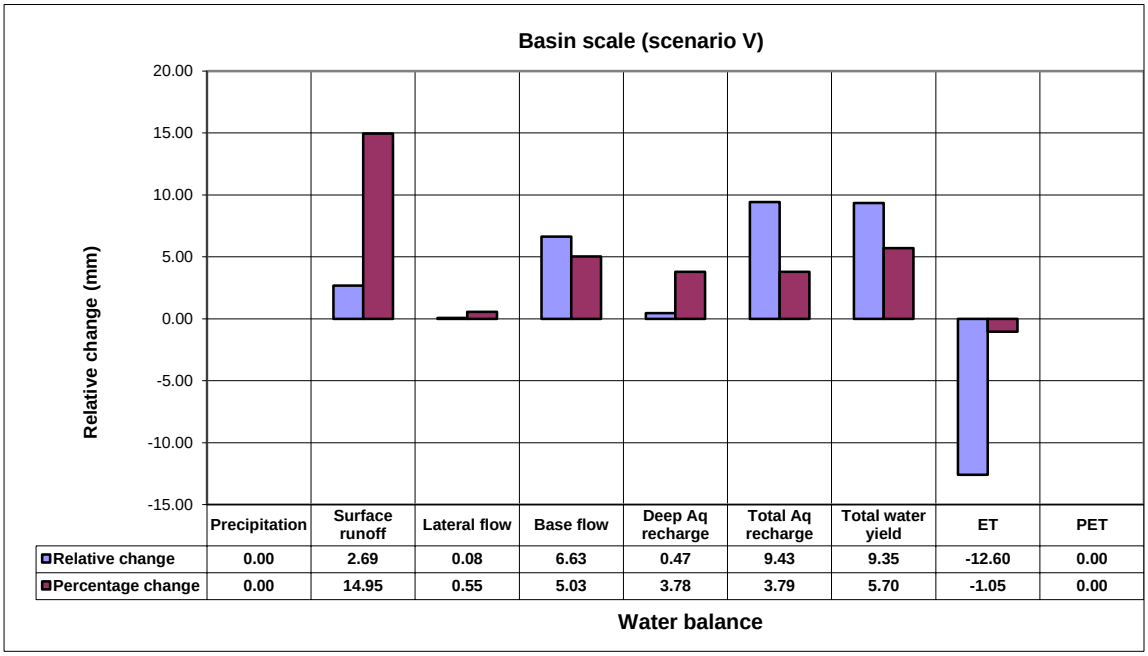

	Precipitation	Surface runoff	Lateral flow	Base flow	Deep Aq recharge	Total Aq recharge	Total water yield	ET	PET
Relative change	0.00	2.69	0.08	6.63	0.47	9.43	9.35	-12.60	0.00
Percentage change	0.00	14.95	0.55	5.03	3.78	3.79	5.70	-1.05	0.00

Figure 8.27: Basin scale water balance change, scenario V

8.4.7 Hydrologic impact of experimental land use scenario VI

The sixth scenario represents mainly agricultural development with little plantation forest in the semi-arid region. The hydrologic response indicates a general increase in surface runoff in most sub-basins with the exception of sub-basins 2, 3, 11, 12, 16, 20 and 23 (Figure 8.28).

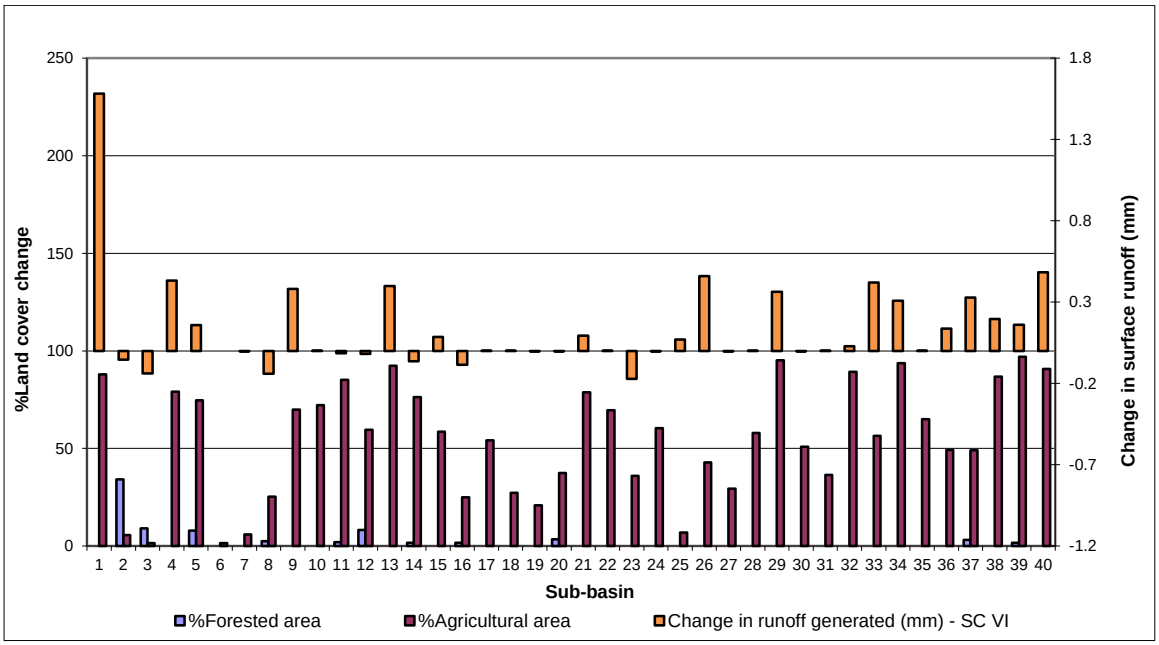

Figure 8.28: Surface runoff generation response to land cover change in scenario VI

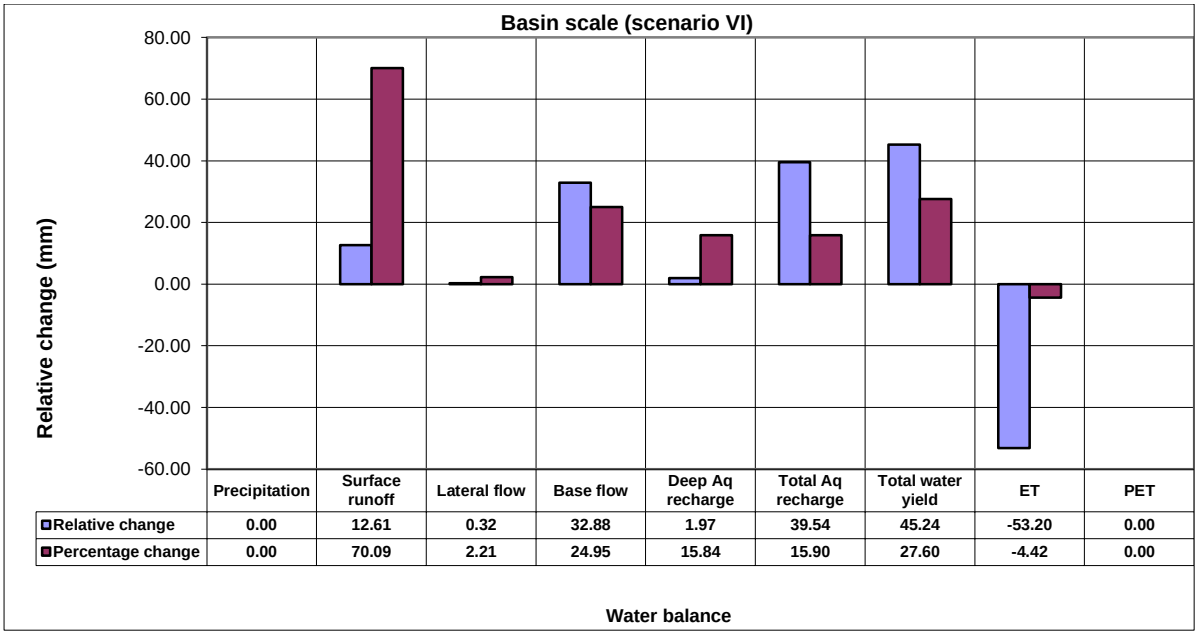

	Precipitation	Surface runoff	Lateral flow	Base flow	Deep Aq recharge	Total Aq recharge	Total water yield	ET	PET
Relative change	0.00	12.61	0.32	32.88	1.97	39.54	45.24	-53.20	0.00
Percentage change	0.00	70.09	2.21	24.95	15.84	15.90	27.60	-4.42	0.00

Figure 8.29: Basin scale water balance change, scenario VI

Analysis of the water balance at basin scale indicate significant increase in surface runoff by 70.09 %, baseflow by 24.95 %, total aquifer recharge by 27.60 % and total water yield by 27.60 %.

8.5 The effect of spatial location and extent

To demonstrate the effect of spatial location and extent of land use change on hydrologic process, nine sub-basins representing spatial heterogeneity in climate were chosen for analysis, three sub-basins from each climatic region. Table 8.8 shows sub-basins chosen to represent each climatic zone.

Table 8.8: Sub-basins chosen for spatial analysis

Sub-basin	Climatic region
2, 6, and 19	Very Dry & Dry
1, 16 and 20	Moderately Wet & Wet
26, 35 and 40	Very wet

8.5.1 The effect of land use change in the dry region

The analyses of the hydrologic responses in the three sub-basins located in the dry region are presented in figures 8.30 (a, b & c). The percentage change in land cover and the difference in surface runoff were plotted to determine if there is any relationship. In all the

three sub-basins in the dry region, changes in forest cover had mixed responses. However in general there was insignificant (< 0.05 mm) decrease in surface runoff in the sub-basins 6 and 19 following changes in forest and agricultural land cover.

According to published findings, water yield response to land cover changes is more significant in areas with deep soils and high annual precipitation and less significant in areas with less precipitation (Brooks et al., 2003). The response in these sub-basins does support this hydrologic principles, it however did not prove that afforestation reduces water yield in the dry climates. Reason to this could be due to inherent complexity and uncertainty in the model structure in simulating semi-arid hydrologic response. Changes in evapotranspiration are shown to significantly affect water yield (Bosch and Hewlett, 1982). Evapotranspiration of watershed can be manipulated by changing the structure and or composition of vegetation. Evapotranspiration process in the dry climate however, is dominated by the soil evaporation. The hydrologic model SWAT model computes evaporation from soil and plants separately as described by Ritchie (1972). Potential soil water evaporation is estimated as a function of potential evapotranspiration and leave area index (area of plant leaves relative to the area of the HRU) and plant transpiration is simulated as a linear function of potential evapotranspiration and leaf area index. Thus, increase in leave area index would result into increase in transpiration and decrease in soil water evaporation. The proportionate increase in transpiration and decrease in soil water evaporation however determines the net change in evapotranspiration.

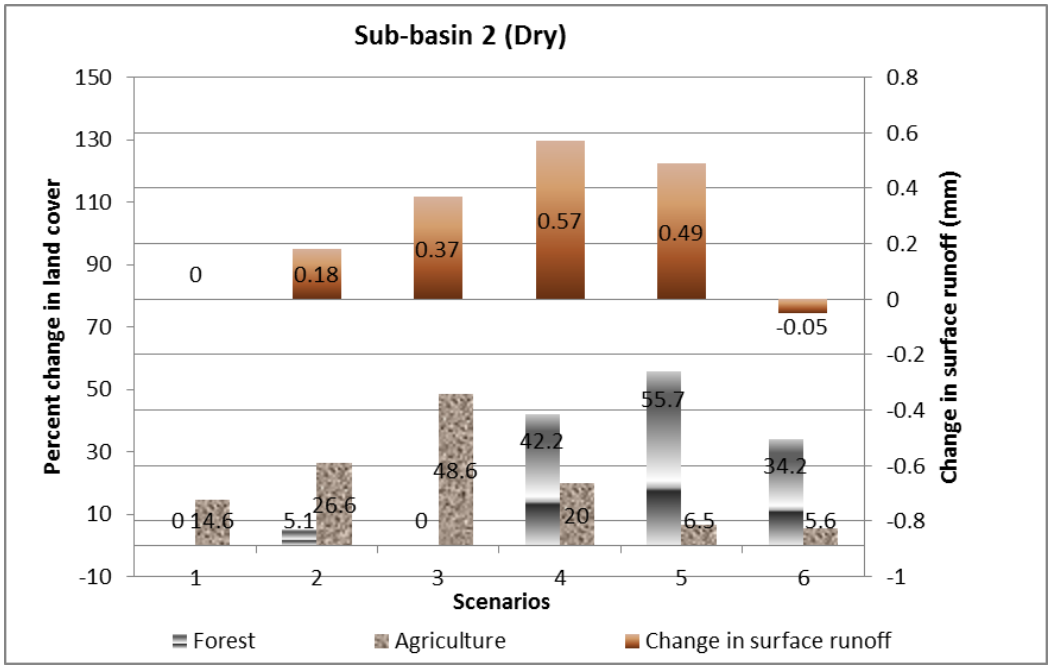

Figure 8.30a: Relationship between land cover extent and difference in flow in dry region

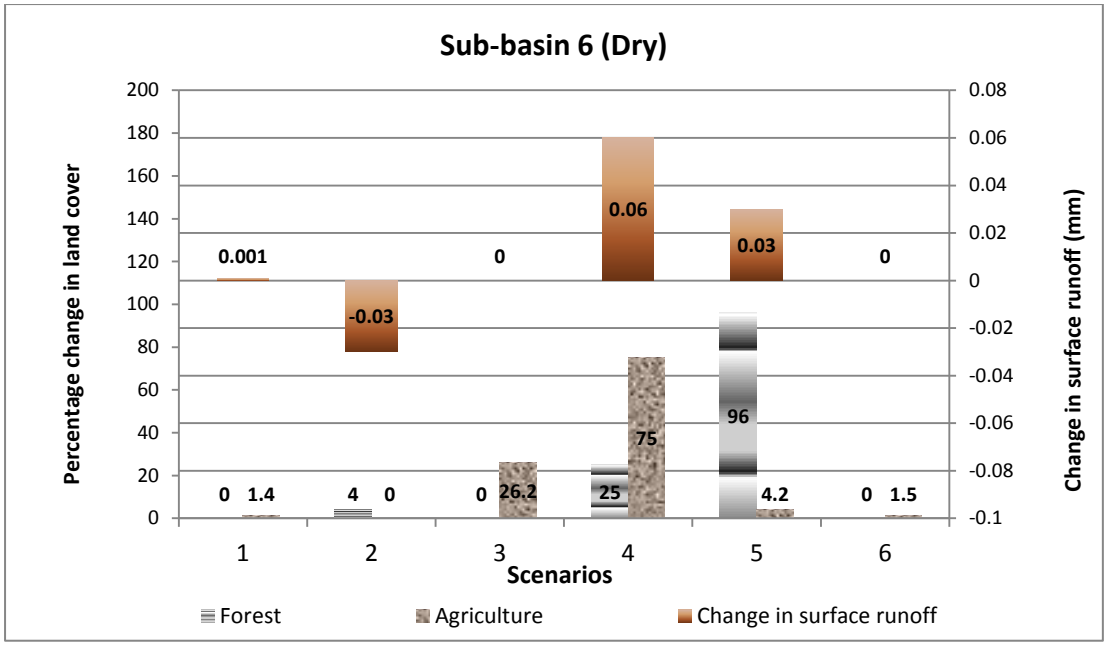

Figure 8.30b: Relationship between land cover extent and difference in flow in dry region

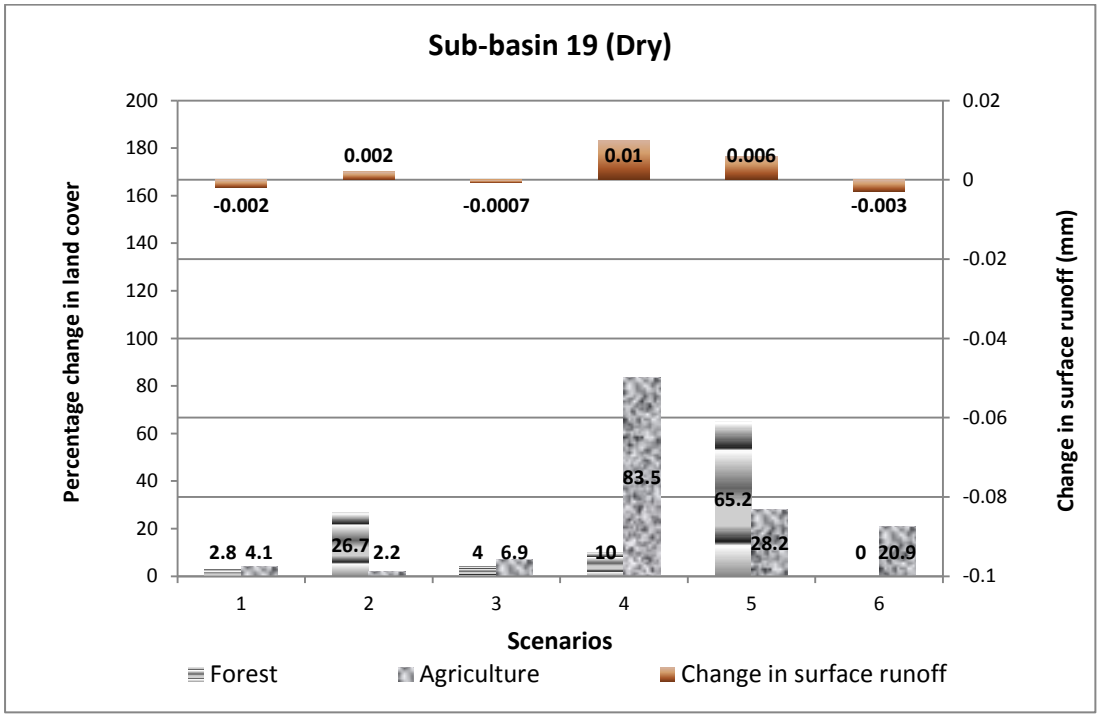

Figure 8.30c: Relationship between land cover extent and difference in flow in dry region

8.5.2 The effect of land use change in wet region

The effects of agricultural land and forest land cover extent on surface runoff in the wet zone of the basin are presented in figures 8.31 (a, b & c). The analyses in sub-basin 20 showed that increasing agricultural land use significant increases surface runoff, while

increase in forest land cover decreases surface runoff. In sub-basin 13, increase in forest land cover by 82 % decreases surface runoff by 0.9 mm, meanwhile expansion of agricultural land by 92 % increases surface runoff by of 0.4 mm.

Increase in water yield as result of increase in agricultural land cover could be the results of decreasing evapotranspiration due to replacement of high water demanding range lands cover with less water demanding agricultural land cover. Sub-basin 16 however showed different responses, which could be due to composition of land cover (present of wetland) or soil characteristics (shallow soil).

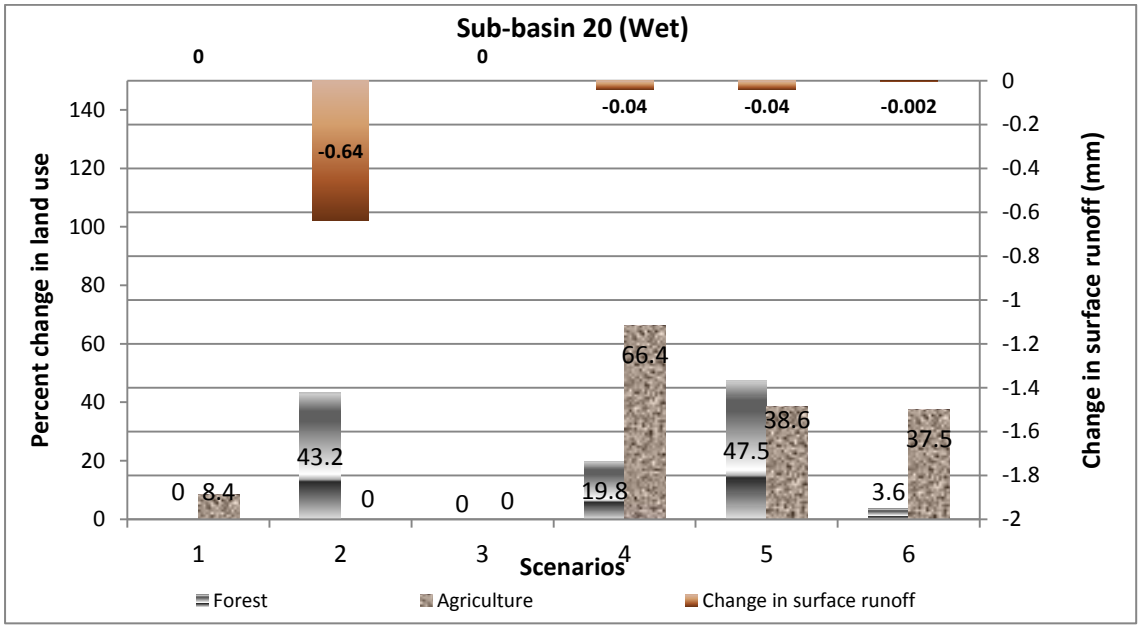

Figure 8.31a: Relationship between land cover extent and difference in flow in wet region

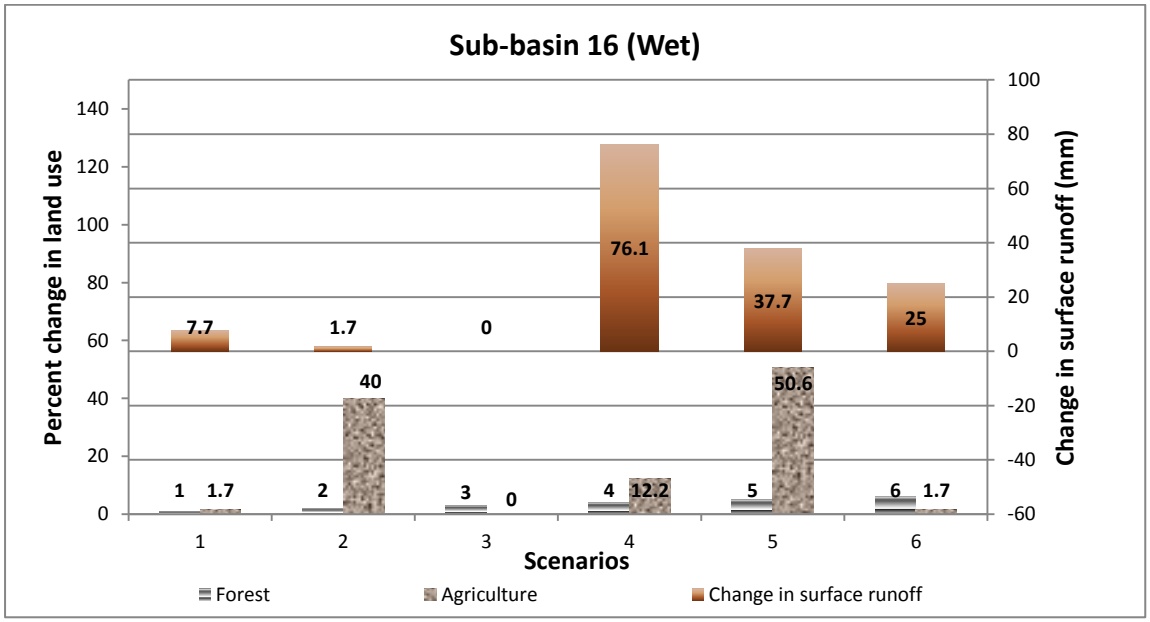

Figure 8.31b: Relationship between land cover extent and difference in flow in wet region

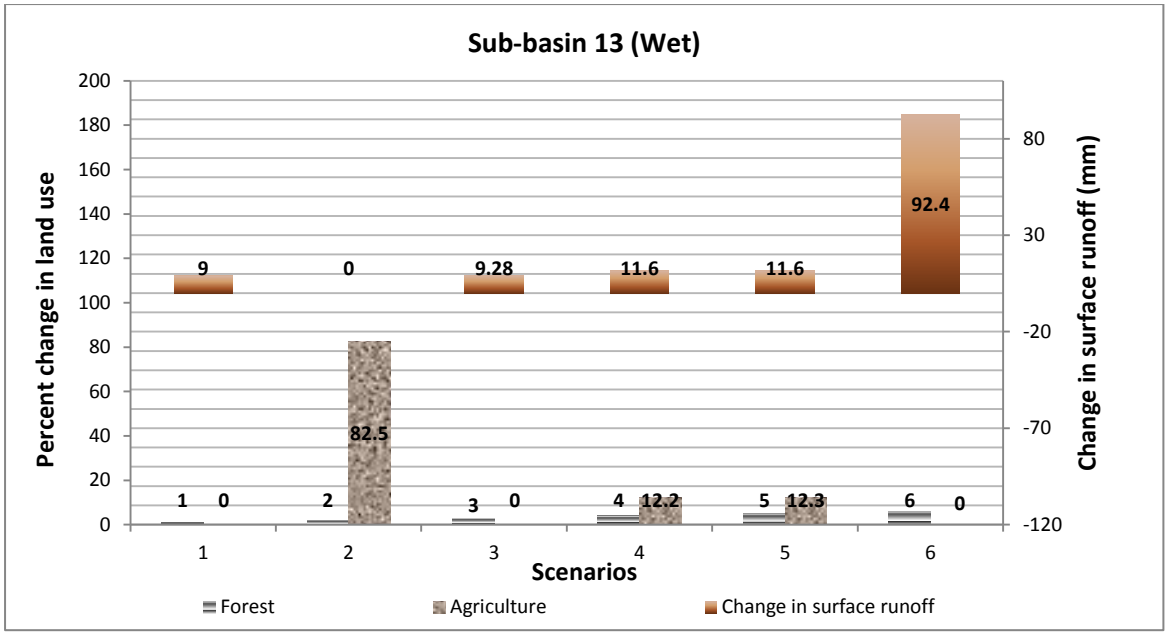

Figure 8.31c: Relationship between land cover extent and difference in flow in wet region

8.5.3 The effect of land use change in very wet region

The impact of afforestation and expansion of agricultural land cover (Figure 8.32; a, b & c) in very wet sub-basins are quite similar to the wet sub-basins. However, the impacts of afforestation on surface runoff generation were more pronounced in very wet sub-basin than in the wet sub-basins. In sub-basin 40 for example, 72% afforestation decreases surface runoff by 0.72 mm. Meanwhile, expansion of agricultural land cover by 90 % increases surface runoff by 0.48 mm. Sub-basin 40 was originally dominated by agriculture (38 %) and range land brush (34 %). The response in this sub-basin therefore was associated with replacement of range land brush with agriculture and agriculture and with plantation forest.

However, in sub-basin 26 the effect of afforestation on surface runoff generation was less noted compared to other sub-basins. Reasons could be that afforestation replaces rangeland grass, with similar water use requirement. Rangeland grass covered up to 44 % of the sub-basin area.

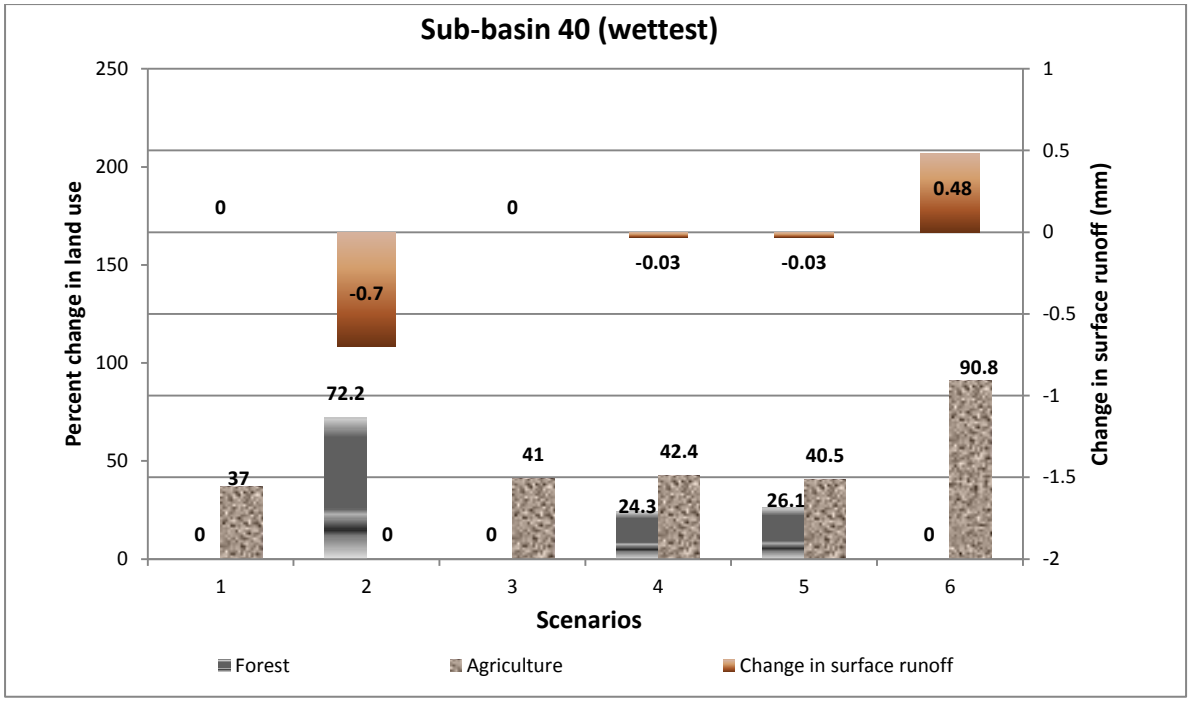

Figure 8.32a: Relationship between land cover extent and difference in flow in wettest region

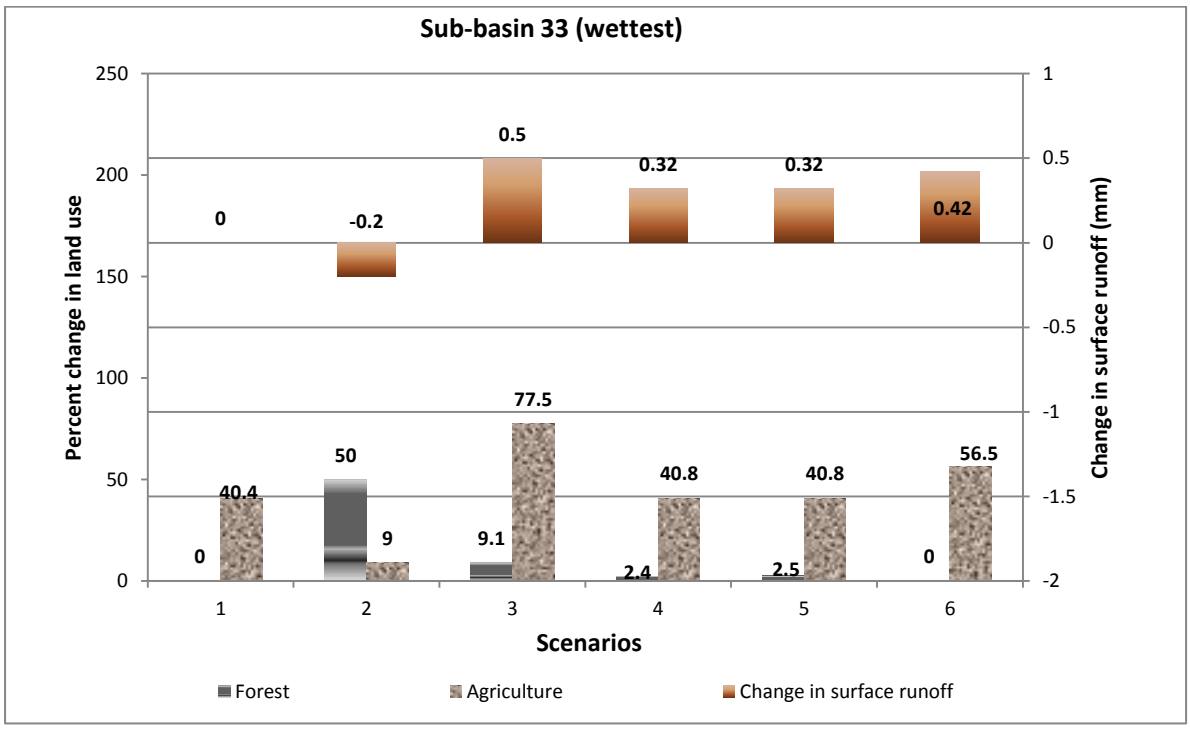

Figure 8.32b: Relationship between land cover extent and difference in flow in wettest region

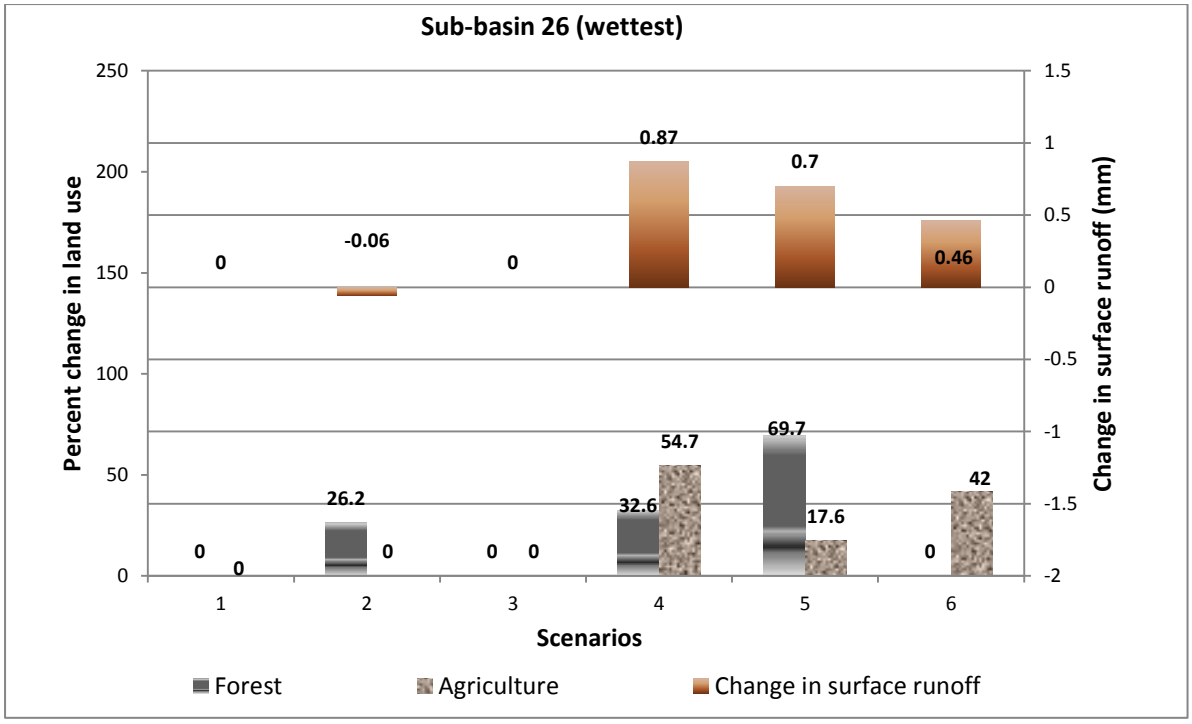

Figure 8.32c: Relationship between land cover extent and difference in flow in wettest region

8.6 Conclusion

The analyses of the hydrologic impact of afforestation and expansion in agricultural land cover presented in this chapter leads to three major conclusions.

I. Land use types, which in this study were restricted to plantation forest and generic agriculture, land use extent and location of the land use with respect to precipitation rate and amount, greatly influence the hydrologic process of the basin and the net water yield.

II. Afforestation in the dry sub-basins produces less impact on the hydrologic processes. However, in the wet sub-basins, afforestation had notable impact on surface runoff generation. Insignificant impact of afforestation in the dry zones can be used as an opportunity to offset afforestation pressure on the wet sub-basins and to meet the objective of environmental protection. However, if afforestation is required in the wet zones, then the extent of afforestation must be carefully assessed with respect to the future water demand.

III. Last but not least, the land cover change "successions order" showed great effect on the hydrologic impact of changing land use. For the benefit of increasing water yield in the basin, replacing grassland with agricultural land cover showed great potential.

Chapter 9

9. Impact evaluation

9.1 Introduction

In chapter six, seven and eight, the hydrologic model SWAT was applied to study the hydrologic impact of afforestation and expansion in agricultural land cover. In chapter six and seven, the model was used to quantify the water balance variables in the year 1986 and 2001 and to examine the impact of land use change in the reference years (1986 & 2001). In chapter eight, the application of the model was extended to assess the hydrologic impact of the experimental land use scenarios.

In this chapter, the analyses of the hydrologic impact of experimental land use change scenarios were carried out to answer fundamental questions that formed the basis of this study, formulated as: (1) "*to what degree can water yield be manipulated by altering the vegetation cover at basin and sub-basins scale*?" and (2) "*can vegetation be manipulated to complement water resources management objectives in the study area*?"

9.2 The degree of changing water yield by altering the vegetation cover.

9.2.1 Basin scale analysis

At basin scale, the summary of the hydrologic impact of experimental land use scenarios are presented in table 9.1.

Table 9.1: Basin scale water balance response

Scenarios	Percentage change in land cover		Percentage change in water balance				
	Agriculture	Forest	Surface runoff	Baseflow	Total aquifer recharge	Total water yield	ET
1	12.4	7.5	-15.51	-5.72	-3.31	-6.09	+0.90
2	6.2	37.5	-35.69	-14.89	-21.60	-15.85	+2.35
3	22.5	4.6	+7.45	+1.82	+1.43	+2.26	-0.42
4	52.0	23.2	+61.48	+22.44	-8.68	+24.85	-4.05
5	32.3	42.9	+14.95	+5.03	+3.79	+5.70	-1.05
6	53.7	2.6	+70.09	+24.95	+15.90	+27.60	-4.42

-indicate decrease, +indicate increase

Looking at the extreme two cases presented in scenario II and scenario VI, the analyses of the hydrologic impact revealed that afforestation decreases water yield at basin scale and expansion in agricultural land increases water yield at basin scale. In scenario II, the impact of 37.5% afforestation and 6.2% expansion in agricultural land was a reduction of total water yield by 15.85%, an upsurge in actual ET by 2.35%, a reduction in total aquifer recharge by 21.6%, a reduction in baseflow by 14.89% and a reduction in surface runoff by 35.69%. In scenario VI, however, expansion of agricultural land cover by 53.7% and increasing forest extent by 2.6% had a net hydrologic impact equivalent to 27.60% increase in total water yield, 70.09% increase in surface runoff, 24.95 % increase in baseflow and 15.9% increase in total aquifer recharge.

Not all the afforestation scenarios were able to decrease water yield at basin scale. In scenarios III, IV and V, the water yield at basin scale was increase regardless of significant level of afforestation. This unique response was earlier on attributed to the "replacement/succession order" of the plantation forest and the spatial location of the plantation forest in the basin. The replacement order was defined as substitution of the existing land cover with the new land use.

9.2.2 Sub-basin scale analysis

The discussion in the previous chapter noted that the effect of land use change on hydrologic processes at basin scale is controlled by the location of the land cover in the basin, and the extent. The analyses at sub-basins were therefore performed to reveal the relationship between the spatial extent of afforestation and agricultural land expansion on basin water yield.

In scenario I, 7.5 % increase in plantation forest was mainly in the wettest regions. The impact observed for this spatial location and extent of afforestation was a reduction in total water yield by 6.09 %. In scenarios IV and V, the plantation forests were located mainly in the less wet zone of the basin and the net impact was an increase in the basin water yield by 24.85% and 5.7%.

In general, in the wet region, replacement of less water demanding range lands with high water demanding plantation forest had more impact on the hydrologic process than in the dry zone.

9.3 Manipulation of vegetation covers to complement water resources management objectives in the study area

9.3.1 Technical background

Water resources management in Uganda is focusing on attainment of the UN Millennium Development Goals, which includes reducing poverty and hunger, diseases and environmental degradation, including halving the proportion of people without access to basic drinking water and sanitation services. The water and sanitation sector was recognized as a key area under the 2004 Poverty Eradication Action Plan (PEAP), Uganda's main strategy paper to fight poverty. Crucial issues facing the water and sanitation sector in the country are degradation of natural resources caused by limited ability to plan and manage the resources.

In Aswa basin, this study evaluated how vegetation manipulation can complement water resources management objectives on reducing environmental degradation, and meeting the water needs in agriculture and household. The evaluation looked at mainly the replacement or succession orders of vegetation and how this affects the water resources availability. The evaluation of vegetation replacement (afforestation and agriculture) with the indigenous range lands on water resources were treated at two levels.

In the first level, the evaluation looked at how the soil moisture storage (green water resources) could be impacted by the vegetation changes, which could affect the sustainability of the traditional rainfed agricultural systems. In the second level, the evaluation looked at the water yield (blue water resources), which could determine the potential of water harvesting technologies and future irrigated agriculture, required to boost agricultural production.

9.3.2 Options for green and blue water management

Green water management paradigm proposed by Falkenmark and Rockström (2006) focuses on how precipitation can be separated at the soil into soil moisture/green water (transpired by plant) and water that infiltrates the soil and reaches aquifers and streams commonly refers to as blue water. The management principles of green water looked at three fundamental issues: increasing infiltration, reducing destructive surface runoff and reducing

unproductive evaporation. By reducing runoff and increasing soil storage, groundwater recharge and baseflow are also increased.

The analysis of water demand (evapotranspiration) for the different land cover types (Figure 8.14) indicate agriculture as having the least water requirement, followed by mixed forest cover, brush land, semi-arid range, grass land, wetland and plantation forest (considered to be pines and eucalyptus) in that order. By expanding less water demanding agricultural land into range lands, the unproductive evaporation in range lands are reduced and water availability for humans and ecosystems downstream increased. Analysis indicates that total water yield can be increased by 27.6 % after expansion of 53.7 % of agricultural land (scenario 6). However expanding agricultural land may cause other related environmental issues (erosion and water pollution). This therefore present a trade-offs in expansion of agricultural land to augment basin water yield for crops and humans.

The expansion of plantation forest into range land on the other hand reduces blue-water availability for humans and ecosystems downstream. Plantation forest consumes large proportion of infiltrated rain leaving little to generate runoff or recharge groundwater. Analysis indicates that introduction of 37.5% plantation forest decreases surface runoff by 35.69%, baseflow by 14.89 % and total water yield by 15.85 % and increases evapotranspiration (water consumption) by 2.35 %.

However, determining the needs to manage green and blue water resources depend on the financial incentives and on the environmental requirements. In ASWA basin, it can be noted that land cover changes provides great opportunity to manage the green water and blue water resources.

9.3.3 Options for infrastructure and technologies

The choice of future water infrastructure and technologies depends on how the availability of water in the basin is managed. The choice extends across the whole spectrum of technical and institutional complexity, which may range from a simpler in-situ land management practices on individual farms to a more complex technologies such as drainage systems, check dams and percolation ponds, which may require more institutional involvement. The appropriate infrastructure and technologies should be able to address issues of water scarcity during the period of shortage; and excess flow during period of abundant.

For example, the choice of soil and water conservation approach through agronomic and engineering procedures depends on the needs to prevent erosion, improve soil moisture availability, and increase the period of water availability for human, livestock and crops.

In case of decreasing water yield due to afforestation scenario, effort to improve soil moisture availability would be uneconomical. The green water reserve would instead be consumed by the non-beneficial evapotranspiration from plantation forest. In such a case, even groundwater recharge would be reduced. The appropriate infrastructure and technologies would be the construction of percolation ponds and dams to stores water for livestock, crops and recharges the groundwater. The ponds can be constructed in large numbers at the foot of hills slopes and hilly areas. The storage facilities would attenuate the floods during storms; ensure soil moisture for good growth of trees downstream, recharging the groundwater in the region and making available more water for drinking and irrigation water.

However, when water yield is increased due to agricultural scenarios, efforts to improve soil moisture availability, reduce erosion, and harvest excess flow for use during scarcity are crucial. The appropriate technologies may include contour bunds and contour barriers (vegetative and stone), required to prevent soil erosion and obstruct the flow of runoff water. The obstructed water increases the soil moisture and also recharges the groundwater in the area. Check dams made of locally available materials may also be used to obstruct the soil and water removed from the watershed. The dam stores little water above, and may also help in supplementing the groundwater.

9.4 Conclusion

In conclusion, the water yield of the basin can be significantly decreased by over 15%, if more than 37% of the plantation forests are introduced in the wet zone. However, the introduction of plantation forest in the less wet region (semi-arid region) up to 42 % did not show any significant effect on water yield. Expansion of agricultural land by 53% can increase the water yield in the basin, by up to 27 %. The response of agricultural land to water yield was however less sensitive to climatic zones. Note that agriculture in this study was treated as generic, meaning that response of specific agricultural land cover could be different.

Replacement order of forest plantation and agriculture with the existing land cover was very crucial in management of green and blue water resources. Increase in runoff due to expansion of agricultural land into rangelands present great opportunities to rainwater harvesting and supplemental irrigation. However, the constrain lies in the environmental degradation due to potential increase in sedimentation and siltation of rivers and streams. Decrease in surface runoff due to afforestation in the wet zone limits the potentials of rainwater harvesting and supplemental irrigation. Insignificant impact of afforestation in the dry zone, however present great opportunity of offsetting the afforestation pressures in wet zones.

Chapter 10

10. Summary and conclusion

10.1 Background information

Identifying and quantifying hydrological consequences of land use change are complex exercises limited by: 1) the relatively short length of hydrological records; 2) the relatively high natural variability of most hydrological systems; 3) the difficulty in controlling land use changes in a catchments; and 4) the challenges involved in extrapolating or generalizing results from such studies to other systems (DeFries and Eshleman, 2004).

Contemporary approach to understanding the effects of land use on hydrology is based on controlled manipulations of the land surface while observing the hydrologic processes using the hydrologic process model. The physically based and spatially distributed hydrologic models have been extensively used in the study of land use change impact on hydrology. These models present great advantage in being more flexible, rigorous and enabling mechanistic interpretation. In addition the results are provided immediately to the resource planner or manager.

The drawback in the use of process hydrologic modelling however relies on their dependence on the field data and observation for their construction, calibration and validation and therefore have a lot of uncertainty. The recent development made in observing land cover changes using satellite data offset some of the burden in data construction required and make the study of hydrological impact of land use changes more feasible.

In the interest of planning and managing land use for environmental sustainability, modelling land use change impact requires more of the "object-oriented" than "problem-oriented" approach. For decades, the study of hydrologic impact of land use change has been focused on identifying the impact of a particular land use change on hydrologic systems, (Bosch and Hewlett 1982; Li et al., 2007) and providing solution to the problems.

The present study explores object-oriented modelling of land use impact on hydrologic processes for resource management. The key assumptions used in the study is that, the knowledge of relationships between the land use change attributes (defined here as land use

extent, land use location and land use type) and the hydrologic processes present great opportunity to the management of land and water resources. This however may be limited by number of issues such as complexity involved in the systems and luck of adequate representation of the processes that link vegetation dynamics and hydrology in the hydrologic process model SWAT used in this study. Other limitations are; lack of fundamental data (detail land cover information, meteorological data and hydrological data), which normally affect the scale and representativeness of such study and the absent of optimization algorithm, which can define the optimal allocation and extent of a particular land use while maximizing environmental benefit and minimizing environmental degradation. There may still be limited attempts by scientist to optimize land use for environmental benefits.

The main scope of this study was to explore the opportunities land use change may offer in management of water resources using the spatial distributed hydrologic model SWAT. The emphasis was not to predict, but to understand the trend in land use and how it affects the hydrologic process and subsequent management of water resources. The overall objectives of the study were formulated into four broad sections:

1- Land use change evaluation
   a. To develop land cover maps using remote sensing image classification techniques
   b. To analyse the changes in the land cover
2- Land use change scenarios
   a. To develop GIS based multi-criteria approach to simulate anticipated forest land cover and agricultural land cover changes in the basin
3- Hydrologic impact assessment of land use change
   a. To setup hydrologic process model SWAT
   b. To calibrate and validate the hydrologic model for scenario simulation
   c. To quantify the hydrologic processes in the basin using the model &
   d. To simulate the hydrologic impact of land use change scenarios
4- Impact evaluation
   a. To examine how the hydrologic impact of land use change affects water resources availability, capacity and technological choices in sustaining future water demand in agriculture and other sectors.

10.2 Quantification of land use change using remote sensing

Due to limitation in data and information access, this thesis explored the use of spectrally based image classification algorithms (both supervised and unsupervised) for mapping land cover in ASWA, Northern Uganda, and for assessing the change in land cover between 1986 and 2001.

The results of the classification indicate that supervised image classification is more superior to unsupervised classification in identifying mixed rural land cover with accuracy of 81.48% and 70.37% and Kappa statistics of 0.7816 and 0.6609 respectively. The study has also demonstrated that the spectral based supervised image classification remains very useful even when limited information is available.

Land cover maps for 1986 and 2001 were prepared by using supervised image classification. Post classification analysis included using majority filter with moving windows of 3x3. The thematic land cover maps generated were analysed for change detection in land cover using ArcGIS software. The analysis of land use change between 1986 and 2001 indicated some significant change in forest land cover (decreased by 3.4%), settlement (increased by 0.3%), and agriculture (decreased by 6.4%).

10.3 GIS-Multi-criteria analysis and land use scenarios development

Recently, there have been attempts to use GIS to model site suitability and use the suitability map as a guide to subsequent allocation of land to potential uses (Jones et al. 1995; Campbell et al. 1992; Carver 1991; Diamond and Wright 1988). GIS capabilities for supporting spatial decisions (Malczweski, 1999), offers a unique opportunities to spatial land use allocation and configuration, which this study explored in developing land use change pattern. GIS based land use change model also offer great flexibility to spatial configuration of land cover change, by assigning different weights to land transformation.

Simples but consistent sets of assumptions about biophysical and socio-economic parameters driving land use change in the study area were developed. The multi-criteria decision making approach using the AHP was used to assign weights to the different

parameters, which were later used in the GIS interface for land use scenarios modeling. The weights were assigned using the scales of relative importance according to (Saaty, 1980).

The set of biophysical parameters developed were: relief, climate, vegetation cover, and water availability. The only socio-economic parameters used were accessibility and population. It was assumed that the general economic environment are influenced mainly by population, which provides for example market force and labours and by the biophysical parameters such as climate, topography, soil characteristics and water availability, which are fundamentals to land productivity. The parameters were presented as map layers in GIS for modeling land use change.

The land use suitability models were built by stringing together Euclidian distance tool, reclassification tool, weighted overlay tool, and the conditional tool "con". The weighted overlay tool was used to perform 'weighted overlay of the parameter maps' in the ArcGIS spatial analyst environment. The result of the overlaid maps was a suitability maps that was analyzed using the condition tool "con" to determine site suitability for the land allocation. The site suitability maps were transformed to scenario map through aggregation, using the reference land cover map (2001 land cover map) as base map.

10.4 The hydrologic process model SWAT; set-up, calibration and validation

In chapter 5, the hydrologic process model SWAT was set up through customization and calibration. A great deal of time was spent in preparing the input data required by the model and generating the parameters for the custom weather generator. Daily data on precipitation and temperature were available for input from three meteorological stations (Gulu, Lira and Kitgum). Daily data on wind speed, relative humidity and radiation were simulated using the custom weather generator.

SWAT model was successfully calibrated by using observed streamflow data from 1970 to 1974, with a coefficient of determination (R2) equals to 0.64 and the Nash-Sutcliffe efficiency (NSE) of 0.47. Validation of the model was carried out using independent set of streamflow record between the periods 1975 and 1978. Validation result indicated that the model performance was even better in the validation periods with a coefficient of determination obtained to be 0.56 and the model efficiency (NSE) was 0.66.

10.5 Application of the hydrologic model SWAT for the year 2001

The application of the calibrated model SWAT in simulating hydrologic processes in 2001 and the hydrologic impact of experimental land use scenarios was validated by comparing the actual evapotranspiration fractions at sub-basin scale simulated using SWAT model with the actual evapotranspiration fractions estimated by using a simplified surface energy balance model (Senay et al., 2007) with the thermal MODIS images data.

It was observed that, the simulated actual ET fraction using the hydrologic model SWAT and the estimated ET fraction using the energy balance method and the MODIS LST product (MDIS11A2) correlate fairly well, with correlation coefficient of 0.45 in most wet months of the year. In the dry months (January, February, March, November and December) the correlation coefficient was however rather low. The low correlation in the actual ET fraction estimates in the dry months was believed to be due to the two extreme conditions; the wetlands vegetation and dry grasslands vegetation, which affected the choice of the "cold" and "hot" pixel temperature.

10.6 Simulation of the hydrologic processes and the hydrologic impact of land use change

The aims of the hydrologic process simulation were threefold; first was to quantify the hydrologic processes in the basin using the reference conditions, defined in this study as the 1986 and 2001 scenarios, the second aim was to simulate the hydrologic impact of land use change both in the reference periods and using experimental land use scenarios derived in chapter IV and the third aim was to evaluate the hydrologic impact of land use change on water resources availability, capacity and technological choices in sustaining future water demand in agriculture and other sectors.

Using the process hydrologic model SWAT customized and calibrated in chapter V, the hydrologic process simulations were performed using the reference land cover dataset to quantify the available water resources in Aswa basin. The analyses indicated that more water was available in 2001 than in 1986. It was revealed that this increase was due to mainly two factors. The first factor was precipitation difference and the second factor was changes in land use. The year 2001 was relatively wetter than the year 1986. The aggregated effect of land use change and precipitation difference had a net increase in water yield by 9.2 mm

($112.10^6 m^3$). Subtracting the effect of precipitation variation, using single climate simulation, the effect of land use change only had a net increase in water yield by 2.52 mm ($30.10^6 m^3$).

The analyses of the hydrologic impact of experimental land use scenarios (afforestation and expansion in agricultural land cover) revealed that land use types, which in this study were restricted to plantation forest and generic agriculture, land use extent and location of the land use with respect to precipitation rate and amount, greatly influenced the hydrologic process of the basin and the net water yield.

The afforestation in the dry sub-basins was noted to produce less impact on the hydrologic processes. However, in the wet sub-basins, afforestation had notable impact on surface runoff generation. Insignificant impact of afforestation in the dry zones can be used as an opportunity to offset afforestation pressure on the wet sub-basins and to meet the objective of environmental protection. However, if afforestation is required in the wet zones, then the extent of afforestation must be carefully assessed with respect to the future water demand.

Land cover change order referred to in this study as "successions order" showed great influence on the hydrologic impact of changing land use. For example, it was noted that the water yield in the basin can be significantly increased by replacing grassland with agricultural land. Increase in runoff due to expansion of agricultural land present great opportunities to rainwater harvesting and supplemental irrigation. However, the constrain lies in the environmental degradation due to potential increase in sedimentation and siltation of rivers and streams. Decrease in surface runoff due to afforestation in the wet zone was noted as constrains that limits the potentials of rainwater harvesting and supplemental irrigation.

10.7 Remarks

Vegetation dynamics and hydrologic processes are systematically linked. This link presents great opportunities for manipulating the hydrologic processes through controlling land surface vegetation for the benefit of transforming the hydrologic input variables to the output variables desired. The present study recognised that the outlooks into future sustainable land and water resources management in Aswa basin depends on spatial planning of land use with the objective of optimizing the environment benefit such flood protection, erosion protection and water availability. The study further recognises that the use of GIS-

Multi-criteria methodology for land use planning and the hydrologic process model SWAT in the simulation of the hydrologic impact of land use changes, opens new perspectives in adaptive management of water resources. In particular, the use hydrologic process model SWAT in object oriented simulation of the hydrologic impact of land use change in this study was innovative and demonstrate the importance of the model as a tool for planning. While the GIS-Multi-criteria methodologies approach in simulating potential land use changes, using simple straightforward assumption was another innovation that sowed great potential for use in water resources management and land use planning.

References

Abbott, M. B., J. C. Bathurst, J. A. Cunge, P. E. O'Connell, & J. Rasmussen, 1986a. An Introduction to the European Hycirological System-Systeme Hydrologique European 'SHE' 1: History and Philosophy of a Physically-Based, Distribu ted Modeling System. J. Hydrol. 87:45-59.

Abbott, M. B., J. C. Bathurst, J. A. Cunge, P. E. O'Connell, & J. Rasmussen, 1986b. An Introduction to the European Hydrological System-Systeme Hydrologique Europeen, 'SHE' 2: Structure of Physically-Based, Distributed Modeling System. J. Hydrol. 87:61-77.

Ahuja L.R., D.L. Brakensiek & A. Shirmohammadi, 1993. Infiltration and soil movement. In D. R. Maidment (Editor): Handbook of Hydrology. McGraw-Hill, New York (U.S.A.); Chapt.5

Allen R. G., L. S. Pereira, D. Raes & M. Smith, 1998. Crop evapotranspiration - Guidelines for computing crop water requirements - FAO Irrigation and drainage paper 56, Water Resources, Development and Management Service. FAO Rome.

Allen R. G., M. Tasurmi, A. T. Morse, & R. Trezza, 2005. A land based Energy balance and evapotranspiration model in Western US Water Rights Regulation and Planning. Journal of Irrigation and Drainage systems, 19 (3-4): 251-268(18).

Anderson, J. R., E. E. Hardy, J. T. Roach & R. E Witmer, 1976. A Land Use and Land Cover Classification System for Use with Remote Sensor Data. U.S. Geological Survey Professional Paper 964.

Arnold, J.G., R. Srinivasan, R. S. Muttiah, & J. R. Williams, 1998. Large area hydrologic modeling and assessment. Part I. Model development. Journal of the American Water Resources Association 34: 73–89.

Banai-Kashani, A. R. 1989. New method for site suitability analysis - the Analytic Hierarchy Process, Environmental Management, 13(6):685-693.

Bastiaanssen, W. G. M., M. Meneti, R. A. Feddes & A. A. M. Holtslag, 1988. A remote sensing surface energy balance algorithm for land (SEBAL: 1) Formulation. Journal of hydrology, 212 (213):213-229

Beven, K. J. 2001. Dalton Medal Lecture: How far can we go in distributed hydrological modelling? Hydrology and Earth System Science, 5 (1):1-12.

Beven, K., 1993. Prophecy, Reality, and Uncertainty in Distributed Hydrological Modelling. Advances in Water Resources 16(1):41-51.

Beven, K.J., & A.M. Binley, 1992. The future of distributed models: Model calibration and uncertainty prediction, Hydrol. Process, 6:279-298.

Beven, K.J., 1995. Linking parameters across scales: sub-grid parameterisations and scale dependent hydrological models, Hydrological Processes, 9:507-526.

Beven, K.J., 1996a. Equifinality and Uncertainty in Geomorphological Modelling, In B L Rhoads and C E Thorn (Eds.), The Scientific Nature of Geomorphology, Wiley, Chichester, 289-313.

Beven, K.J., 1996b, A discussion of distributed modelling, Chapter 13A, In J-C Refsgaard and M B Abbott (Eds.) Distributed Hydrological Modelling, Kluwer, Dordrecht, 255-278.

Blaney, H. F. & W. D. Criddle, 1962. Determining Consumptive Use and Irrigation Water Requirements. Agricultural Research Service, U. S. Department of Agriculture, Technical Bulletin No. 1275.

Borg, H., & D. W. Grimes, 1986. Depth development of roots with time: an empirical description: In Panigrahi, B., Panda, S. N., 2003. Field test of a soil water balance simulation model. Agricultural water management Journal. 58: 223-240

Bossel, H. 1986. Systems Analysis: An Introduction. Ecological Systems Analysis, German Foundation for International Development, chapter 1.

Briassoulis, H., 2000, Analysis of Land Use Change: Theoretical and Modeling Approaches, Regional Research Institute, West Virginia University

Bronstert, A., 2004. Rainfall-runoff modeling for assessing impacts of climate and land use change. Hydrology process. 18:567-570.

Brooks, K. N., P. F. Ffolliott, H. M. Gregesen & L. F. Debano, 2003. Hydrology and the management of watershed. Blackwell Publishing, 2121 State Avenue, Ames, Iowa 50014.

Bruijnzeel, L.A., 1990. Hydrology of moist tropical forests and effects of conversion: a state of knowledge review. In: UNESCO International Hydrological Program, 224 pp.

Campbell, J. C., J. Radke, J. T. Gless & R. M. Wirtshafter. 1992. An Application of Linear Programming and Geographic Information System: Cropland Allocation in Antigua. Environment and Planning. 24:535-549.

Carver, S.J. 1991. Integrating multi-criteria evaluation with geographical information systems.
International Journal of Geographical Information Systems. 5(3):321-339.

Chankong, V. & Y. Y. Haimes, 1983. Multiobjective Decision Making: Theory and Methodology, Elsevier-North Holland (New York).

Chow, V.T., D. R. Maidmeni & L. W. Mays, 1988. Applied Hydrology. McGraw-Hill. United Sate of America.

Congalton, R. 1991. A Review of Assessing the Accuracy of Classifications of Remotely Sensed Data. Remote Sensing of Environment, Vol. 37: 35-46.

Croke, B. F. W., W. S. Merritt, & A. J. Jakeman, 2004. A dynamic model for predicting hydrologic response to land covers changes in gauged and ungauged catchments. J. Hydrol 291:115–131.

D'urso G., 2001. Simulation and Management of On-Demand Irrigation Systems: A combined agrohydrological and remote sensing approach. PhD Thesis, Wageningen University, Wageningen, The Nertherlands, 174p. Pp 46-47

DeFeries, R., & K. N. Eshleman 2004. Land-use change and hydrologic processes: a major focus for the future. Hydrological processes, 18: 2183-2186

Diamond, J. T., & J. R. Wright, 1988. Design of an integrated spatial information system for multiobjective land-use planning, Env. And Planning B, 15(2):205-214.

Dingman, S. L., 2002: Physical Hydrology, 2nd Ed.: Upper Saddle River, New Jersey. Prentice Hall.

Dooge, J.C.I., 1973. Linear theory of hydrologic system. Technical Bulletin No 1468. Agricultural Research Service, USDA. Washington D.C.

Duan, Q., S. Sorooshian, & V. Gupta, 1992. Effective and efficient global optimisation for conceptual rainfall-runoff models, Water Resour. Res., 28:1015-1031

Dunn S. M., & R. Mackay, 1995. Spatial variation in evapotranspiration and the influence of land-use on catchment hydrology, Journal of Hydrology 171:49–73.

Eastman, J. R., L. A. Solórzano, & M. E. V. Fossen, (2005). Transition Potential Modeling for Land-Cover Change. In: Maguire, D., Batty, M., Goodchild, M., (eds). GIS, Spatial Analysis, and Modeling: California, ESRI Press, p. 357-385.

Eastman, J. R., P. A. Kyem, J. Toledano, & W. Jin, 1993. GIS and Decision making, UNITAR, Geneva.

Eastman, J. R., W. Jin, P. Kyem, & J. Toledano. 1992. Participatory procedures for multi-criteria evaluations in GIS. Proceedings, in GIS'92, pp. 281–88. Buffalo, N.Y.

Falkenmark, M. & J. Rockström, 2006. The new blue and green water paradigm: breaking new ground for water resources planning and management. Journal of Water Resources Planning and Management, 132:129–132.

Geneletti, D. & B. G. H. Gorte, 2003. A method for object-oriented land cover classification combining Landsat TM data and aerial p”hot”ographs. International Journal of Remote sensing, 24:1273-1286.

Gerten D., S. Schaphoff, U. Haberlandt, W. Lucht, & S. Sitch, 2004. Terrestrial vegetation and water balance- hydrological evaluation of a dynamic global vegetation model. Journal of Hydrology 286:249-270

Grizzetti, B., F. Bouraoui, K. Granlund, S. Rekolainen, & G. Bidoglio, 2003. Modelling Diffuse Emission and Retention of Nutrients in the Vantaanjoki Watershed (Finland) Using the SWAT Model. Ecological Modelling 169(1):25-38.

Hibbert, A. R. 1983. Water yield improvement potential by vegetation management on western rangelands. Water Resources Bulletin 19(3): 375-381.

Holling, C.S. (ed.) (1978). Adaptive Environmental Assessment and Management. International Institute for Applied Systems Analysis. Wiley Chichester, New York.

Howards, K. W. F., M. Huges, D. L. Charlesworth, & G. Ngobi, 1992. Hydrogeologic evaluation of fracture permeability in crystalline basement aquifers of Uganda, Hydrogeology Journal, 1:55-65

Immerzeel, W. W., & P. Droogers, 2007. Calibration of a distributed hydrologic model based on satellite evapotranspiration. Journal of hydrology (in press)

James, L. D. and S. J. Burges, 1982. Selection, Calibration, and Testing of Hydrologic Models. In: Hydrologic Modeling of Small Watersheds, C.T. Haan, H.P. Johnson, and D.L. Brakensiek (Editors). ASAE Monograph, St. Joseph, Michigan, pp. 437-472.

Jensen, J. R. (ed.) 1983. Urban/Suburban Land Use Analysis. In: Colwell, R.N., ed. Manual of Remote Sensing, Second Edition. American Society of Photogrammetry, Falls Church, Virginia. pp. 1571-1666.

Jensen, J. R. 1996. Introductory digital image processing: A remote sensing perspective. Prentice Hall, Upper Saddle River, New Jersey.

Jensen, M. E., R. D. Burman & R. G. Allen (ed). 1990. Evapotranspiration and irrigation water requirements. ASCE Manuals and Reports on Engineering Practice No. 70 ASCE New York.

Jiang, H. and J. R. Eastman, 2000. Application of fuzzy measures in multi-criteria evaluation in GIS. Int. J. Geographical Information Systems, 14:173-184.

Jones, C. B., G. L. Bundy, & J. M. Ware, 1995. Map Generalization with a Triangulated Data Structure. Cartography and Geographic Information Systems, 22(4):317-331.

Jorgensen, H. O., 2006. Population Dynamics and Agricultural Land Depletion. The World Bank

Kangas, J. 1992. Multiple-use planning of forest resources by using the Analytic Hierarchy Process. Canadian Journal of Forest Research, 7:259–68.

Kangas, J. 1993. A multi-attribute preference model for evaluating the reforestation alternatives of a forest stand. Forest Ecology and Management, 59: 271–88.

Kati L. W., & I. Chaubey, 2005. Sensitivity analysis, calibration, and validations for a multisite and multivariable SWAT model. Journal of the American Water Resources Association (JAWRA) 41(5):1077-1089.

Keeney, R.L. and H. Raiffa, 1976. Decision with Multiple Objectives: Preferences and Value Tradeoffs. New York: John Wiley & Sons.

Kiersch. B & S. Tognetti, 2002. Land-water linkages in rural watersheds: Land use and water resources research, Results from the FAO electronic workshop FAO Land and Water Development Division, Rome, Italy.

Li K.Y., M. T. Coe, N. Ramankutty, R. De Jong 2007. Modeling the hydrological impact of land-use change in West Africa, Journal of Hydrology. 337.258– 268

Lillesand, T. M., & R. W. Kiefer. 1987. Remote Sensing and Image Interpretation. New York: John Wiley & Sons, Inc.

Malczewski, J., 1999. GIS and Multicriteria Decision Analysis, John Wiley and Sons, 392 pp., New York, NY.

Mendoza, G. A. 1997. Introduction to Analytic Hierarchy process: Theory and applications to Natural Resources Management. In Proceedings of 1997 ACSM/ASPRS Annual Convention. Vol 4. Resource Technology. April 7–10. Seattle, WA. pp.130–39.

Molden, D, (ed). 2007. Water for food, water for life: A comprehensive Assessment of water management in Agriculture, IWMI, Summary.

Moriasi, D. N., J. G. Arnold, M. W. Van Liew, R. L. Bingner, R. D. Harmel, & T. L. Veith, 2007. Model evaluation guidelines for systematic quantification of accuracy in watershed simulations, T. ASABE, 50:885–900.

Nash, J. E. & J. V. Sutcliffe, 1970. River flow forecasting through conceptual models, Part I - A discussion of principles, J. Hydrol., 10:282–290.

Neitsch, S. L., J. G. Arnold, J. R. Kiniry, & J. R. Williams, 2005. Soil and Water Assessment Tool – Theoretical Documentation, Version 2005. Texas, USA.

Organisation for Economic Cooperation and Development (OECD); Water management in industrialized river basins, Paris (1980).

Pagan, P., & L. Crase, 2004. Does adaptive management deliver in the Australian water sector. 48th Annual Conference of Australian Agricultural and Resource Economics Society, Melbourne, 11-13 February 2004

Parker, D., T. Berger, S. Manson, S. Mcconnel, 2002. Agent-Based Models of Land-Use /Land-Cover Change. Report and Review of an International Workshop., Irvine, California, USA, LUCC Project.

Peterson, D. L., D. Silsbee, & D. L. Schmoldt, 1994. A case study of resource management planning with multiple objectives. Environmental Management, 18(5): 729–42.

Priestley, C. H. B. & R. J. Taylor, 1972. On the assessment of the surface heat flux and evaporation using large-scale parameters. Monogram of Weather Rev. 100, 81-92

Rallison, R. E., & N. Miller, 1981. Past, present and future SCS runoff procedure, in Rainfall-Runoff Relationships, Proceeding of the International Symposiums on rainfall-runoff Modeling, May 18-21, Mississippi State University, Water Resource Publications, Littleton, CO, pp 355-364.

Reynolds, K. M., & E. Holsten, 1994. Relative importance of risk factors for spruce beetle outbreaks. Canadian Journal of Forest Research, 24(19):2089–95.

Saaty, T. L., 1980. The analytical hierarchy process. McGraw-Hill, New York.

Saaty, T. L., 1983. Priority settings in complex problems. IEEE, Transactions on Engineering Management, 30:140-155.

Saaty, T. L., 1994. Fundamentals of Decision Making and Priority Theory with the Analytic Hierarchy Process. RWS Publications, Pittsburgh PA., p 337.

Santhi, C., J. G. Arnold, J. R. Williams, L. M. Hauck, & W. A. Dugas, 2001a. Application of a Watershed Model to Evaluate Management Effects on Point and Nonpoint Source Pollution. Transactions of the American Society of Agricultural Engineers 44(6):1559-1570.

Savenije, H. H. G., 1995. New definitions for moisture recycling and the relation with land-use changes in the Sahel. H. Hydrol. 167:57–78.

Saxton, K. E., W. J. Rawls, 2006. Soil water characteristic estimates by texture and organic matter for hydrologic solutions. Soil Science Society of America Journal, 70:1569-1578.

Scotter, D. R., B. E. Clothier, & M. A. Turner, 1979. The soil water balance in a Fragiaqualf and its effect on pasture growth in central New Zealand. Australian Journal of soil research, 17, 455-465

Senay, B. G., M. Buddle, J. P. Verdin & A. M. Melesse, 2007. A Coupled Remote Sensing and Simplified Surface Energy Balance Approach to Estimate Actual Evapotranspiration from Irrigated field. Sensor, 7:979-1000

Soares-Filho B. S., G. C. Cerqueira & C. L. Pennachin, 2002. DINAMICA- a stochastic cellular automata model designed to simulate the landscape dynamics in an Amazonian colonization frontier. Ecological Modelling 154, 217-235

Tanji, K. K., and C.A. Enos, 1994. Global water resources and agricultural use: In Tanji K.K., and B. Yaron (Eds.) Management of Water Use in Agriculture, Springer-Verlag Berlin Heidelberg, Pp 1

Thornthwaite, C. W., 1948. An approach toward a rational classification of climate: Geographical Review, 38:55–94.

Thornthwaite, C. W., and J. R. Mather, 1955. The Water Balance. Publications in Climatology, 1: 1-104, Drexel Institute of Climatology, Centerton, NJ.

Tou, J. T., & R. C. Gonzalez, 1974. Pattern Recognition Principles. Addison-Wesley Publishing Company. Reading, Massachusetts, pp 97-104.

Uganda National Water report (2005). Chapter two: Review of the water sector http://www.unesco.org/water/wwap/wwdr/wwdr2/case_studies/uganda/pdf/2_overview_uganda_water_sector.pdf Accessed on 12/2/2009

Van Liew, M. W., J. M. Schneider, & J. D. Garbrecht, 2003. Stream Flow Response of an Agricultural Watershed to Seasonal Changes in Rainfall. In: Proceedings, 1st Interagency Conference on Research in the Watershed, Renard, K. G., S. A. McElroy, W. J. Gburek, H. E. Canfield, & R. L. Scott (Editors). U.S. Department of Agriculture, Agricultural Research Service, Benson, Arizona.

Veldkamp, A., & L. O. Fresco, 1996. CLUE-CR: an integrated multi-scale model to simulate land use change scenarios in Costa Rica. Ecological modelling, 91:231-248.

Verburg, P. H., A. Veldkamp, L. Willemen, K. P. Overmars, & J. P. Castella, 2004. Landscape level analysis of the spatial and temporal complexity of land-use change. In: De Vries, R., Houghton, R. (Eds.), AGU Monograph

Verburg, P. H., B. Eickhout, & V. Meijl, 2008. A multi-scale, multi-model approach for analyzing the future dynamics of European land use. Annals of Regional Science, p. 57 - 77.

Verburg, P. H., G. De Koning, K. Kok, A. Veldkamp, & J. A. Bouma, 1999. Spatial explicit allocation procedure for modeling the pattern of land use change based upon actual land use. Ecological modeling, 116:45-61, 1999.

Verburg, P. H., K. Kok, R. G. Pontius, A. Veldkamp, E. F. Lambin, H. J. Geist, 2006. Modeling land use and land cover change. Land-use and landcover change. Local processes and global impacts, Springer, Berlim.

Verburg, P. H., P. P. Sc"hot", M. J. Dijst, & A. Veldkamp, 2004. Land use change modeling: current practice and research priorities. GeoJournal, 61(4): 309-324.

Verburg, P. H., W. Soepboer, A. Veldkamp, R. Limpiada, & V. Espaldon, 2002. Modeling the Spatial Dynamics of Regional Land Use: The CLUE-S Model. Environmental Management, 30(3):391-405.

Walker, G. R. & L. Zhange, 2001. Plot scale models and their application to recharge studies. In: Zhang, L., and Walker, G. R. (eds), Studies in catchment hydrology. The basics of recharge and discharge. Melbourne, CSIRO Publishing.

Wandera, S. A. Izama, A. 2009. World Bank to reward Ugandaa for planting trees. Ecology Press (http://www.ecologypress.com/2009/10/06/world-bank-to-reward-uganda-for-planting-trees/) Accessed 10/1/2010

Williams, J. R. & W. V. LaSeur, 1976. Water yield model using SCS curve numbers. ASCE Journal of Hydraulics Division, 102, 1241-1253.

Williams, J. R. 1995. The EPIC Model: In SWAT Models, Input/Output file documentation, Version 2005.

Xiang, W. & D. L. Whitley, 1994. Weighting land suitability factors by the PLUS Method. Environment and Planning B: Planning and Design. 21:273–304.

Zhang L., G. R. Walker, & W. R. Dawes, 2002. Water balance modeling: concept and applications. In: McVicar, T. R., R. Li, J. Walker, R. W. Fitz-Patrick, & C. Liu (eds). Regional Water and soil assessment for Managing Sustainable Agriculture in China and Australia, ACIAR Monograph No. 84, 31-47.

Appendix A

Table A.1: Locally available meteorological station obtained from FAO-NILE used in generating rainfall map

Station ID	Station name	Lon	Lat	Altitude	Start year	End year
86320000	Kitgum Centre VT	32.88	3.30	940.00	1914	2000
86320030	Palabek Divisional Hqs	32.58	3.43	980.00	1939	1981
86320090	Padibe	32.82	3.50	1080.00	1943	1983
86320170	Acholi Ranch	32.55	3.27	984.00	1970	1985
86330000	Kitgum Matidi	33.05	3.27	1000.00	1943	1982
86330010	Kalongo Hospital	33.37	3.05	1120.00	1956	1981
86330020	Paimol	33.42	3.07	1150.00	1943	1980
86330030	Agoro	33.02	3.80	1120.00	1943	1984
86330050	Orom	33.47	3.42	1080.00	1943	1983
86330060	Karenga	33.72	3.48	2655.00	1952	1977
86330070	Naam	33.33	3.35	1040.00	1943	1983
86330080	Mucwini Gombolola	33.07	3.33	1020.00	1963	1978
86330140	Madi Opei	33.10	3.60	1020.00	1965	1998
86330230	Kacheri	33.78	3.20	1050.00	1977	1991
86340000	Kotido PWD	34.17	3.02	1200.00	1947	1980
86340010	Kaabong	34.10	3.55	1500.00	1946	1966
86340020	Kotido	34.10	3.02	1260.00	1947	1991
86340030	Loyoro [County Dodoth]	34.22	3.37	1470.00	1947	1963
87320000	Gulu Met Station	32.28	2.78	1105.00	1937	2000
87320020	Ngetta Farm	32.93	2.32	1110.00	1943	1999
87320040	Atura Port KUR	32.33	2.12	990.00	1943	1962
87320060	Boroboro CMS	32.92	2.18	1200.00	1943	1962
87320070	Amar	32.08	2.62	1200.00	1943	1976
87320080	Minakulu Verona FM	32.37	2.52	1043.00	1943	1985
87320100	Comboni College	32.92	2.30	1110.00	1943	1977
87320110	Lira	32.90	2.25	1068.00	1943	1979
87320120	Awere	32.80	2.70	1000.00	1943	1998
87320130	Pajule	32.93	2.97	1050.00	1943	1980
87320190	Ogur	32.93	2.43	1080.00	1943	1975
87320200	Bardyang Forest Station	32.95	2.02	1050.00	1943	1982
87320210	Attanga	32.72	3.00	1050.00	1943	1982
87320220	Alito	32.83	2.45	1080.00	1943	1979
87320230	Anyeke Oyam	32.52	2.37	1140.00	1944	1968
87320240	Opit Forest Station	32.48	2.62	1102.00	1946	1984
87320320	Lakwatomer	32.40	2.70	900.00	1953	1959
87320360	Aboke Group Farm	32.63	2.33	1080.00	1965	1990
87320370	Adyeda Group Farm	32.53	2.27	1053.00	1965	1978
87320390	Lira Ngetta AgroMet Station	32.93	2.28	1300.00	1964	1999
87330000	Amuria Dispensary	33.67	2.03	1233.00	1943	1951
87330010	Alebtong	33.23	2.27	1200.00	1943	1978
87330020	Alanyi Catholic Mission	33.27	2.10	1050.00	1943	1977
87330030	Omoro MHM	33.37	2.25	1110.00	1943	1951
87330070	Morulem	33.77	2.62	1440.00	1951	1998
87330080	Patong	33.32	2.77	1020.00	1943	1998
87330090	Adilang	33.48	2.75	1100.00	1943	1976
87330100	Pader	33.12	2.87	1020.00	1943	1978
87330130	Alerek	33.72	2.80	1350.00	1946	1979